Converting an ice storage facility to a chilled water system for energy efficiency on a deep level gold mine

DC Uys

21663394

Dissertation submitted in fulfilment of the requirements for the degree *Magister* in Mechanical Engineering at the Potchefstroom Campus of the North-West University

Supervisor: Prof M Kleingeld

May 2015

ABSTRACT

Title: Converting an ice storage facility to a chilled water system for energy efficiency on a deep level gold mine

Author: Dirk Cornelius Uys

Supervisor: Prof. M. Kleingeld

Faculty: Engineering

Degree: Master of Engineering (Mechanical)

Keywords: ice storage; deep level gold mine; energy management; refrigeration system

The South African gold mining sector consumes 47% of the mining industry's electricity. On a deep level gold mine, 20% of the energy is consumed by the refrigeration system. The refrigeration system cools 67 ˚C virgin rock temperatures underground. Underground cooling demand increases significantly with deeper mining activities. Various cooling systems are available for underground cooling. This study focuses on the electricity usage of an ice storage system versus a chilled water system for underground cooling.

An energy-savings approach was developed to determine possible power savings on the surface refrigeration system of Mine M. The savings approach involved converting an ice storage system to a chilled water system and varying the water flow through the system. The water flow was varied by installing variable speed drives on the evaporator and condenser water pumps. The feasibility of the energy-efficiency approach was simulated with a verified simulation model.

Simulation results indicated the feasibility of converting the thermal ice storage to a chilled water system and implementing the energy-efficiency approach on Mine M. Simulated results indicated a 9% electricity saving when using a chilled water system. Various problems encountered by the mine were also a motivation to convert the thermal ice storage system.

Energy management is achieved through the monitoring, controlling and reporting of the implemented savings approach.

Converting the glycol plant and recommissioning the chilled water plant gave the mine an additional chiller as backup to sufficiently meet underground demand. An annual summer power saving of 1.5 MW was achieved through the conversion and control strategy. It is concluded that conversion of the thermal ice storage system on Mine M results in an energy- and cost saving.

ACKNOWLEDGEMENTS

My Saviour for providing me with the ability and perseverance to complete this study.

Thank you to TEMM International (Pty) Ltd and HVAC International (Pty) Ltd for the opportunity, financial assistance and support to complete this study.

Prof. Eddie Mathews for providing me with the opportunity to complete the study.

Dr. Marius Kleingeld for his guidance and assistance throughout the course of the study.

Dr. Abrie Schutte for mentoring and assistance in the project implementation and dissertation editing.

Andre Pretorius, Dirk Botha, Frits Schutte and Flip Stols at Mine M for assisting with the project implementation.

Colleague and friend Declan van Greunen for assisting with the project implementation.

Close friends Lötter Els and Wynand Breytenbach for their continued support throughout the course of the study.

Family members JJ, Minda and Duené Uys for their continued support throughout the study.

LAYOUT OF CONTENTS

LIST OF FIGURES

LIST OF TABLES

NOMENCLATURE

Δ	change	-
A	flow admittance	m^4
AEU	annual energy used	kWh
AU	periodic symbol for gold	-
C	cooling capacity	kW
Cp	specific heat at constant pressure	J/g˚C
η	efficiency	%
h	specific enthalpy	J/kg
H	system head	m
hr	operating hours	hrs
m_{CO_2}	mass CO_2 emissions	kg
ṁ	mass flow rate	kg/s
N	rotational speed	rev/min
P	power	kW
pd	pressure difference	Pa
ρ	density	kg/m^3
Q	flow rate	ℓ/s
RH	percentage relative humidity	%
T	dry-bulb temperature	˚C
T_{wb}	wet-bulb temperature	˚C
w_c	compressor work input	kW

x_1	total flow from chillers	ℓ/day
x_2	ambient temperature	˚C

ABBREVIATIONS

AC	alternating current
BAC	bulk air cooler
BEP	best efficiency point
COP	coefficient of performance
DB	dry-bulb
DC	direct current
EMS	energy management system
ESCO	energy services company
FP	fridge plant
HT	high transmission
HVAC	heating ventilation and air conditioning
IDM	integrated demand management
kW	kilowatt
LT	low transmission
MCC	master centre controller
MV	manipulated variable
NPSH	net positive suction head
PID	proportional integral derivative
PV	process variable
SCADA	supervisory control and data acquisition
SP	set point
TES	thermal energy storage
THD	total harmonic distortion

VSD	variable speed drive
WB	wet-bulb

CHAPTER 1: INTRODUCTION

[1]

South Africa's energy usage has been a key concern for the past six years. The mining industry is largely accountable for electricity consumed in South Africa. South African gold mines dominate as the deepest in the world. At these depths, underground conditions become difficult to work in and cooling is required. Additional cooling leads to an increase in electricity consumption. Cooling systems on South African mines are identified as having major energy-saving potential.

[1] http://nelspruitpost.co.za/179456/notice-interruption-electricity-supply-2/

1.1 ENERGY USAGE IN SOUTH AFRICA

The affects of the load shedding that occurred in 2008 is still felt economically in South Africa. During this period the mining industry could not hoist, or do any cooling and ventilation, and was forced to stop all underground operations. Energy consumers were forced to undertake energy investigations to prevent load shedding from recurring in South Africa in the near future [1].

The worldwide electricity demand is projected to increase by 33% between 2010 and 2030 [2]. The industrial sector consumes 37% of the world's total delivered electricity, more electricity than any other end user [2]. Eskom supplies 95% of South Africa's electricity [3], [4].

The 95% electricity sales can be split into the various sectors, as illustrated in Figure 1 [1]. From the 95% of electricity supplied by Eskom, 14.6% is consumed in mining activities and 23.8% in industrial applications [1], [3]. Mining activities play an important role, as South Africa's economy relies on the amount of minerals mined and processed.

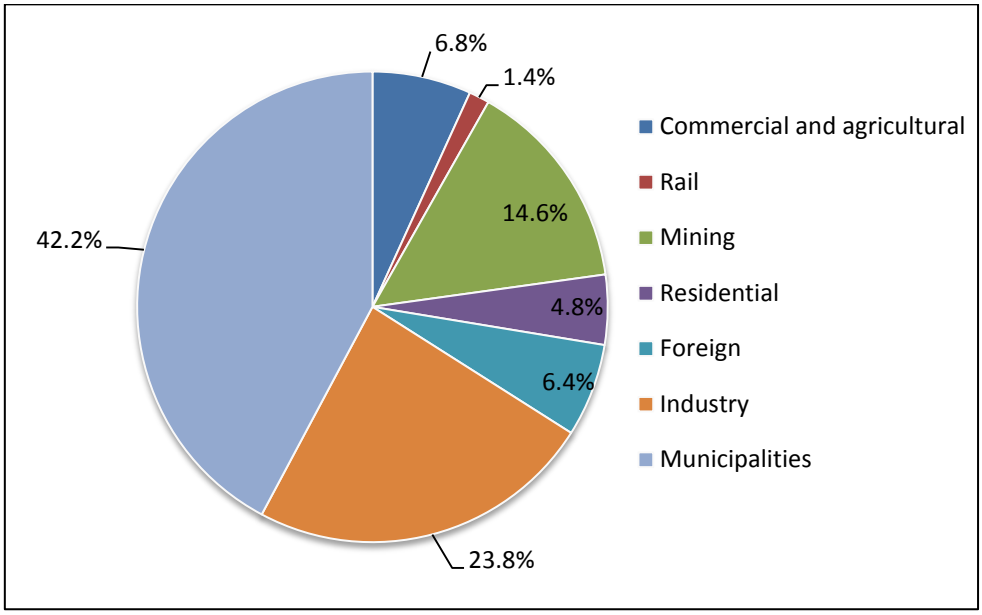

Figure 1: Eskom's electricity sales by customer for the year ended 31 March 2013 (adapted from [1])

Electricity distribution to rural communities is an inclusive growing economy and has led to an increase in South Africa's energy consumption [5]. South Africa's mass electrification programme from 2012 includes the distribution of electricity into rural areas. This increased the electricity demand and is expected to double by 2030 [5]. Industrial disputes in the

mining industry have caused major delays in mining production. In addition, the economy has been negatively influenced by this [6].

Energy management has become a great priority of the mining industry's top management [2]. Energy management is to minimise energy cost/waste without affecting production, product quality, and to reduce environmental effects [2]. There are four main sections that should be adhered to in energy management programs. They are firstly analysis of historical data, secondly energy audit and accounting, thirdly energy analysis and investment proposals based on viability studies, and lastly personnel training and information [2].

Time-of-use (ToU) is a time schedule developed by Eskom. This schedule can be characterised into peak-, standard- and off-peak hours. This schedule is further characterised into weekdays, Saturdays and Sundays for operations consuming more electricity on weekdays than on weekends. Eskom's focus is to reduce the electricity consumption during weekdays [7].

The schedule allows Eskom to force the industry into load management of their power usage from peak hours to off-peak hours. The mining industry falls under the Megaflex non-local authority tariff. The Megaflex tariff is seasonally and time-of-use differentiated [7]. The ToU Megaflex grid, under which mining operations are characterised is illustrated in Figure 2 [8].

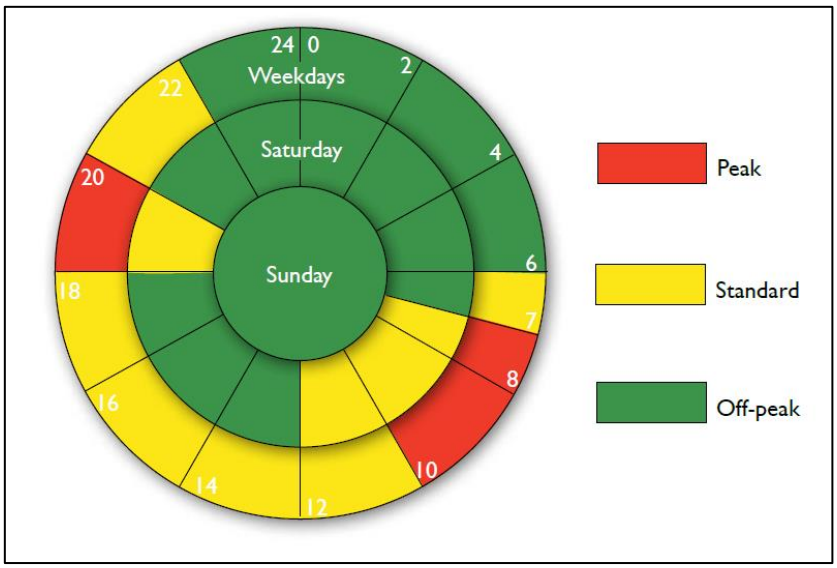

Figure 2: Megaflex time-of-use periods (adapted from [8])

Morning peak hours range between 07:00 and 10:00 and evening peak hours between 18:00 and 20:00. There are three integrated demand management (IDM) interventions, namely load

shifting, peak clipping and energy efficiency. Load shifting is when the electricity usage is shifted from peak hours to off-peak and standard hours. The daily consumed electricity remains the same, but the high peak tariff charges are avoided. Peak clipping is when the electricity consumption is reduced during peak hours, like load shifting. The difference with peak clipping is that the reduced load is not recovered as with load shifting [9]. Energy efficiency includes a decrease in daily electricity consumption [9], [10].

Studies in the USA have shown that it is more economically viable to conserve energy on existing electricity generation plants than to construct a new generation plant [11]. Eskom has an IDM programme that aims to lower the national electricity consumption. The IDM programme aims to lower the daily electricity usage through energy-efficiency programs.

Further IDM strategies include consumed electricity load shifted out of peak hours. This avoids the high electricity costs during weekday peak hours [12]. During the year ended 31 March 2014, an annualised energy saving of 19 GWh was achieved through new IDM projects [12].

Eskom has, in addition, an integrated energy plan to achieve a peak load reduction of 1.37 GW by 2015 and 5 GW by 2025 [13], [14]. Eskom further introduced a scheme that will reward and penalise customers based on their energy usage [14]. Eskom manages the electricity supply and demand and can therefore address the rising electricity demand in South Africa. In 2010 Eskom generated 44 175 MW of electricity. Additional electricity generated in South Africa was 2 400 MW from municipalities and 800 MW from private companies [14].

Non-renewable energy contributes to 85% of South Africa's electricity [1]. Energy reduction of the non-renewable sector will therefore remain significant for a few years to come. Eskom generates the majority of its electricity by burning coal. Using this process for generating electricity makes South Africa the 14th highest emitter of greenhouse gasses, one of them being CO_2 [14].

From 2003, rising electricity cost has forced mines to participate in energy-saving initiatives to stay competitive. South Africa's mining production increased by 3.1% in January 2014 calculated year-on-year [15]. Eskom makes use of Energy Services Companies (ESCOs) to implement IDM projects. The energy efficiency, peak clipping and load shifting projects are managed by these companies [13], [14].

Gold mines are the largest users of electricity in South Africa across all sectors [16]. Gold is one of three most important minerals mined in South Africa. Figure 3 shows the annual revenue per commodity in ZAR billion for the year ended 2013. This indicates an income of R70 billion for gold production in 2013[17] .

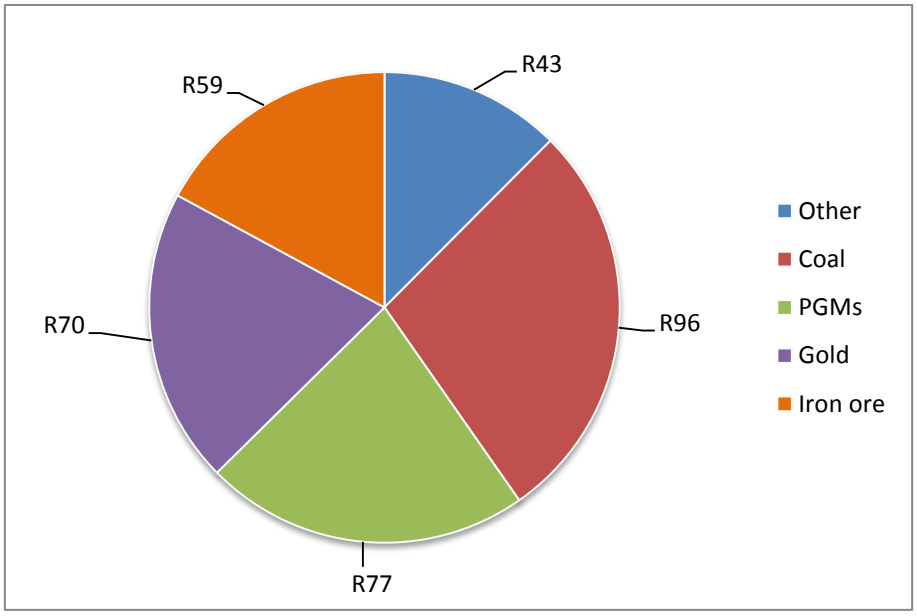

Figure 3: Annual revenue per commodity for 2013 in ZAR billion (adapted from [17])

There is still a significant amount of electricity-saving opportunities available within the mining sector in South Africa. Energy-saving management is of high priority to both the mining industry and Eskom. Energy consumption on the mines can be reduced, as long as production and quality are not affected. From Figure 3 it is evident that coal, non-renewable energy, accounts for an output of R96 billion. Non-renewable energy is therefore the primary energy source today and the consumption thereof should be managed [18].

1.2 SAVING POTENTIAL ON SOUTH AFRICAN MINES

Various energy consumers are found on South African mines. The gold-mining industry in South Africa is the largest energy consumer within the mining industry, consuming 47% of the industry's electricity [1], [19]. Before identifying saving potential on a gold mine, the mine's total energy usage needs to be broken down. The electricity usage breakdown of a typical gold mine in South African is illustrated in Figure 4 [19].

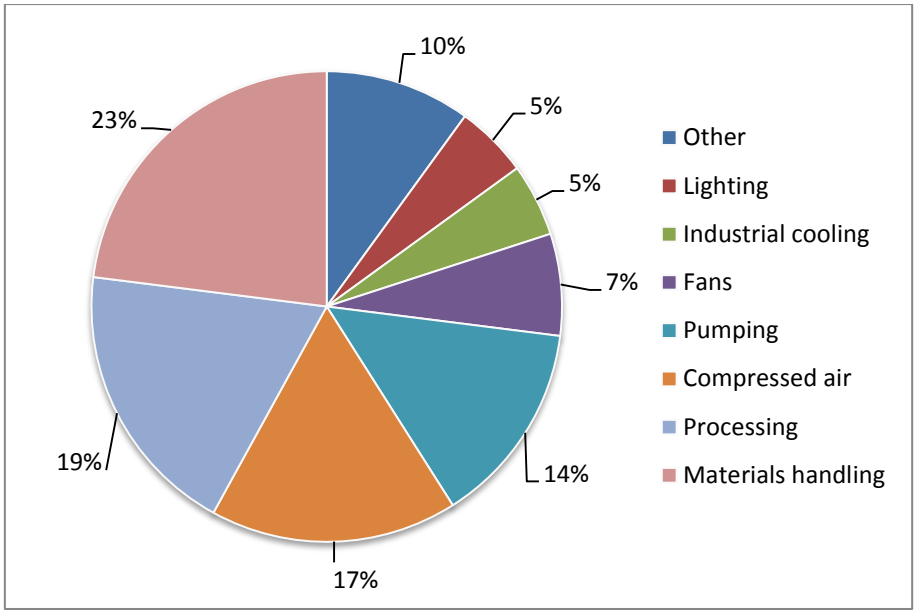

Figure 4: Electricity usage breakdown of a typical gold mine (adapted from [19])

The global mining industry is encouraged by government to move towards sustainable development [20]. Numerous investigations and energy saving projects have been implemented on compressed air networks. This is due to compressed air consuming 17% of the electricity on mines, as shown in Figure 4 [19].

Industrial cooling contributes to 5% of electricity saving potential on a typical gold mine. Fewer studies have therefore been performed on industrial cooling. However, the 5% electricity usage for industrial cooling amounts to a significant amount of a mine's annual electricity bill [21]. This presents an electricity cost-saving potential on industrial cooling. Cooling methods used on mines include air cooling, water cooling and ice cooling [22].

Not only has South Africa experienced an energy crisis, but also a water supply shortage. The mining industry accounts for 2-3% of the water demand in South Africa [23]. One ton of processed ore typically requires between 300 and 700 litres of water [20], [22]. Water usage should therefore be maintained and controlled.

Up to 42% of energy consumed on a deep level gold mine can be attributed to the water reticulation system. Recent studies performed on water reticulation systems showed 13% cost-saving in mining electricity. The chillers, underground water supply and de-watering system forms part of the water reticulation system [24].

Pumping and cooling of mine water are the main contributors to energy usage of the mine's water reticulation system. Studies have shown that 30% to 50% of energy consumed by pumping systems can be saved through control system changes [25]. Various cost-saving strategies have been implemented on the cooling and ventilation of deep level mines.

When cost-savings are suggested, it is important to look at the possible savings of the equipment lifespan. The pump efficiency can have an effect on the amount of energy consumed to pump a certain head. A more efficient pump consumes less energy to pump the same head than a less efficient pump [26].

Pumping cleaner water reduces wear and tear on pipes and pumps and indirectly reduces maintenance cost. Mine water could be re-used to save on water cost. Processes to treat reused water includes filtration, clarification, evaporation, ion exchange and electro-dialysis [20]. Maintenance should regularly be done on pipelines, pumps and equipment where build-up can occur. This maintenance ensures more efficient pumps and compressor equipment and expands the equipment's lifespan [26].

In order to develop a sustainable mining industry, energy efficiency must be increased and water usage reduced. The reduction in energy and water can be induced by improving the water network design [20].

1.3 DEEP LEVEL GOLD MINE COOLING

South Africa is leading as one of the largest gold-producing countries in the world [27]. In 2013 South Africa was the sixth largest gold-producing country, with 145 million ton produced [28]. South Africa was the world's largest gold producer in 2006 and accounted for 11.2 % of global production [27], [29]. From 2002 to 2011 South Africa produced an annual average of 274 tons of gold [30]. A gold sale of R68.8 billion was achieved in 2011 [30].

Gold mining is the backbone of South Africa's economy and therefore sustained development thereof is important for South Africa's future. Large capital investments and specialised equipment is required on deep level gold mines [31]. Development in the technical capacity of deep level gold ore has made South Africa a world leader in deep level mining technology [27]. This led to gold mining in South Africa becoming more capital intensive. One gram of gold is the result of 0.42 tonnes of processed ore [32].

Long lead times are associated with the development of deeper mines until the actual production of gold is seen [31]. For this reason mines have to manage their capital investment in such a manner that it will be sufficient until production starts [31]. The energy used to mine one ton of gold increases as the underground depth increases [16].

Most of the gold within 1 km below surface has been mined, and mines have followed gold reefs to great depths. South Africa is home to the world's deepest gold mines [33]. In some cases gold mine depths in South Africa can be in excess of 3.8 km below the surface [34]. Plans are being made to mine as deep as 4.5 km below the surface in the near future [34]. The depth of today's mines requires that shaft systems have to be split into two or three stages before reaching the bottom.

As the underground depth increases, the virgin rock temperature increases. One of many health risks that corresponds with working under high temperature conditions is heatstroke. Workers mining in extremely hot conditions underground are more at risk of accidents occurring. The productivity of underground workers decreases as the underground temperature increases [35]. Figure 5 illustrates the statement above [36].

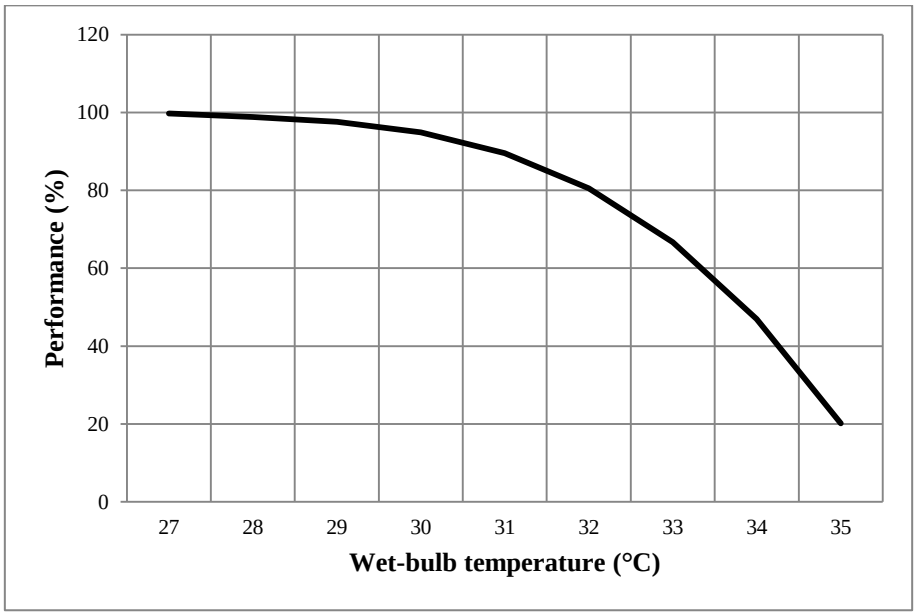

Figure 5: Underground worker performance as a function of underground conditions (adapted from [36])

In Figure 5 the work conditions of between 27 ˚C and 32 ˚C wet-bulb to deliver a work performance of between 80% and 100% can be seen. This ensures that workers work for up to eight hours underground to produce a sustainable gold production rate. Within the mining industry in South Africa, the maximum wet-bulb temperature in working areas is limited to

27.5 ˚C for sustainable mining at 100% workforce performance [1], [24], [21]. Wet-bulb temperatures are used as reference, as it is the most significant variable affecting body cooling [37].

At depths of 3.8 km, virgin rock temperatures can rise up to 67 ˚C [34]. It is therefore important to have sufficient water cooling and air ventilation on deep-level mines. Not only is surface refrigeration therefore required, but underground cooling facilities also need to be in place. Integrated cooling systems typically consume 23% of the total electricity used on deep level gold mines exceeding depths of 1600 m [38]. The contribution to the underground heat load can be broken down into the following sources, as illustrated in Figure 6.

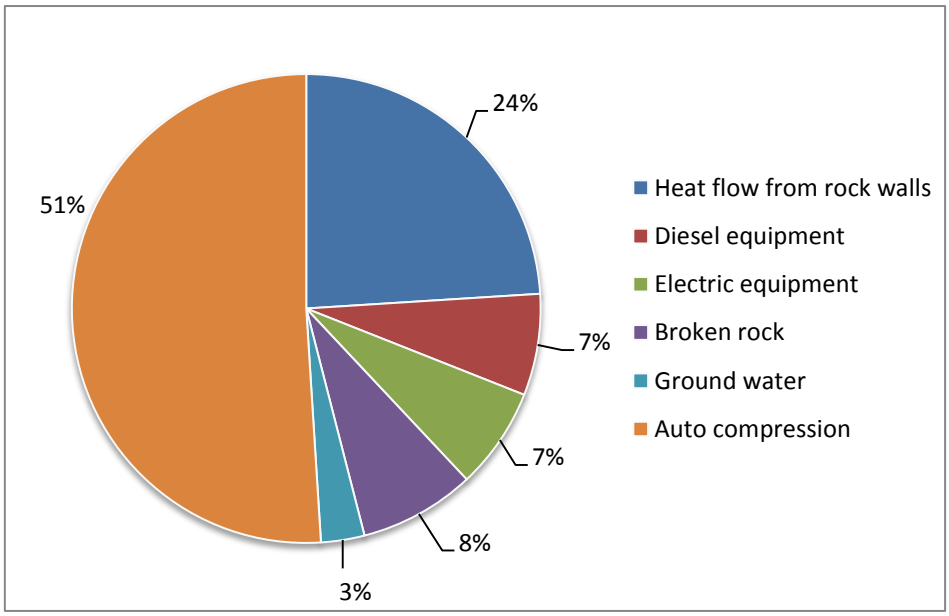

Figure 6: Underground heat contributions, excluding the impact of surface changing temperature (adapted from [39])

To keep underground conditions within limits, large refrigeration systems are found on deep level mines. Refrigeration systems supply chilled service water and cooled air for underground cooling and ventilation purposes. More capital is therefore required for ventilation, cooling, hoisting and underground tunnelling on deep level mines [27]. Furthermore, as mines deepen, electricity and maintenance costs increase [40].

Keeping underground conditions safe should be regarded as the number one priority when performing energy-saving studies on surface cooling systems [41]. As the mine depth increases the efficiency of the surface bulk air cooler (BAC) is lost. The bulk air cooler is used for underground ambient cooling and ventilation. At these depths it is more cost

effective to use underground air cooling [22]. As mines deepen, different cooling methods are required. Table 1 shows the virgin rock dry-bulb temperature and cooling required when reaching a certain depth [22].

Table 1: Dry-bulb virgin rock temperature and cooling method versus depth on deep level mines [22], [42]

Depth (m)	**Virgin rock DB temperature (˚C)** [42]	**Cooling method**
0 – 100	28	Ventilation system only
600 – 1000	34	Surface BAC conventional
1000 – 1400	39	Surface BAC ultra-cold
1400 – 1900	43	Surface chillers
1900 – 2000	46	Underground air cooling
2000 – 2500	50	Underground chillers
2500 +	60	Ice from surface

Going beyond 2 km below surface, underground chillers (often referred to as fridge plants on a mine) are more cost effective than surface chillers. This is due to the energy loss in the distribution of the cold water from the surface and pumping it back. The increase in mine depths led to various advanced cooling methods. Skilled workers are required to operate and maintain these refrigeration systems. Additional personnel are also required to optimise the refrigeration system, indirectly reducing energy usage [22].

In the twenty years post 1994 the number of unskilled mining personnel decreased by 71 %. The reason for the reduction is the restructuring of the gold-mining process and the movement towards newer technology [31].

Mechanised mining is one of today's major aspects in the gold mining industry. It is estimated that mechanised mining will expand the lifetime of the gold-mining industry. This enables industry to mine lower-grade ore and employ smaller groups of skilled and productive workers. Other developments forming part of the mechanised mining focus on trackless mining, backfilling and hydro power [27].

For underground workers it is vital to ensure that machines operate under their manufacturing temperature limits [24]. It will therefore be important to continue underground cooling, even though mechanised mining is taking over labour-intensive mining.

Newer technologies on the deep level mines are sending hard ice and crushed ice to underground ice dams. On a deep mine, ice is sent underground at 120 tons per hour to ensure cooler conditions [34]. This use of technology for underground cooling has shown remarkable energy-saving results. However, the ice process requires chilled water at 5 ˚C to produce sufficient ice [40].

It is important that the underground workforce performs at its best without being affected by unbearable temperatures underground, in order to maintain the high gold production that South Africa delivers for a sustainable economy. Chilled water is required underground, be it for machines operating underground or labour-intensive mining. There is however a question between two surface methods used for water cooling on deep level mines. The question will be addressed in the following section.

1.4 RESEARCH QUESTION

Refrigeration systems are used to chill water on deep level mines. The chilled water is used for cooling the underground environment. In 2006 the procedure of thermal ice storage on mine cooling systems was used to chill water on deep level mines. By this time, various thermal ice storage systems have been implemented on the air-conditioning of buildings. South Africa was the first and today the only country that makes use of thermal ice storage on deep level mines [43].

Presently only two mines in South Africa utilise thermal ice storage systems for underground cooling. A study was undertaken on the thermal ice storage system on one of these mines. The mine where the study was conducted will from hereon be referred to as Mine M. There are two methods of cooling underground water on Mine M, and will be referred to as method A and method B.

Method A includes glycol chilled with a York chiller and sent through pipes into an ice dam filled with water. Ice forms on the outside surface of the pipes. Chilled water is pumped over the ice, melting the ice before it is sent underground. Method B includes a York chiller that

constantly delivers cold water to a storage dam. Chilled water is fed by gravity from the storage dam to underground.

Research is required and comparisons have to be made to determine the most energy-efficient method for underground cooling. Factors that need to be compared are average energy usage, energy cost-savings, water temperature to underground and chiller performance. This study will determine if it is more energy efficient to use method A or method B.

1.5 OVERVIEW OF STUDY

Chapter 1

A background of South Africa's energy usage is given. The contribution of the mining industry to the electrical energy consumed in South Africa is briefly discussed. South African gold mines dominate as the deepest in the world. Additional cooling is therefore required on these deep level mines. Additional cooling leads to an increase in electricity consumption and cost. Cooling systems on South African mines thus have major energy-saving potential.

Chapter 2

Underground conditions are kept below maximum wet-bulb conditions through refrigeration systems. At a certain depth underground, refrigeration is required. This chapter focusses on two surface refrigeration systems used on deep level gold mines. One process is chilled water refrigeration and the other process includes thermal ice storage.

Chapter 3

An overview of the refrigeration system on Mine M is given. A savings approach is investigated, followed by a simulation model based on the savings approach. Simulation results indicate an energy-saving potential for the refrigeration system of Mine M. This strategy includes the conversion of the ice storage system to a chilled water system. Furthermore, ways of controlling the refrigeration system is described.

Chapter 4

From the energy strategy there are changes to be implemented on the refrigeration system of Mine M. Results of the existing thermal ice storage system are shown. Results after implementation are given. The amount of energy savings achieved by operating a chilled

water system rather than a thermal ice storage system is determined in this chapter. Varying the water flow through the chillers with a VSD also resulted in additional energy savings.

Chapter 5

This chapter conveys the conclusion and recommendations of this study. It is concluded that converting an ice storage system to a chilled water system resulted in energy efficiency.

1.6 CONCLUSION

Eskom requires South Africa to reduce their electricity usage. IDM projects contributed to a large extent to energy savings for the year ended 31 March 2014. There is however a significant amount of potential energy savings available. Eskom has a target to reduce the power usage by 5 GW by 2025. At the moment, Eskom places their focus on reducing energy consumption during weekdays.

South Africa's economy mainly depends on the gold-mining industry. The need to sustainably supply electricity to gold mines is therefore of great concern. There is however numerous opportunities to reduce the energy consumption on a deep level gold mine, particularly the refrigeration systems. It was investigated and determined that cooling contributes to 23% of electricity consumed on typical gold mines exceeding a depth of 1600 m.

Gold mines are forced to mine deeper in order to maintain production rates. It was found that the performance of underground workers decreases as the temperature underground increases. During the investigation of energy-saving projects, underground cooling requirements should therefore be the first priority. As underground depth increases, the cooling requirement also increases. Additional refrigeration leads to an increase in electricity consumption.

Investigation of the various methods used to chill water led to a particular question between two methods used to chill water. The first method produces ice to cool water and the second uses the traditional water-chilling method. The following chapter will discuss the processes in more detail.

CHAPTER 2: LITERATURE REVIEW

[2]

Underground conditions are kept within workable limits through the use of refrigeration systems. This chapter focuses on two surface refrigeration systems used on deep level gold mines. One process is chilled water refrigeration, and the other thermal ice storage. From research it is evident that insufficient research has been conducted on the ice storage systems in the industry. This led to a case study on the ice storage systems of a deep level mine.

[2] http://yayimages.com/photo/blog-web-design/melting-ice-cubes/image-5958904

2.1 INTRODUCTION

Mining in a deep level gold mine requires chilled service water to cool the rock surface temperature. The constant high virgin rock temperature underground, as discussed in Chapter 1, requires continuous underground cooling throughout the year. This enables underground workers to mine within workable conditions. Underground temperature does not fluctuate as much as ambient surface temperature. Surface ambient temperatures in the North-West province can drop as low as 4 ˚C dry-bulb temperature during the winter months. This enables the refrigeration system to decrease the load during the winter months [44].

Various types of cooling methods can be found on deep level mines. This chapter provides background on different cooling systems found on gold mines. As described in Chapter 1, certain cooling methods are required when a certain depth is reached.

Operating refrigeration systems efficiently is a constant challenge for any mining operation. Each mine's refrigeration system is unique and designed for the conditions on that specific mine. Refrigeration systems are designed to handle the worst temperature conditions found in the area where it's located. Potential energy savings on the refrigeration system can therefore be achieved during days when it's below the worst ambient temperatures.

For the past 54 years chillers have been used to chill water for underground activities [45]. Each chiller is designed to deliver the maximum amount of cooling. Most deep level mines therefore require more than one surface chiller.

The first glycol thermal ice storage system was introduced to the gold-mining industry in 2006 [43]. This concept and technology have successfully been implemented on the air-conditioning systems of buildings. However, thermal ice storage is new to mine cooling and results are therefore limited. Other ice-cooling methods include sending soft ice and hard ice to the underground storage dams. This method of cooling is only used on mines that are deeper than 3.5 km.

The simplicity and accessibility of surface cooling systems has forced various underground chillers to be disabled [46]. Although various underground cooling systems are available, this study will focus on the surface refrigeration system.

2.2 CHILLED WATER REFRIGERATION SYSTEMS

Background

The use of chilled water refrigeration systems keeps underground conditions within workable limits. Different sources of cooling are used on mines for underground cooling. Chilled surface water is used in drills and for dust suppression [46]. The mine's total cooling capacity is used during the summer months when ambient conditions reach up to 36 ˚C dry bulb, in the North-West [47].

The cooling capacity of 1.0 ℓ/s of water sent underground at 4 ˚C requires refrigeration of 100 to 120 kW [46]. On deep level mines that require large refrigeration, the circulating costs of the chilled water sent underground can justify replacing it with ice [46]. Taking the latent heat of fusion of the ice into account, sending ice underground increases the cooling capacity of 1.0 ℓ/s of ice with 400 kW refrigeration. Using ice reduces the amount of water that needs to be pumped back to the surface [46].

The depth where surface ventilation alone no longer provides sufficient cooling is approximately 600 to 800 m underground [22]. Spot coolers are used underground and serves as miniature standalone heat exchangers, which absorb heat from the air and then transfer it to the water. Spot coolers can deliver a cooling capacity of up to 500 kW refrigeration [46].

Underground return air is required as discharge air for the underground condensing circuit [48]. Return air enters at high temperatures and humidity throughout the year. This prevents load reduction on the underground units during the winter months [48].

The cooling capacity of hard ice can remove 4.5 times the heat load as the same flow of chilled water. A reduction in mass flow can be achieved due to the latent heat capabilities of the ice [40]. Hard ice is sent to the underground storage dams to lower the water temperature. Cooling underground dams reduce the return pumping cost from underground to surface refrigeration machines. Maintenance on underground systems tends to be greater than on surface refrigeration [48].

Various cooling components used on mines include:

- pre-cooling towers,

- chillers,
- condenser towers, and
- bulk air coolers (BACs).

These components are linked to each other. Each component has a different purpose in the refrigeration system. The functionality and purpose of each component follows below. A layout of a typical refrigeration system used on a gold mine is illustrated in Figure 7.

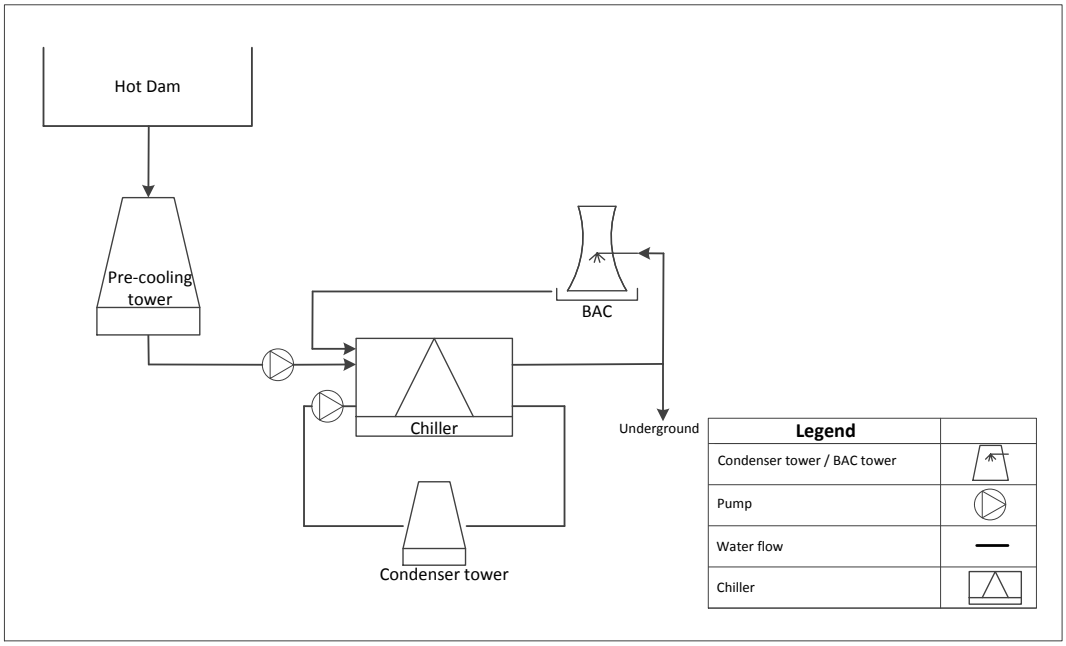

Figure 7: Typical mine refrigeration system

Pre-cooling towers

The pre-cooling tower makes use of surrounding air to directly extract the heat from the warmer water to the colder ambient air. Hot water at around 26 ˚C is sent from underground. Water in a pre-cooling tower is distributed in the tower through nozzles, splash bars or film type fills. These distribution methods expose a large contact area of the water to the ambient air. Surface ambient air is displaced through the tower by means of fans, convective currents, wind currents and through the induction effect of the spray [49].

Pre-cooling towers are used on the surface to cool hot water from underground before entering the refrigeration system. The efficiency of a pre-cooling tower is affected by poor water quality and broken fans. Maintenance on the pre-cooling system is performed during the winter months when pre-cooling is required less and more cooling capacity is available in

the system [50]. Pre-cooling towers can cool the water within 3 to 6 ˚C of the ambient wet-bulb temperature [49].

The determining factor for the amount of water that can be cooled is restricted by the amount of water pumped from underground. The maximum amount of water able to flow through the pre-cooling towers is a restriction on the number of chillers that can be used.

Chillers

There are two refrigeration cycles used in the industry. These are the vapour compression (shell-and-tube heat exchanger) and the ammonia absorption cycle (plate heat exchangers) [46], [51]. The major difference between the cycles is the way in which compression is achieved and the types of working fluids used. In the absorption cycle, low-pressure ammonia vapour is absorbed in water and the liquid solution is pumped to a high pressure. The low-pressure ammonia leaving the evaporator is absorbed in the weak ammonia solution as it enters the absorber.

During this absorption, heat must be transferred to the surroundings at temperatures slightly higher than the surrounding ambient temperature. The strong ammonia solution is pumped through a heat exchanger to the generator. In the generator a higher pressure and temperature is maintained to drive the ammonia vapour from the solution. In the evaporator the ammonia absorbs heat from the water, cooling the water.

The ammonia vapour goes to the condenser where it condensates before entering the expansion valve and evaporator. The weak ammonia solution is then returned to the absorber through the heat exchanger [51]. From here on forward, focus will be placed on the vapour compression cycle.

In the ideal vapour compression refrigeration cycle, illustrated in Figure 8, refrigerant changes phase during the cycle. Refrigerant refers to the working substance in the vapour-compression refrigeration cycle. Halogenated hydrocarbons, trade names Freon and Genetron, have been the principal refrigerant for many years. Refrigerant needs to be chemically stable at ambient temperatures. Chillers use refrigerant in a cycle to cool down water that is sent underground [46].

Generally the ideal cycle is used to analyse the vapour compression refrigeration cycle. However, the actual refrigeration cycle differs from the ideal cycle. In the actual refrigeration cycle, pressure drops occur due to fluid flow and heat transfer to and from the surroundings. Other deviations from the ideal cycle are pipe lengths and pipe insulation [49].

Three important considerations when selecting refrigerant are the temperature at which the refrigeration is needed, the type of equipment to be used and whether it will be used for surface or underground refrigeration. On the condenser side of a heat exchanger, water is usually used as heat transfer medium to remove heat from the refrigerant [49].

The refrigerant undergoes a phase change during the heat transfer and heat rejection process. During these phases the refrigerant is in the saturation pressure. Low pressures mean large specific volumes, likewise large equipment. High pressures mean smaller equipment that is able to withstand high pressures.

The type of compressor used has a particular behaviour on the type of refrigerant used. Reciprocating compressors are normally used for low specific volumes at high pressures. For high specific volumes at low pressure, centrifugal compressors are most suitable. The work related between process 1 to 2 and 3 to 4 is adiabatic and therefore isentropic [51].

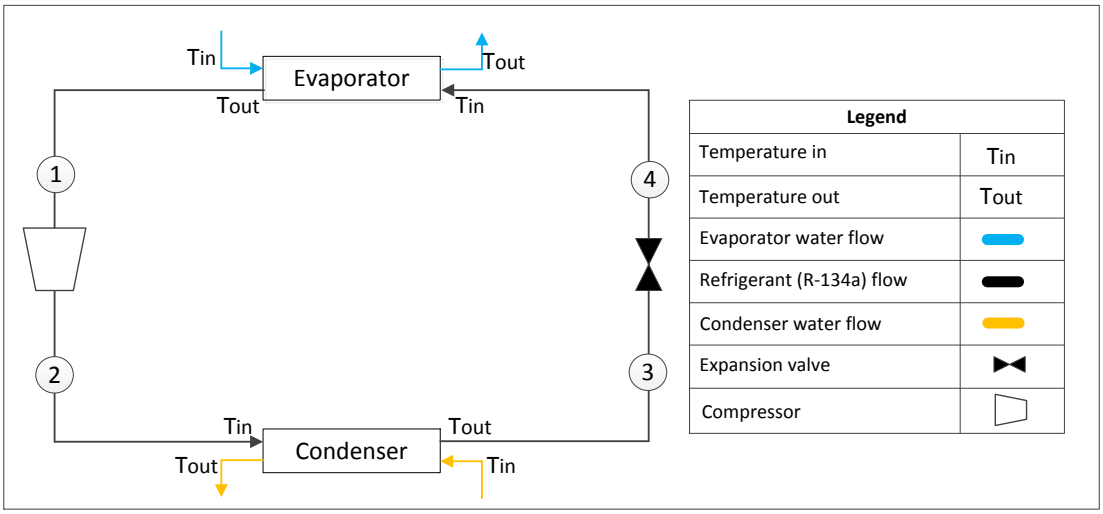

Figure 8: Ideal vapour compression refrigeration cycle (adapted from [51])

In Figure 8, the vapour entering the compressor, process 1, will be superheated. During the compression phase a heat transfer to or from the surroundings can occur due to the nature of the surroundings and refrigerant. A heat transfer to the refrigerant, process 4, causes an

increase in entropy, whereas heat transfer from the refrigerant causes a decrease in entropy, process 2 [51].

The pressure of the liquid leaving the condenser, process 3, will be less than the pressure of the vapour entering. The temperature of the refrigerant in the condenser will be higher than the surroundings. On a typical mine refrigeration system, condenser water is the source for transferring heat to and from the water to the surroundings. Normally the temperature of the liquid leaving the condenser is lower than the saturation temperature [51].

An expansion valve is placed between the condenser and evaporator. The valve expands the high pressure of the refrigerant to a low pressure. Refrigerant entering the evaporator has a low enthalpy, process 4. This allows for more heat to be transferred to the refrigerant in the evaporator. A slight pressure drop occurs as the refrigerant flows through the evaporator [51].

Refrigerant leaving the evaporator may be superheated. Due to the temperature around the piping between the evaporator and compressor, a temperature increase occurs in the refrigerant. The temperature increase indicates a loss due to the compressor work increasing, since the fluid entering the compressor has an increased specific volume.

A chiller operates within design constraints. Failing to operate within these limits could result in pipes bursting and components malfunctioning [22]. The measure of the performance of a chiller is rated using the term coefficient of performance (COP). The COP of a chiller indicates the amount of cooling capacity achievable (C) against the compressor work input (w_c). The COP calculation is shown in Equation 1 [52].

$$\boldsymbol{COP = \frac{C}{w_c} = \frac{h_1 - h_3}{h_2 - h_1}} \quad (1)$$

Condenser tower

A condenser tower is a heat rejection device that extracts heat from water to the atmosphere. The type of heat rejection is termed evaporative, due to a portion of water evaporating into the atmosphere as the air moves through, providing significant cooling to the rest of the water. Heat transferred from the water to the airstream raises the air temperature and its relative humidity to 100% [53]. The thermal performance of a cooling tower depends on the entering air's wet-bulb temperature [49].

Hot water enters the condenser tower at the top and is fed onto packing known as fill. The fill creates a cascade of water droplets as the water hits the fill. The fill increases the contact surface of water for efficient heating of the air and evaporation to take place [53].

Figure 9 illustrates a typical temperature relationship between the air and water in a counter flow condenser cooling tower. As the temperature of the water drops, a wet-bulb temperature rise in the air leaving the tower is seen. The wet-bulb temperature drop of the water from point A to B is called the range. At steady state the range of the tower will be the same as the temperature rise through the heat exchanger [49]. The range is determined by the heat load and water flow rate through the heat exchanger.

The difference between (B), the leaving water temperature, and the entering air's wet-bulb temperature (C) is called the approach, illustrated in Figure 9. A larger cooling tower delivers a closer approach, a colder leaving water temperature for a given heat load, flow rate and entering air condition [49].

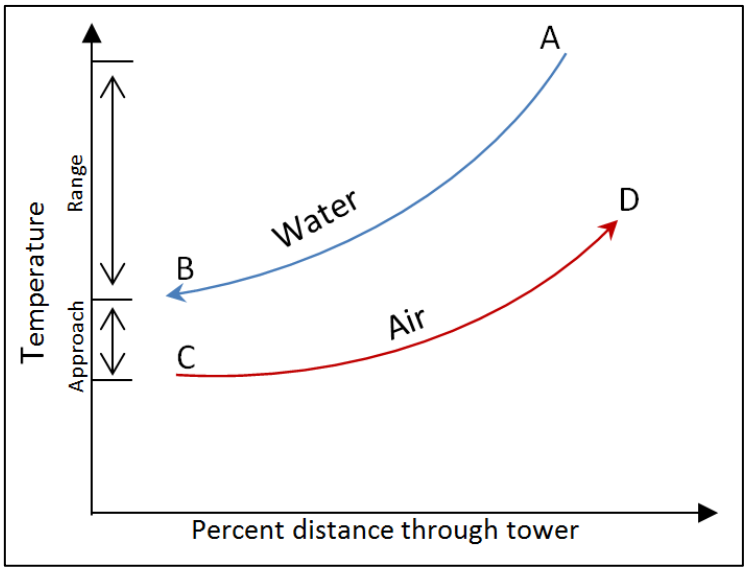

Figure 9: Temperature relationship between air and water in a counterflow cooling tower (adapted from [49])

Indirect or closed cooling tower circuits involve no direct contact between air and water. They are normally used in cases where a water or glycol mixture is cooled [53]. The thermal capability of a cooling tower is defined by the temperature of water entering and leaving, wet-bulb temperature entering the tower and water-flow rate [49]. The amount of heat transferred from the water to the air is proportional to the enthalpy difference in the entering and leaving air.

Condenser towers used on mine refrigeration cycles are used in a closed loop with the condenser side of the chiller. Most cooling towers used on mines make use of open-circuit cooling towers. In an open-circuit cooling tower there is direct heat extraction from the water to the air occurs, also known as a direct contact evaporative cooling tower [53]. A good rule of thumb is to operate one condenser tower for each operating chiller[3].

Bulk air cooler (BAC)

The main purpose of a BAC is for underground cooling and ventilation. Ventilation provides sufficient air to all underground working stations [46]. Ventilation air dilutes the unwanted contaminants, such as dust and gases in the underground air [54].

BACs are normally located near the shaft. This allows for less heat loss in the cooled air sent underground. In a BAC, heat is transferred from the warmer ambient air to the chilled water. Chilled water normally enters the BAC at 4 ˚C [55]. BAC fans ensure that chilled air is blown underground at 7 ˚C. Extraction and ventilation fans are operated on the outlet air side of the underground to extract the warm and humid air [54].

In the BAC, water in the air condensates due to chilled water being cooler than the surrounding air. Condensation occurs at the surrounding dew-point temperature. Air less humid than the ambient air is therefore sent underground. Through the condensation, some water is thus added to the BAC sump. Depending on the ambient conditions, the discharged air at the extraction fan is not always 100% saturated [56].

Underground temperature is measured in wet-bulb temperature. Dry-bulb temperature and relative humidity is measured and converted to wet-bulb temperature using Equation 2 [57].

$$T_{WB} = Tatan[0.151977(RH + 8.313659)^{1/2} + \text{atan}(T + RH) - \text{atan}(RH - 1.676331) + 0.00391838(RH)^{3/2}\,\text{atan}(0.023101RH) - 4.686035 \quad (2)$$

Pump affinity laws

There are two major classes of pumps used in water processes, namely the centrifugal pump and the rotary positive displacement pump [58]. This study will focus on the operation of a

[3] Dirk Botha_Chiller Foreman_Anglogold Ashanti
Cell: 083 332 3713 Email: dbotha@anglogoldashanti.com

centrifugal pump. If the speed of a pump is increased with 10%, the volume flow increases with 10%, the power with 33% and the head with 21% [59].

If we can therefore reduce the flow with 10%, a 33% electricity saving can be achieved [2], [59]. Equation 3 shows the relationship between the impeller velocity and pump power [59], [60]. Power is therefore proportional to the cube of the motor speed [61]. Subscripts 1 and 2 represent the value before and after respectively.

$$\frac{P_1}{P_2} = (\frac{N_1}{N_2})^3 \quad (3)$$

Refrigeration system control

The first refrigeration system controlled to minimise electricity cost and load shift during peak hours was implemented in 2005 [62]. Replacing old refrigeration equipment is avoided in times of economic pressure. Energy therefore needs to be saved on present equipment, inherently saving cost. Capital savings can then be used to invest in new equipment.

There are presently two IDM initiatives that can be performed on the refrigeration systems. The one initiative is load shifting of the fridge plants. This includes shifting the refrigeration load from morning- and evening peak to the standard- and off-peak hours. This is done through ensuring that there is enough chilled water storage available to be able to meet demand during peak hours, without having to start a chiller. The chillers should also be able to deliver enough cooling water during standard- and off-peak hours to meet the demand and at the same time fill the storage dams.

The second initiative is energy efficiency. Energy efficiency is the reduction of the electricity demand over a 24-hour period. This is done through controlling the power consumers to deliver only the required outputs. Lowering the flow through the evaporator and condenser will increase the time for heat exchange to take place. This will result in reduced back pass to the evaporator, at the same time meeting the required water demand [63].

Shorter distances between cooling systems have shown less heat loss through the piping system [48]. Distributing chilled service water in insulated pipes prevents unnecessary chilled water heat loss [22].

Variable speed drives

A variable speed drive (VSD) is an electronic power converter that generates a multi-phase, variable frequency output. The VSD frequency output is used to drive an alternating current induction motor, control and modulate the motor's speed, torque and mechanical output [2]. Pumps not running at full speed expand the lifespan of the pumps and bearings [64], [61].

A VSD adjusts the rotational speed of the pump. By regulating the speed, the pump will continuously try to maintain pressure within the system at a prescribed level by adapting to an optimum flow rate [65].

To date the variable speed control is the most cost-efficient way of adjusting pump performance. The pump power reduces as the pump speed is reduced [61]. The most popular VSD is the variable frequency drive (VFD). The VFD controls the motor (rotational or impeller) speed of an alternating current electrical motor by adjusting the voltage and frequency applied to the motor [58].

Bearings operating at reduced speeds last longer than bearings operating at full speed. The VSD characteristically soft starts the motor. This soft start expands the lifespan of the bearings and motor and reduces the motor's belt wear and tear [2]. Soft starting ensures that the motor is brought up to its running speed without an abrupt start, placing less mechanical stress on the motor [61]. Over a period of time this ensures less maintenance required on the motor. VSDs optimise pump efficiencies and pump control [58].

VSDs control the pump flow and therefore control the pump pressure. In most cases pressure management in water supply systems has proven to reduce water loss [61]. VSDs have successfully been tested on centrifugal pumps [61].

Pressure control on water supply systems is where the operating pump performance constantly adapts to the actual demand pressure. VSD pump control results in lower leakages, lower electricity consumption and increases the pump lifespan [61]. The implementation of VSDs on water supply systems with negligible demand variation results in minor savings [61]. Other uses of VSDs are for efficient control of fans in industrial and commercial boilers [66].

The required pump power (P) to drive the pump increases as the flow rate increases, as illustrated in Figure 10. The $NPSH_R$ is the minimum absolute pressure that has to be present

at the suction side of the pump to avoid cavitation. The net positive suction head required ($NPSH_R$) increases as the flow (Q) increases, and decreases as the flow decreases [61].

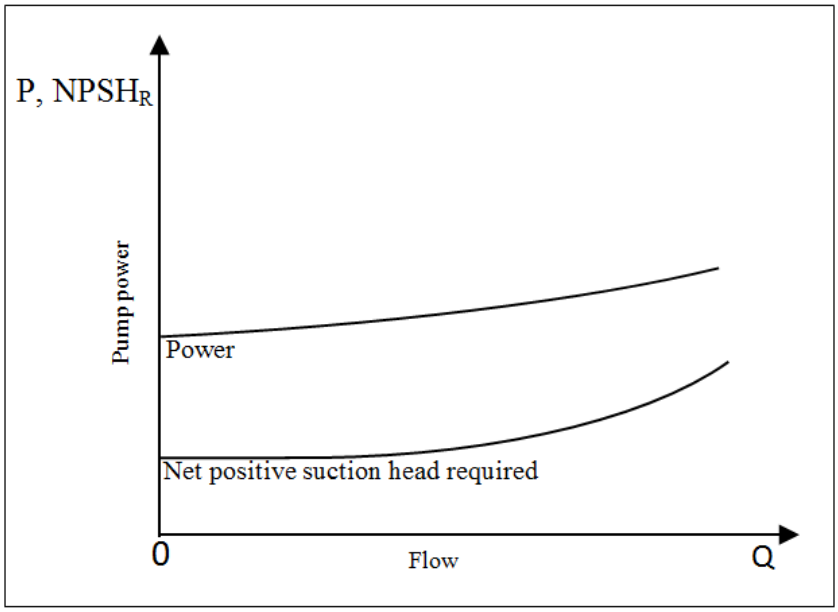

Figure 10: Power of centrifugal pump versus flow (adapted from [61])

A 50 Hz frequency is equal to the motor at full speed and 0 Hz frequency to the motor not operating. As the frequency is reduced, the motor speed also reduces. The VSD on the evaporator can be controlled by dam level or evaporator outlet temperature. The VSD on the condenser can be controlled through temperature difference across the condenser tower or ambient enthalpy [61].

Figure 11 represents the performance of a typical centrifugal pump with constant revolutions per minute (rpm), N. The flow is the independent variable Q, whereas the pump head is symbolised by H and the pump efficiency by η. The QH-curve in Figure 11 represents the head that the pump can deliver at a certain flow [61].

The pump efficiency is always zero at no-flow and increases to a maximum, 80-90%, peak at about 0.6 Q_{max}. At point Q^* the best efficiency point (BEP) is achieved at $\eta = \eta_{max}$ [61]. Good practice on the operation of a centrifugal pump is to operate it within 15% from its BEP, as illustrated in Figure 11 [58].

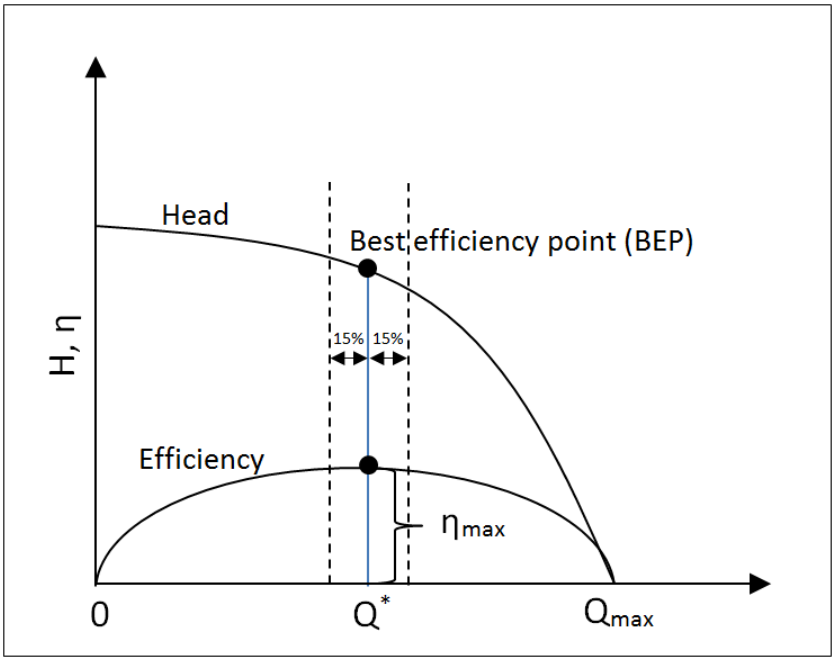

Figure 11: Typical centrifugal pump performance curves at constant impeller-rotation speed (adapted from [58])

Harmonic distortion is the degree to which a waveform deviates from its pure sinusoidal curve [67]. An ideal sine wave has zero harmonic components [67]. The total harmonic disturbance (THD) on a voltage sine wave gives a percentage as result. The higher the percentage, the more distortion is present on the main lines. The upper limit on voltage harmonics is set at 5% THD and 3% THD for any single harmonic. Keeping low THD values ensure proper operation of equipment and a longer equipment lifespan [67].

Full automation of a refrigeration system includes temperature sensors, pressure sensors, flow meters, communication equipment and actuated valves [68]. Control on the chillers can be done through the programmable logic controller (PLC) [69]. If there are components on the chiller that are operating over the required specifications, the plant will trip to prevent major damages on the chiller.

In order to fully automate the chillers it is necessary for the plants to be shut down. Fewer chillers are required to operate during the winter months, due to low ambient wet-bulb temperatures [62]. Winter is therefore the season for mine refrigeration system automation and system maintenance, and an ideal time for implementations to be done on a refrigeration system [62].

Reduced carbon emissions

Reducing electricity consumption reduces the amount of CO_2 emissions. For every kWh reduced, 0.99 kg of CO2 emissions is reduced. The mass CO_2 saving achieved can be calculated using Equation 4 [70].

$$m_{CO_2} = 0.99(AEU) \tag{4}$$

2.3 THERMAL ICE STORAGE SYSTEMS

Concept

The concept of thermal energy storage can be illustrated by Figure 12. Scenario one indicates the ice storage time and cooling release time to be the same. Scenario two indicates a longer storage time, yet a large release of refrigeration cooling in a short period. Scenario three requires large refrigeration cooling to release a smaller amount of cooling over a longer period [71]. Thermal energy storage (TES) is a method used for adjusting the time difference between power supply and demand [71].

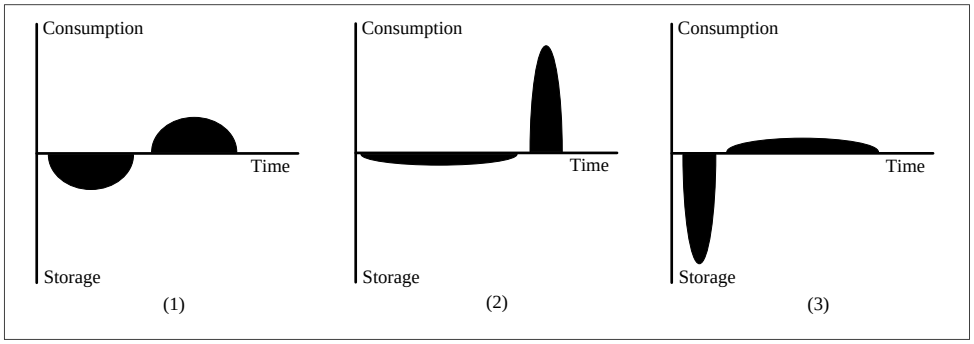

Figure 12: Concept of thermal energy storage (adapted from [71])

Thermal energy storage

Thermal energy can be stored in a material as sensible or latent heat [71]. The development of mine refrigeration systems is greatly influenced by the air-conditioning industry [46]. Thermal ice storage systems are used with vapour compression refrigerators. They were primarily devised to reduce energy cost by storing cooling capacity during off-peak electricity supply times [72].

Thermal ice storage systems have been developed for both air conditioners and drinks coolers [72]. The two common approaches to store thermal energy in buildings is through

active and passive systems [10]. Active systems make use of storage tanks filled with ice or chilled water during the night, which is discharged during the day. Passive systems use the thermal storage of the building mass to pre-cool the building at night so that stored energy can be released during day peak hours [10], [73]. Thermal ice storage is however recent technology that is implemented in the mining industry.

Ice production is classified as static or dynamic types. In static type ice storage, ice bonds on the cooling surface and in dynamic types ice is produced by removing it from a surface [71]. Ice storage used on the mine refers to static types.

Alternative ice-producing strategies

Mine M uses underground ice slurry storage dams to store enough ice to reduce the load on the refrigeration machines during peak hours [21]. Although the ice-producing plants are more expensive than the chilled water refrigeration plants, capital offset is regained through lower pumping costs, with reduced volumes having the same refrigeration capacity [21]. An ice slurry air-conditioning system usually employs three independent circuits, namely the ice slurry refrigeration circuit, a storage tank and a heat exchanger [71].

At Mine M ice slurry is produced by a vacuum freezing vapour compression process. Six units of 3 MW cooling capacity each are located on the surface, producing 4 200 tons of ice slurry per day cooling depths of 4 km below surface [21]. Each ice slurry unit consists of a 320 m^3/s vapour compression volumetric displacement with a compression ratio of 8:1 [73].

The results achieved with the ice slurry were compared to a conventional thermal ice storage system. The ice slurry consumed 22 MWh more electricity than the thermal ice storage plant. However, hydronic and air distribution cost of the ice slurry was found to be 47 MWh lower than the thermal ice storage. The ice slurry resulted in a 4% overall saving above the thermal ice storage system [73].

Previous studies on ice storage technology used in the air-conditioning of buildings resulted in a lowered air distribution temperature, from 15 ˚C to 12 ˚C [73]. A further decrease in the airflow from 41 m/h to 32 m/h was achieved. The reduced flow resulted in a capital and operating cost saving. The lower temperature potentially resulted in lower humidity and a more comfortable environment.

The Herbis Osaka building in Osaka (Japan) is an example of a crystal liquid ice thermal storage system with heat recovery, seen in Figure 13. The installations include 31 units of heat-recovery ice generators of 260 kW each and 16 sets of ice storage tanks, each with a 140 m^3 capacity. R-134a refrigerant is used in the refrigeration network of the ice slurry system.

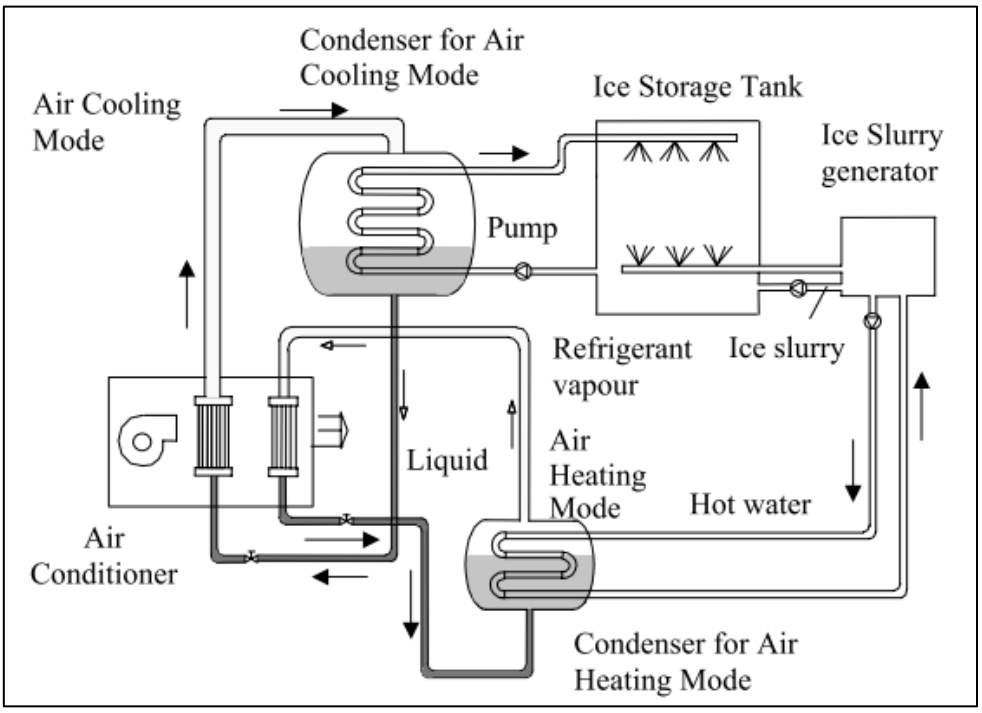

Figure 13: Herbis Osaka building thermal storage system [73]

Ice slurry cooling methods have been installed in many buildings for air-conditioning purposes [73]. Due to the successful results of ice slurry on building air conditioners, ice slurry was introduced to the industrial sector. The increase in mining depths showed great potential for ice slurry. Ice slurry has a four to six times greater cooling capacity than chilled water [74]. By using ice slurry, the same cooling can therefore be provided at a lower flow rate. This saves costs on pumping and the size of equipment used.

The potential energy stored in the water sent underground is lost as heat to the surroundings. A water temperature rise of 2.3 ˚C for every 1 km pipe extending underground has been measured [73]. Ice, on the other hand, will maintain its temperature when sent underground due to its latent heat capacity in melting [21].

In a vacuum ice maker, water is exposed to a deep vacuum to produce ice [21]. A small part of water is forced to evaporate by the vacuum, while the remaining water forms a water-ice

mixture. An ice concentrator is used to separate the water from the ice crystals. Condensation of vapour in the ice maker requires water at 5 ˚C. The 5 ˚C chilled water is supplied from a chiller [75].

Ice can however not be produced without cooling water. Chillers will therefore keep on producing chilled water for underground mining operations. Chilled water is also required for underground drilling, cleaning, dust elimination and air-cooling equipment.

Glycol strategy

Ethylene/propylene glycol systems freeze water by circulating chilled ethylene propylene glycol through tubes situated in a storage dam. During this process conventional shell-and- tube heat exchangers are used to chill the glycol. Instead of water flowing through the evaporator side, a 25% ethylene glycol and 75% water mixture is pumped through the tube side of the chiller. The -5 ˚C ethylene glycol mixture that enters the storage dam through tubes, freezes the water in the storage dam [76]. From here on forward the term glycol will be used when referring to the ethylene/propylene glycol mixture.

A glycol and water mixture at temperatures between -4 ˚C and -10 ˚C is circulated through a winding tube. The tube is submerged in an insulated tank of water for ice to form on the surface of the tube [74]. In the case of ice storage, where ice is melted, latent heat of fusion occurs. When water is sent across the surface, sensible heat is absorbed by the ice [71].

The ice storage tank consists of a low-pressure air pump or in some cases a paddle blade for agitation. The agitation ensures the even formation and melting of the ice. The ice thickness on the tube is measured with a sensor to control the operation [74]. The ice formation occurs in the ice storage tank, as illustrated in Figure 14.

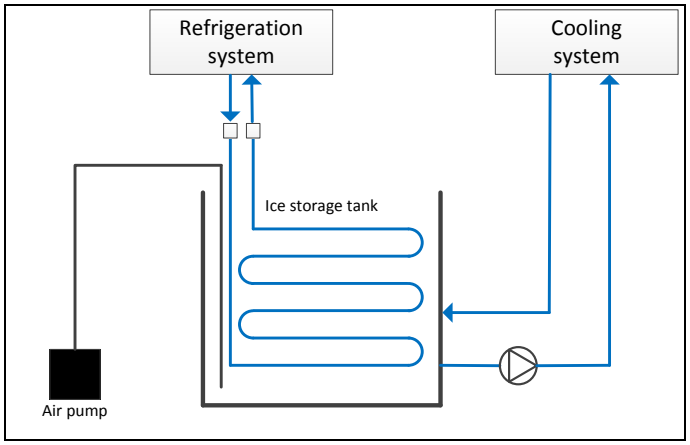

Figure 14: Ice formation on tubes concept (adapted from [74])

The glycol ice-producing machine is fixed in terms of design. This reduces the options to increase the efficiency of the machine. Chilled water systems on the other hand, are more acceptable to change. Equation 5 is used to calculate the cooling capacity of the chiller, where the specific heat capacity, Cp, is taken as the constant value (4.19 J/g ˚C) [49].

$$C = \dot{m}Cp(\Delta T) \tag{5}$$

Glycol is used as anti-freeze in the thermal ice storage system. The glycol is chilled to approximately -5 ˚C. The glycol moves through small pipes through a water dam. Ice starts to form on the outside surface of the pipes. In this process, glycol is chilled by the chiller. The glycol then forms ice and the ice is used to chill the water.

Glycol is food-grade antifreeze used in the chiller. It needs to be mixed with water according to a certain ratio to make it efficient as a coolant. If too much water is present it can freeze, causing the evaporator side to rupture. Too much glycol will reduce the chiller efficiency. Glycol costs R23.00 per kilogram and a typical glycol chiller is refilled with 215 kg of glycol per month[4].

The optimal load shift for ice storage is achieved with a 15 ton ice chiller. For any ice chiller lower than 15 ton savings are not realised. Ice ton chillers larger than 15 ton do not, however, provide additional load-shifting potential [77].

[4] Dirk Botha_Chiller Foreman_Anglogold Ashanti
Cell: 083 332 3713 Email: botha@anglogoldashanti.com

The time for the ice to form when the chiller is supplying the glycol at a certain temperature is seen in Table 2 [78]. The flow rate of the chiller is associated with a flow rate of a water chiller supplying a 2.8 ˚C range.

Table 2: Ice-build performance at various glycol temperatures [78]

Ice formation time (Hours)	**Required chiller temperature supply (˚C)**
8	< -5.5
10	-5.5
12	> -4.0

Various thermal energy storage methods exist to chill water for underground use. These methods have been successfully tested on building refrigeration systems. Fewer studies have however been performed on the thermal energy storage of deep level mines. Section 2.4 draws a glycol and water cooling comparison.

2.4 GLYCOL AND WATER COOLING COMPARISON

In ice-making systems, energy storage is higher than chilled water storage for a given volume. Ice storage systems however operate under less effective conditions compared to chilled water systems [71]. Thermal ice storage systems are new technology used on deep level mines and results of implemented studies are limited.

Recent research using ice storage systems is mostly used on building air-conditioning systems. People working in buildings do not operate on a 24-hour, seven days a week schedule as a mine does. In buildings, cooling is only required for a few hours a day when the building is occupied [79]. The results of a building air-conditioning thermal ice storage system cannot therefore be used as a thermal ice storage system of a deep level mine.

The case study on the implemented thermal ice storage system of Mine M resulted due to insufficient studies being done on mine thermal ice storage systems. Mine M operates option A (thermal ice storage system) and option B (chilled water system), as mentioned in Section 1.4. The results of simulation models and implemented site results will be explained in Chapters 3 and 4 respectively.

Figure 15 is an illustration of an ice storage system versus a chilled water system. The ice storage system uses one chiller to produce ice and one chiller to cool water, whereas the chilled water system has two chillers in parallel that produces chilled water to a storage dam.

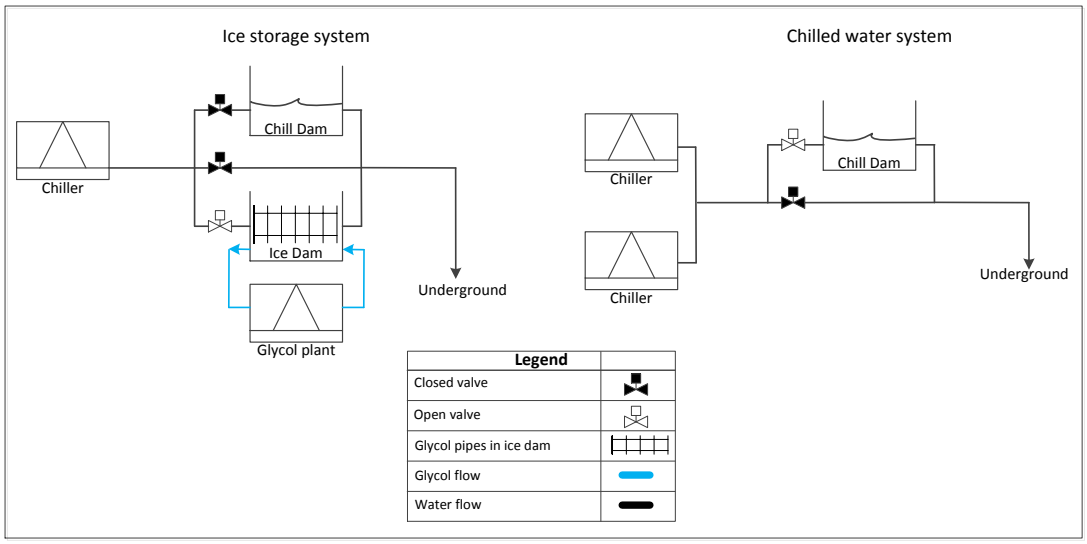

Figure 15: Ice storage system versus chilled water system

The aim of both these methods is to chill water for underground use. The difference is the routes it takes to chill the water. Different routes require different amounts of electricity. Furthermore, through the use of the two different routes, different amounts of energy are lost as heat to the environment.

2.5 CONCLUSION

Due to constant high underground virgin rock temperatures, underground water cooling is required throughout the year. Each mines refrigeration system is unique. However the fundamentals of energy-saving strategies can be applied to the refrigeration system of different deep level gold mines.

Each component in the refrigeration system is linked to each other and has a purpose to produce chilled water. If the cooling capability of one of these components is hindered, the effect will be realised throughout the refrigeration system.

Energy efficiency is achieved by reducing the flow through the chiller and indirectly reducing the pump power and compressor power of the chiller. It was found that a VSD can be used to reduce the frequency to the motor, reducing the flow produced by the pump. VSDs have

proven to deliver outstanding results in the energy-saving field. VSDs have proven to increase the lifespan of the pump motor and pump bearings.

The required time for ice formation is dependent on the glycol outlet temperature. At the lowest glycol temperature, sufficient ice formation can take up to eight hours. Limited research has been conducted on the thermal ice storage of deep level mines. Additional simulations and investigation approaches will therefore follow.

CHAPTER 3: CONVERTING AN ICE STORAGE INTO A CHILLED WATER SYSTEM

[5]

Different cooling systems are used on Mine M to keep underground conditions within workable limits. This chapter gives a system layout and description of the refrigeration system of Mine M. A savings approach and simulations will be developed based on the described cooling system of Mine M. Simulation results indicated the best energy-saving strategy on the refrigeration system of Mine M. This strategy includes the conversion of the ice storage system to a chilled water system. Ways of controlling the refrigeration system are furthermore described.

[5] D. Uys, Personal photograph. "8Mℓ chill dam and condenser cooling towers", West Wits, 2014.

3.1 INTRODUCTION

South Africa's deep level gold reefs 2 km below the surface are becoming exhausted by the day, as described in Chapter 1. The mine is forced to mine deeper in order to sustain production rates. Various surface refrigeration methods are available for underground cooling, as explained in Chapter 2. This chapter focuses on the refrigeration system of Mine M.

A case study was undertaken on the surface refrigeration of Mine M. Production on Mine M is 3.8 km below surface and going deeper. Virgin rock temperatures at Mine M reach up to 54.5 ˚C at 3.8 km below surface [21]. As the depth increases, the demand for underground cooling rises. Additional cooling requires more electricity, which focussed the study on the surface refrigeration system.

Water pumping represents 22% of Mine M's electricity bill [80]. On the particular refrigeration system, an average 30 Mℓ/day of water is cooled from 26 ˚C to 4 ˚C. The surface refrigeration system includes pre-cooling towers, condenser towers and chillers. The electricity cost to cool one litre of water is R0.0013. This totals R22 200/day per chiller operated on a summer day. High electricity costs force the mine to lower the energy consumption and increase the efficiency on the surface refrigeration system.

A York chiller in a closed loop is used in the surface refrigeration system to form ice in an ice storage dam. The York chiller cools glycol to below -5 ˚C. The glycol then passes through tubes with an inside diameter of 15 mm situated in a 2 Mℓ dam. The water in the dam forms ice around the tubes. Water from four Hitachi chillers is continuously sent through the ice dam, melting the ice on the tubes and sending it underground at 4 ˚C. A study was undertaken to compare the ice storage system, where glycol is cooled with a chiller, to water cooled with a water chiller system.

A savings approach illustrates the process flow and cooling delivered on the chillers. One year's data was collected from the mine and used for a thorough case study. Data from the mine was compiled into a simulation model that included a York chiller cooling glycol to form ice. This simulation was compared to a simulation of the York chiller cooling water.

Energy saving was realised by converting the ice storage system to a water chiller and varying the flow through the evaporator and condenser. The ice storage system is affected by other components, therefore a simulation of the whole surface refrigeration process was developed.

3.2 COOLING SYSTEM DESCRIPTION

Background

Gold Mine M is at 3.8 km below surface the world's deepest gold mine and continues to mine deeper. It has an installed refrigeration capacity of 76 MW that includes surface- and underground refrigeration equipment [21], [33]. The refrigeration system circulates 49 Mℓ/day of cooling water through the water-cooling system. Mine M has a life expectancy of 15 to 20 years from 2014 [33][6].

At Mine M, water from underground enters a surface hot dam at 26 ˚C. On average 30 Mℓ/day is pumped from underground to the surface hot dam. From the hot dam, water is gravity-fed through pre-cooling towers into the pre-cooling dam. Water in the pre-cooling dam is at 16 ˚C, within 4 ˚C of ambient wet-bulb temperature. The pre-cooled water is pumped to the evaporator side of four Hitachi chillers, coupled in parallel, to provide chilled water at 4 ˚C.

From the chillers, water is gravity-fed directly to the underground chill dams and working areas or surface chill dam and as make-up water to the BAC. A York chiller in closed loop cools a glycol and water mixture to -5.0 ˚C to form ice in the ice dam. A schematic of the surface refrigeration system is shown in Figure 16. System schematic layouts are used to understand the process flow and the interaction between the system components. The surface refrigeration plant consists of a chilled water plant and a closed-loop BAC plant.

Chilled water from four parallel Hitachi chillers flows into the dam. The glycol and water mixture moves through the tubes and creates an indirect heat exchange with the water in the ice dam to form ice. The load on the Hitachi compressors is lowered during peak hours. Water from the Hitachi plants is fed through the ice dam melting the ice on the surface of the tubes. From the ice dam, water is sent underground or used as make-up water for the BAC.

[6] Dirk Botha_Chiller Foreman_Anglogold Ashanti
Cell: 083 332 3713 Email: dbotha@anglogoldashanti.com

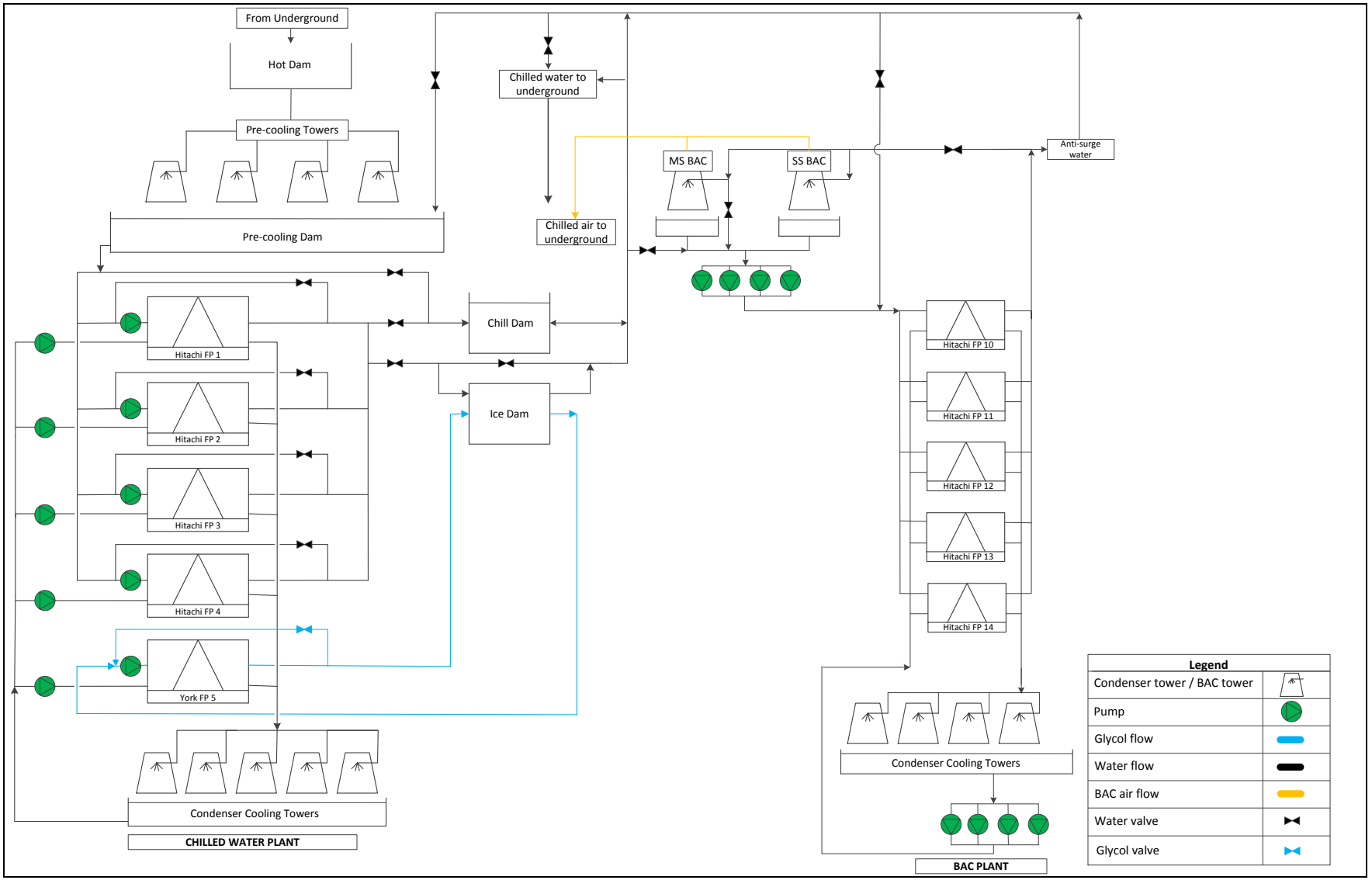

Figure 16: Schematic layout of a refrigeration system on Mine M

The mine only requires three chillers to run simultaneously. The extra chiller is available as backup. The mine requested the glycol chiller not to be removed from the system, but to be converted to a water chiller.

During the energy-saving investigation it was important to identify the layout of refrigeration equipment and how they are linked with each other. It was also important to know the specifications of the equipment used. The chilled water plant specifications of Mine M are shown in Table 3.

Table 3: Chilled water plant specifications

Description	Water	Glycol
Number of chillers	4	1
Make	Hitachi	York
Compressor type	Centrifugal	Centrifugal
Compressor motor rating (kW)	2 100	2 000
Refrigerant	R-134a	R-134a
Voltage (V)	11 000	11 000
Cooling capacity (kW)	10 500	10 500
COP	5	3.5
Evaporator outlet temperature (˚C)	7	-5.0
Condenser inlet temperature (˚C)	21	21
Evaporator water flow (ℓ/s)	330	300
Condenser water flow (ℓ/s)	500	520
Evaporator pump motor rating (kW)	75	160
Number of evaporator pumps	4	1
Condenser pump motor rating (kW)	160	275
Number of condenser pumps	4	1

Condenser

The condenser side of the chiller serves as an indirect heat exchanger between water and refrigerant. Water moves through the tube side counter-current to the refrigerant in the shell side. The water is pumped in a closed loop through a condenser tower. In the condenser tower water is sprayed from the top onto a fill that spreads the water before falling into a sump at

the bottom. The fill is used to increase the contact area of the water for better heat extraction with the air.

A fan at the top of the condenser tower draws ambient air from the side of the tower through the sprayed water and fill. Direct heat transfer occurs from the water to the air in the condenser tower. The surface condenser cooling tower specifications are shown in Table 4.

Table 4: Condenser cooling tower specifications

Description	Quantity
Number of cooling towers	5
Water inlet temperature (˚C)	25
Water outlet temperature (˚C)	21
Water flow (ℓ/s)	525
Air inlet wet-bulb temperature (˚C)	17

BAC

The BAC is closed-loop fed with chilled water from Hitachi chillers 10 to 14. The BAC closed loop receives make-up water from Hitachi chillers 1 to 4. Water is also fed to the anti-surge and back to pre-cooling. Investigations on the chilled water plant therefore led to further investigations on the BAC plant. Water is chilled with Hitachi chillers 10 to 14 and sent to the BAC to cool the air before being sent underground. The specifications of the chillers at the BAC plant are shown in Table 5.

Table 5: Chillers specifications at the BAC plant

Description	Water
Number of chillers	5
Make	Hitachi
Compressor type	Centrifugal
Compressor motor rating (kW)	1 350
Refrigerant	R-134a
Voltage (V)	11 000
Cooling capacity (kW)	10 500
COP	5
Evaporator outlet temperature (˚C)	3

Description	Water
Condenser inlet temperature (˚C)	21
Evaporator water flow (ℓ/s)	250
Condenser water flow (ℓ/s)	350
Evaporator pump motor rating (kW)	160
Number of evaporator pumps	4
Condenser pump motor rating (kW)	160
Number of condenser pumps	4

Water from the chillers is pumped to the top of the BAC. The water is then sprayed from the top onto a fill and into a sump. The BAC operates on the same principle as the condenser tower, however in the BAC direct heat exchange takes place from the air to the water. Air moves counter-current to the sprayed water and is blown underground with the BAC fans and distributed underground at 7 ˚C wet-bulb temperature by means of BAC fans. The BAC plant specifications of Mine M can be seen in Table 6.

Table 6: BAC plant specifications of Mine M

Description	Main shaft	Service shaft
Number of BACs	1	1
Water inlet temperature (˚C)	3	3
Water outlet temperature (˚C)	9	9
Water flow (ℓ/s)	460	100
Air flow (ℓ/s)	270	80
Air inlet wet bulb temperature (˚C)	17	17
Air outlet wet bulb temperature (˚C)	7	7
Pump motor rating (kW)	160	160
Number of pumps	4	2
BAC fans	4	1
BAC fan motor rating (kW)	160	160

3.3 THERMAL GLYCOL ICE STORAGE SYSTEM

The thermal ice storage system forms part of the refrigeration system on Mine M. A study on the energy-savings of the chilled water plant was directed to a study on the thermal ice storage system. A research question in terms of an energy-savings perspective is asked in Section 1.4. This study compares cooling glycol with a chiller to form ice and cooling water with a chiller.

The cost to cool one litre of glycol in a closed loop is R0.0012. Water is cooled from 13 ˚C to 7 ˚C in the Hitachi chiller. From here the water is continuously sent over the ice, melting the ice and is then sent underground at 3.5 ˚C. The cost to cool down one litre of water is R 0.0013. Thus the total cost per day to operate the glycol chiller and a water chiller to reduce the water temperature from 13 ˚C to 3.5 ˚C is R 50 500.00.

On the evaporator side, glycol is cooled through the expansion of R-134a. Glycol flows in a closed loop through a shell-and-tube heat exchanger. As explained in Section 2.3, glycol is antifreeze that Mine M mixes with water in a 30% glycol 70% water ratio[7]. The glycol and refrigerant flows counter current towards each other.

Glycol flows in the tubes and the refrigerant in the shell surrounding the tubes. The shell-and-tube heat exchanger used on a mine is illustrated in Figure 17. This figure illustrates the inside of the heat exchanger with one side open. Shell-and-tube heat transfer is indirect heat transfer. The cooling capacity of the York chiller is 5.5 MW with a COP of 3.5.

[7] Flip Stols_Chiller fitter_Anglogold Ashanti
Email: flipstols@gmail.com

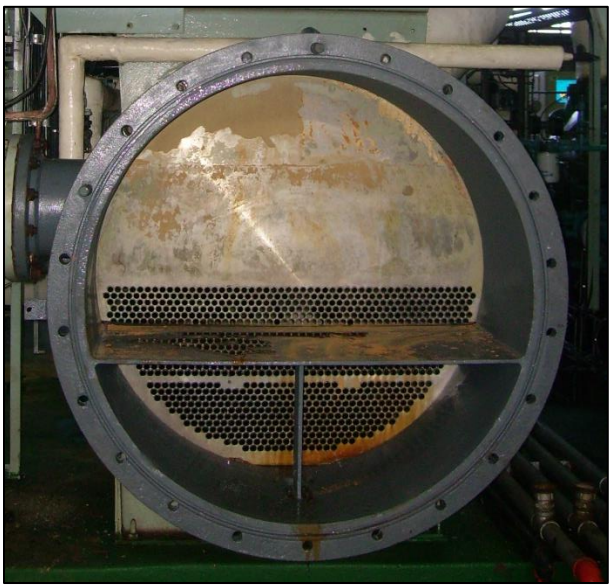

Figure 17: Shell-and-tube heat exchanger

On the condenser side, refrigerant is compressed before it enters into the shell side of the heat exchanger. Water enters through the tubes and heat is transferred from the refrigerant to the water. In the case of a York chiller, R-134a refrigerant is used. The water flows in a closed loop through the condenser and condenser towers. On an average summer day, water enters the condenser at 21 ˚C.

As the refrigerant expands, it undergoes a phase change. It changes from a compressed liquid leaving the condenser, to a gas as it flows through the expansion valve into the evaporator. Heat exchange occurs from the glycol to the refrigerant during the phase change.

Figure 18 shows the ice storage dam. The glycol leaves at -5 ˚C and flows through tubes of 15 mm in diameter. The tubes are layered in the 2 Mℓ dam, as shown in Figure 19. Water from four Hitachi chillers is fed into the storage dam. The water forms ice on the outside surface of these tubes.

The ice storage system can be used as electricity load shifting capacitor by means of recharging the ice storage during off-peak and standard periods [21]. During peak hours the Hitachi chillers can then be switched off whilst the evaporator pumps send water through the ice dam.

In the existing ice storage system there is a continuous flow of chilled water through the ice dam. Water is sent across the surface of the ice by means of the evaporator pump, melting the ice. This results in 3 ˚C chilled water being sent underground through the ice storage dam.

The thermal ice storage system was expected to reduce the peak demand by as much as 10 MW electricity savings.

Figure 18: Ice storage dam

In Figure 19 it can be seen that the tube system is divided into different blocks inside the dam. This is done to ensure that the tube structure fits into the circular-shaped dam. There are, however, various dead spots inside the dam where no ice formation occurs. There are also spots where ice build-up does not melt sufficiently.

Figure 19: Tubes where ice is formed in the ice storage dam.

As stated before, glycol is cooled to form ice and the ice is used to cool water in the ice storage system. Two indirect heat exchanges and one direct heat exchange occur during this process. Through this process, most of the cooling is lost to the surrounding environment. This technique of cooling resulted in an ineffective cooling method on Mine M.

Various problems in using the York chiller to form ice in the ice dam were encountered by the mine. These problems included the tube structure becoming buoyant in the water when ice formed on the tubes. This resulted in only the top layer of water being in contact with the ice.[8] This unplanned excessive build-up of ice on the tubes put strain on the structure.

Additionally, as the demand for underground chilled water increased, the amount of water flowing through the ice storage dam increased accordingly. This decreased the time for water to form ice around the tubes. There was therefore insufficient ice forming on the tubes. A lack of ice formation on the tubes resulted in warmer water being sent underground.

Figure 20 shows the chiller schedule on 2013-01-07 and the ice dam outlet temperature. From this figure it can be seen that the York chiller is operated throughout the day in addition to three Hitachi chillers. In Figure 21 the same chiller schedule can be seen with the flow to underground.

[8] Dirk Botha_Chiller Foreman_Anglogold Ashanti
Cell: 083 332 3713 Email: botha@anglogoldashanti.com

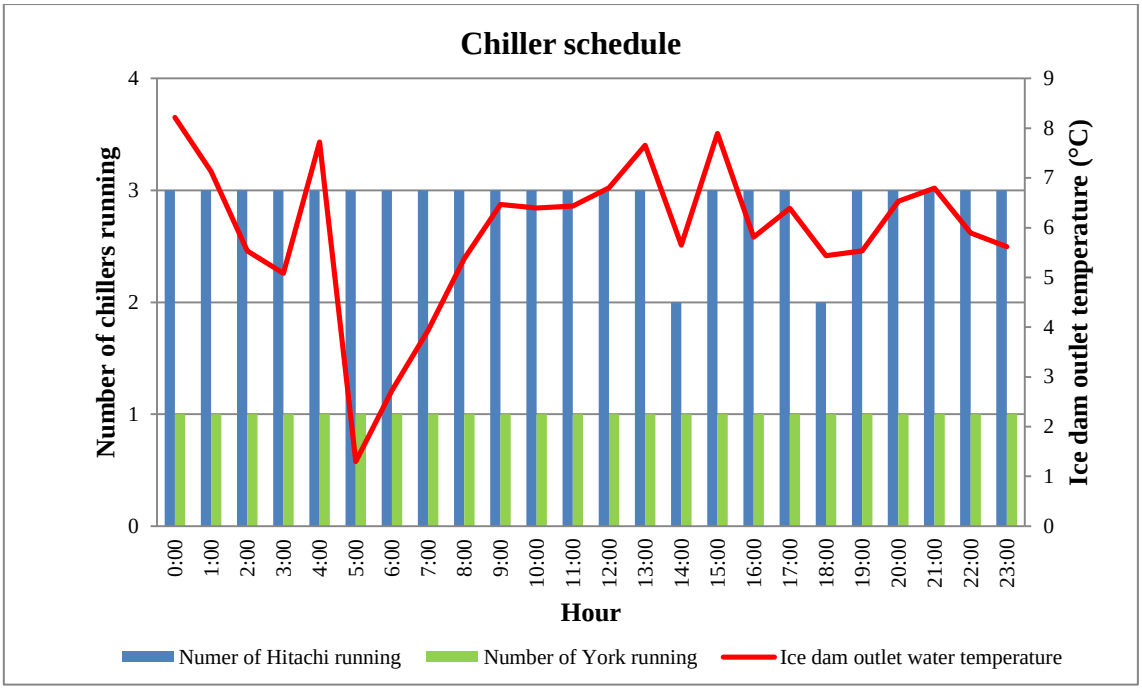

Figure 20: Chiller schedule and ice dam outlet temperature

If there is a delay in the continuous flow of water through the ice dam, the ice build-up around the tubes increases significantly. This build-up can rapidly get to a point where water flow through the ice dam is blocked by the ice. When this problem is encountered, the York machine needs to be switched off long enough for the ice to melt to a desired thickness before water can flow through again.

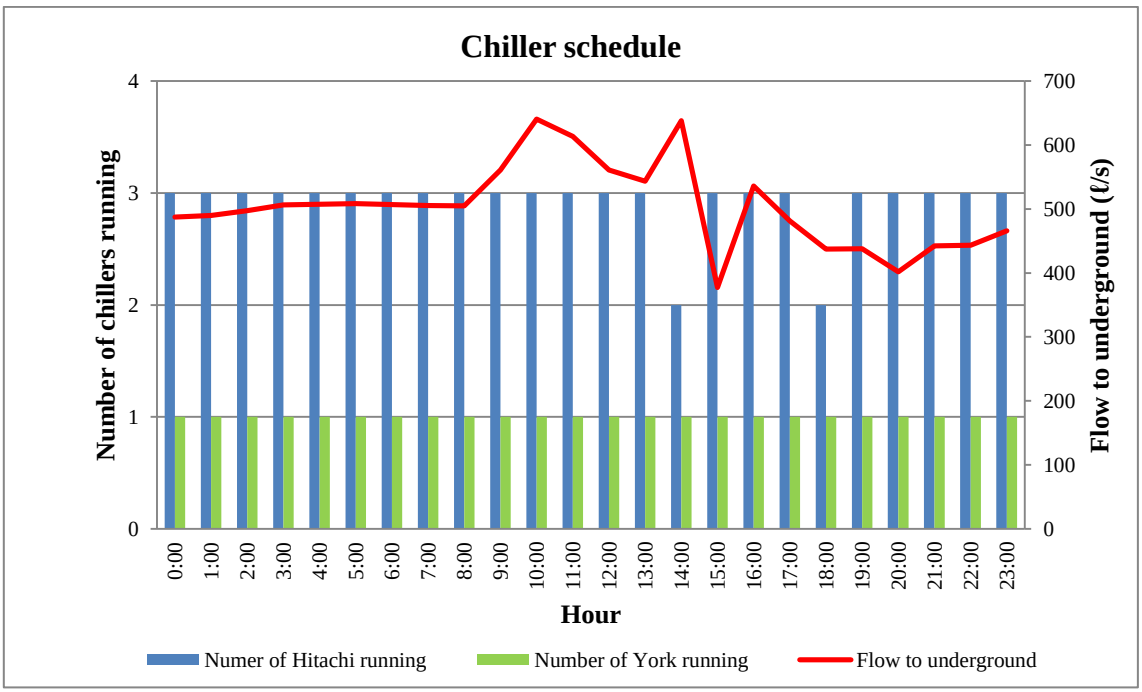

Figure 21: Chiller schedule and flow to underground

The temperature and flow to underground is well within the requirements. However, from Figure 20 and Figure 21 it is clear that no morning and evening peak load shift could be performed. This is due to the stated problem of high demand, resulting in insufficient ice build-up on the tubes.

3.4 ENERGY-SAVING STRATEGY

During the study, refrigeration data was collected from Mine M. The data included evaporator in and outlet temperatures, evaporator flow, condenser in and outlet temperatures, condenser flow, chilled water flow to underground, ambient temperatures, underground temperature and humidity, dam levels and refrigeration system power usage. Underground environmental conditions fully rely on the refrigeration system [62]. For this reason, no risks or compromises are accepted when implementing energy efficiency projects [62].

Dam levels, temperature and flow are measured with sensors. The input to the sensors is 12 V with a 4 - 20 mA feedback. For sustainable and accurate control, measuring sensors need to be calibrated on a yearly basis. The sensor output signals are an input to a Programmable Logic Controller (PLC).

A PLC is a controller block that consists of input and output cards. From the PLC an output signal is sent to the System Controlled and Data Acquisition (SCADA) system. The SCADA system is where the mine monitors and controls the refrigeration system and all other mining operations [69]. Figure 22 illustrates the SCADA layout of the pre-cooling section of Mine M. Control operators make use of the SCADA to monitor and control the refrigeration system. The SCADA has an archive that can store three month's historic data.

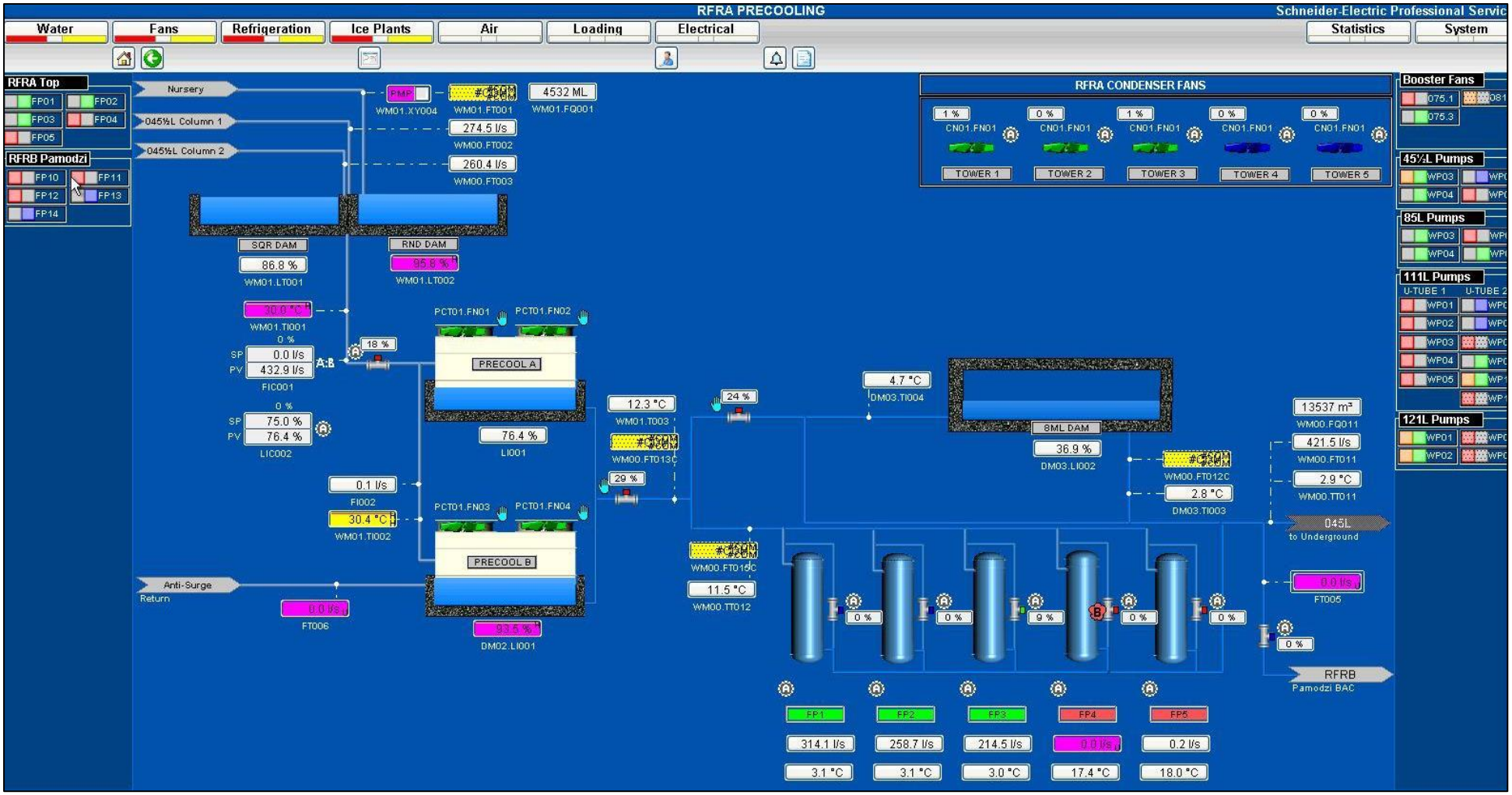

Figure 22: Mine M pre-cooling system and chillers' SCADA layout

When performing an energy investigation, the present energy consumption on the refrigeration system must be analysed. This is also used to identify whether the investigated savings are realistic. The electricity usage for the warmer months of 2013 is illustrated in Figure 23. The installed capacity on the surface refrigeration system of Mine M is 18 615 kW.

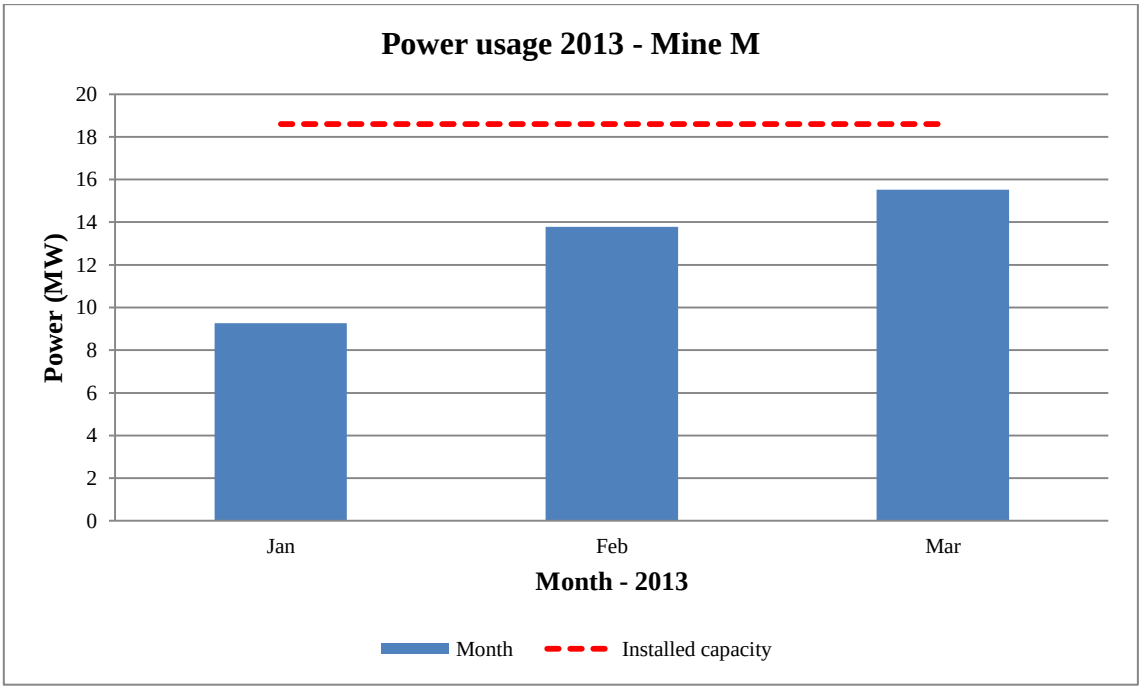

Figure 23: Mine M refrigeration total power consumption

Integrated demand management (IDM) implemented onto a large refrigeration system makes the system energy efficient whilst maintaining demand. In order to apply an IDM project to a refrigeration system, it is important to first understand the process as a complete system. There are different variables that need to be considered when undertaking an IDM project. For a thorough investigation it was important to collect sufficient data from the mine.

The mines inlet and outlet temperatures and flow conditions are gathered with a server installed on site and from the SCADA trends exported to CSV files. Underground flow data and temperatures are downloaded from the mines SCADA system. The total refrigeration power usage, except the BAC power, is logged by the mine in the feeder substation and sent via email.

The BAC is on a circuit with calibrated DENT-loggers installed on the Eskom incomers to log the BAC power data. Underground temperatures and relative humidity are logged by

means of Tiny Tag loggers. Photos of the DENT logger and Tiny Tag are shown in Appendix B, Figure 65 and Figure 67 respectively. Figure 66 in Appendix B shows the current clips of the DENT logger coupled onto the wiring inside the incomer.

Electricity is distributed from Eskom to an incomer substation onsite. Electricity enters a high transmission (HT) substation. The volts are stepped down with a transformer from HT to a lower voltage in the low transmission (LT) substation. Power to the pump is directly fed from a master centre controller (MCC) panel. The MCC panel is located in the LT substation. The MCC feeds the rated power to the specific pump.

Data is processed and calculations are performed on the data to determine the performance of the York chiller. This energy-saving case study is based on converting the glycol plant to a chilled water plant and comparing energy consumption results. The chiller power is logged and is thus available for the calculation. Equation 6 is used to calculate the cooling capacity of the chiller. Equation 7 is used to calculate the coefficient of performance of the chiller. Equation 7 is simplified from Equation 1 in Chapter 2. Cp is the specific heat capacity [52].

$$\boldsymbol{C = \dot{m}Cp\Delta T} \tag{6}$$

$$\boldsymbol{COP = \frac{C}{Chiller\ power}} \tag{7}$$

After studying the York as a water chiller in Section 3.3, a further energy-saving strategy came forth. The strategy includes coupling the York chiller in parallel with the other four Hitachi chillers to produce chilled water. From previous studies energy savings can be achieved by varying the flow through the chiller, as explained in Chapter 2.

From research in Chapter 2 the best alternative to automatically vary the flow whilst saving pumping distribution cost was through VSDs. Installing VSDs on the evaporator and condenser pumps of the York and Hitachi chillers at the chilled water plant was investigated as an energy reducer on the chilled water plant.

The VSD functions between the main centre controller (MCC) and the pump itself. The MCC panel delivers maximum power to the designed specification of the pump. However, the VSD gets a process variable (PV), compares it to a set point (SP) and adjusts the frequency to the pump accordingly. The PV is measured with sensors and connected onto a PLC that is displayed on the SCADA. The manipulated variable (MV) is done by writing an output from

the PLC. Thus the PLC gets a PV input, programmes an output to manipulate the frequency of the VSD so that the PV will strive to be as close as possible to the SP.

The VSD is controlled by means of PID control. The PV of the VSD control on the evaporator side is the evaporator outlet water temperature. The standard evaporator outlet water temperature SP of Mine M is 3 ˚C. The MV is the flow through the evaporator. Each chiller has a designed flow where optimum efficiency is achieved.

The lower the flow through the evaporator, the longer the time for heat exchange to take place. This results in additional heat transfer from the water to the refrigerant. The flow through the evaporator is controlled by means of the VSD frequency output to the pump.

If the evaporator outlet water temperature goes below SP, the output frequency of the VSD increases and vice versa. Higher frequency means more flow and lower frequency less flow. A layout of the suggested control for the refrigeration system of Mine M is shown in Figure 24.

The control of the VSD on the condenser motor makes use of PID control. The PV of the VSD control on the condenser side is the temperature difference across the inlet and outlet water temperature. The MV is the flow through the condenser side of the heat exchanger. The frequency output of the VSD manipulates the flow through the condenser side to maintain the temperature difference according to SP.

The temperature difference SP varies according to the capabilities of the condenser tower. During this control a SP of 6 ˚C across the condenser circuit is selected. As the temperature difference decreases, the frequency output of the VSD will also decrease. As the temperature difference increases, the frequency output of the drive will increase accordingly.

The VSD on the evaporator side of the BAC is controlled with the wet-bulb air temperature to underground as PV. The MV is the flow through the evaporator. The frequency output of the VSD manipulates the flow through the evaporator side to maintain the desired wet-bulb air temperature to underground. As the air temperature decreases to below SP, the frequency output of the VSD increases. As the air temperature increases above SP, the frequency output of the VSD decreases.

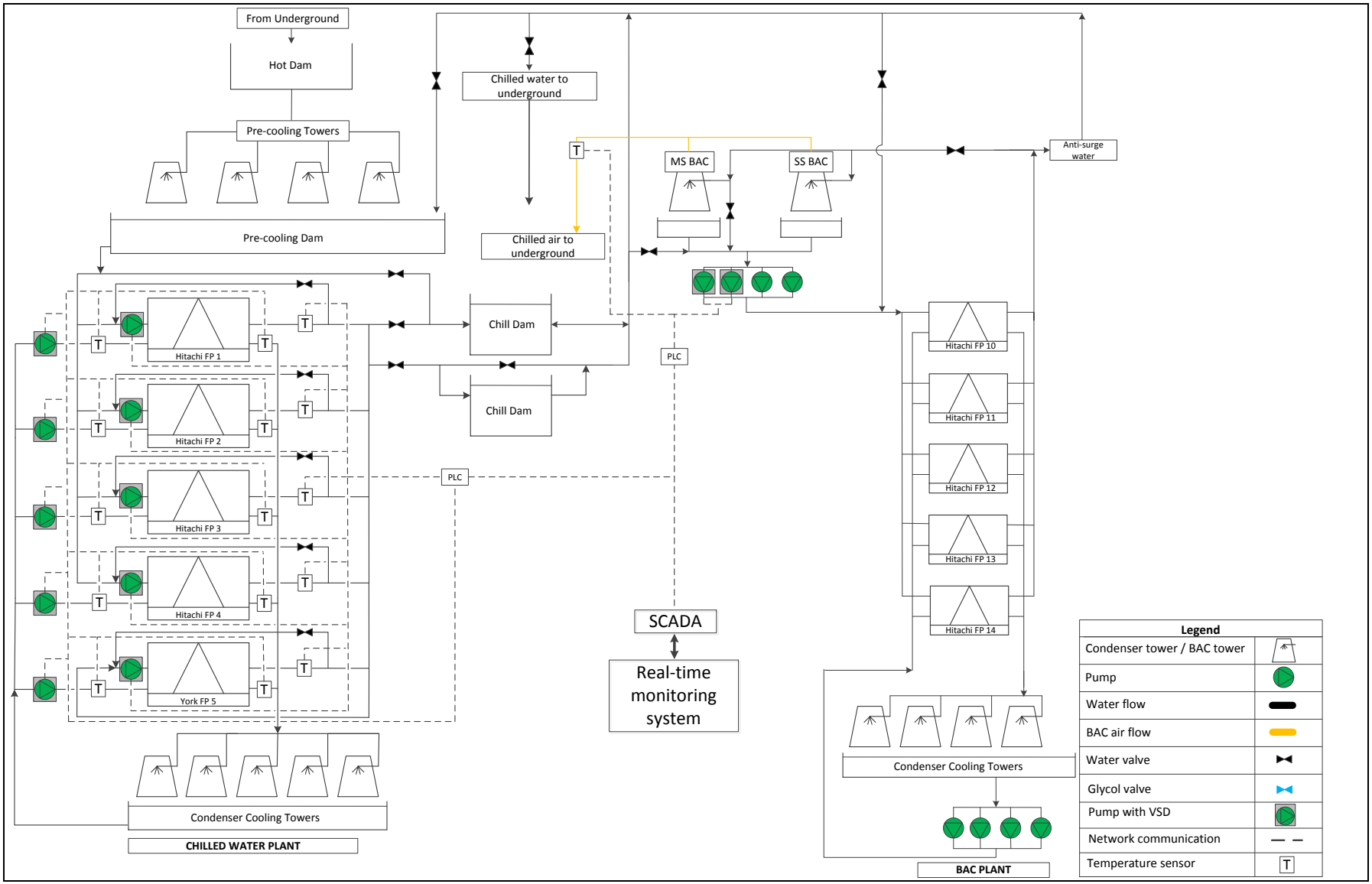

Figure 24: Surface refrigeration with decommissioned ice storage and VSD control

All the required data to control the fridge plant is logged into an energy management system (EMS). The EMS has input and output communication with the SCADA. The EMS monitors on a real-time basis and logs the data of the refrigeration system. Internal calculations can be made within the EMS software and can be written to the SCADA for control.

The control of the refrigeration system needs to be in place in order to establish an energy saving. The control of the equipment can be categorised into various steps of importance. The existing system operation is illustrated in Table 7. The flow through the evaporator of the existing system remains constant, as shown in Table 7.

The existing control strategy uses the chiller evaporator outlet temperature as the PV. From Table 7 it is seen that, as the evaporator outlet temperature rises above the SP, the first reaction is to fully open the guide vanes of the compressor, followed by opening the back pass valve. Guide vanes at 100% means that the compressor is working at maximum load. When the guide vanes of a chiller are below 40%, that chiller can be switched off. As the guide vanes close, the chiller compressor power reduces.

If the evaporator outlet temperature decreases below SP, the back pass valve closes and the guide vanes cut back. If the temperature keeps on reducing, the back pass will remain closed and the guide vanes will cut back to their minimum. The aim is to operate the chiller as efficiently as possible. On the existing control the best system efficiency will be produced when the guide vanes are fully opened and the back pass valve is closed. This results in maximum heat exchange without back-passing the chilled water to be cooled again.

Table 7: Existing control strategy on Mine M

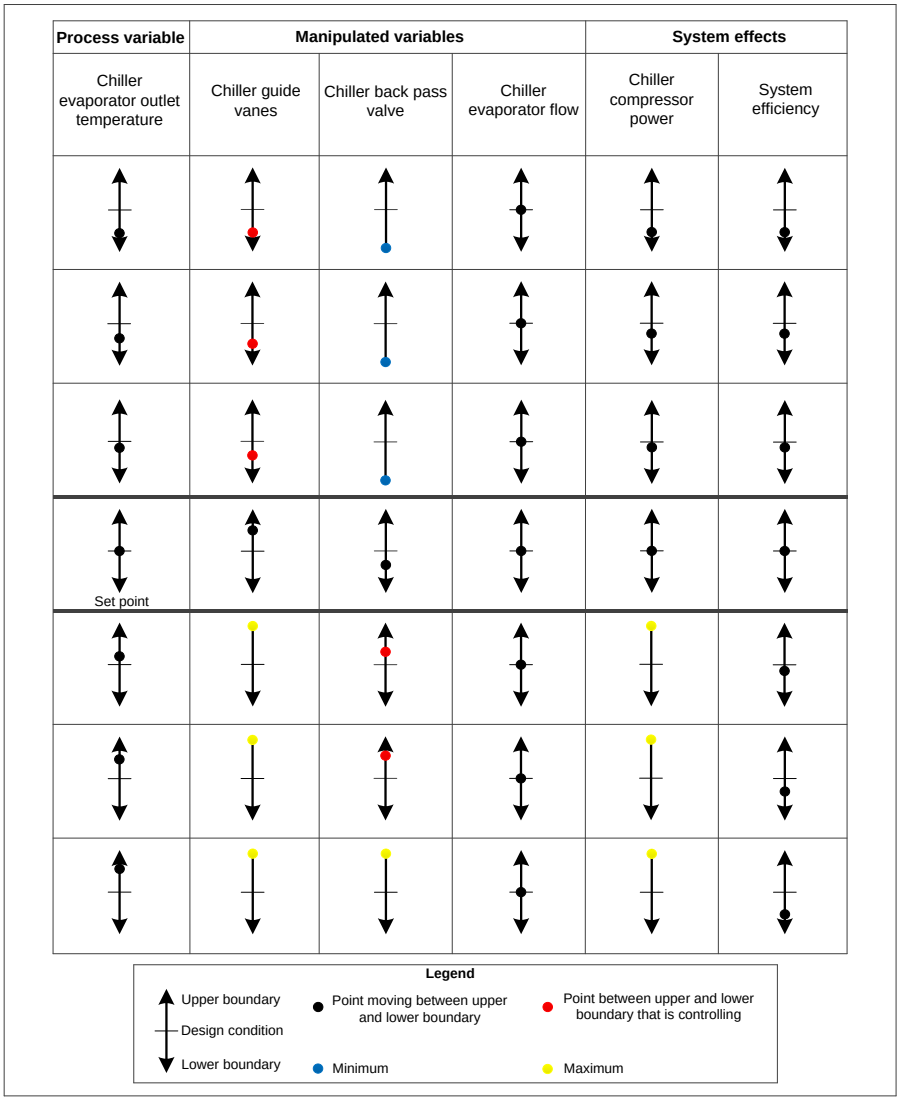

It is suggested that the refrigeration system should follow the steps indicated in Table 8. The control strategy also uses the evaporator outlet temperature as PV. However, if the evaporator outlet temperature rises above the SP, the first reaction should be to reduce the flow through the evaporator.

As the evaporator flow reduces, the guide vanes must be fully opened with no back pass. If the outlet temperature increases, the evaporator flow should be reduced to its design minimum. When the minimum flow through the evaporator is reached, the next reaction should be to open the back pass valve.

If the evaporator outlet temperature decreases below SP, the flow through the evaporator should be increased. If the temperature continues to decrease, the flow through the evaporator

should be increased to maximum design condition. When the maximum flow through the evaporator is reached, the next reaction should be to cut back on the guide vanes.

Following this control strategy will increase the cooling efficiency and reduce the water distribution cost. The amount of cooling is increased when the system is operating at maximum efficiency. The energy-saving strategy will therefore result in reduced electricity consumption for the same amount of cooling achieved when following the existing control strategy.

Table 8: Energy-saving strategy on Mine M

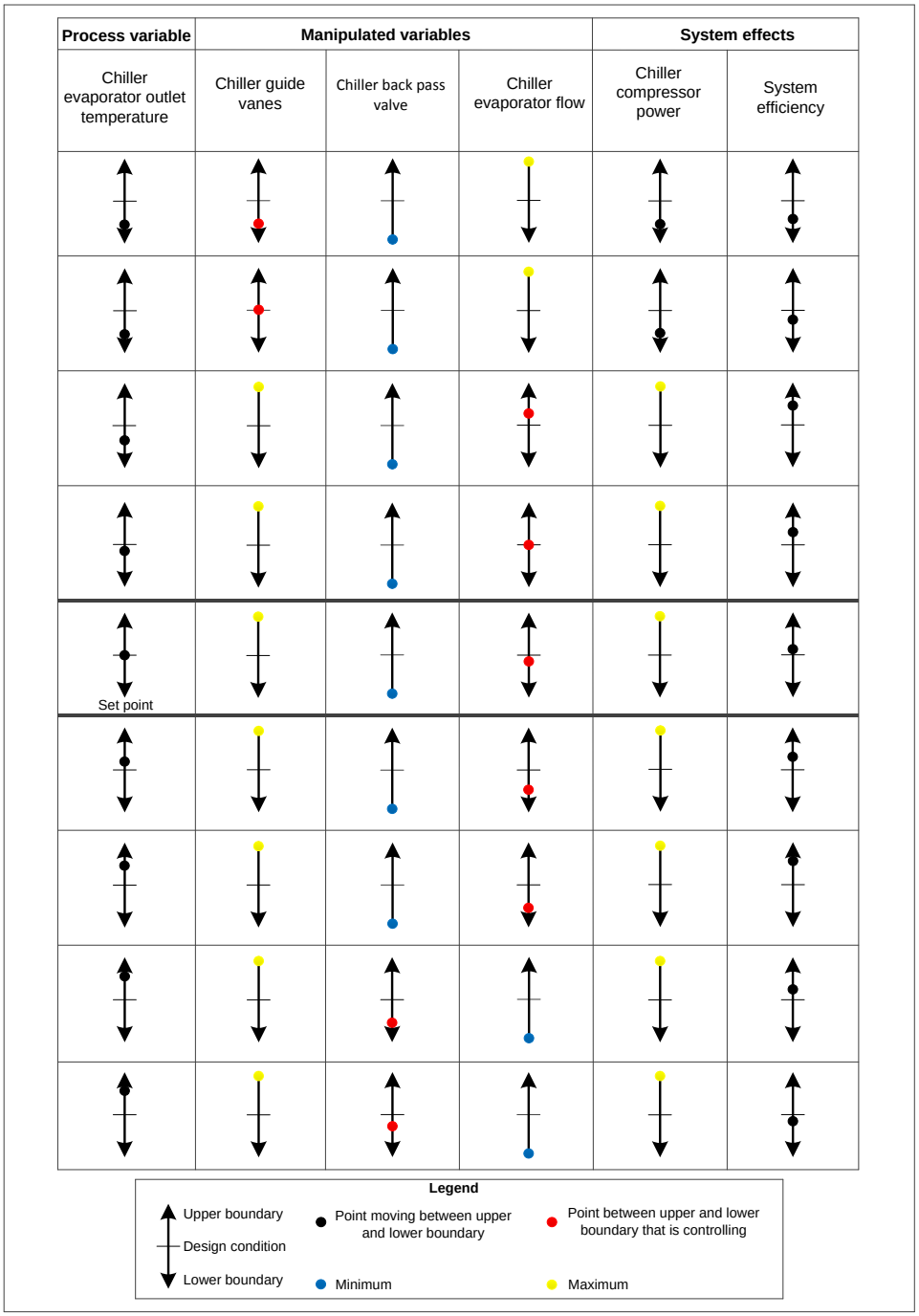

Savings approach

A flow layout of the refrigeration system was developed to determine the feasibility of an energy saving strategy. The flows and temperatures of the existing refrigeration operation were incorporated into the refrigeration layout. Average values of 2013's summer months were used in the savings approach. Figure 25 shows the existing water flow and temperature through the refrigeration system.

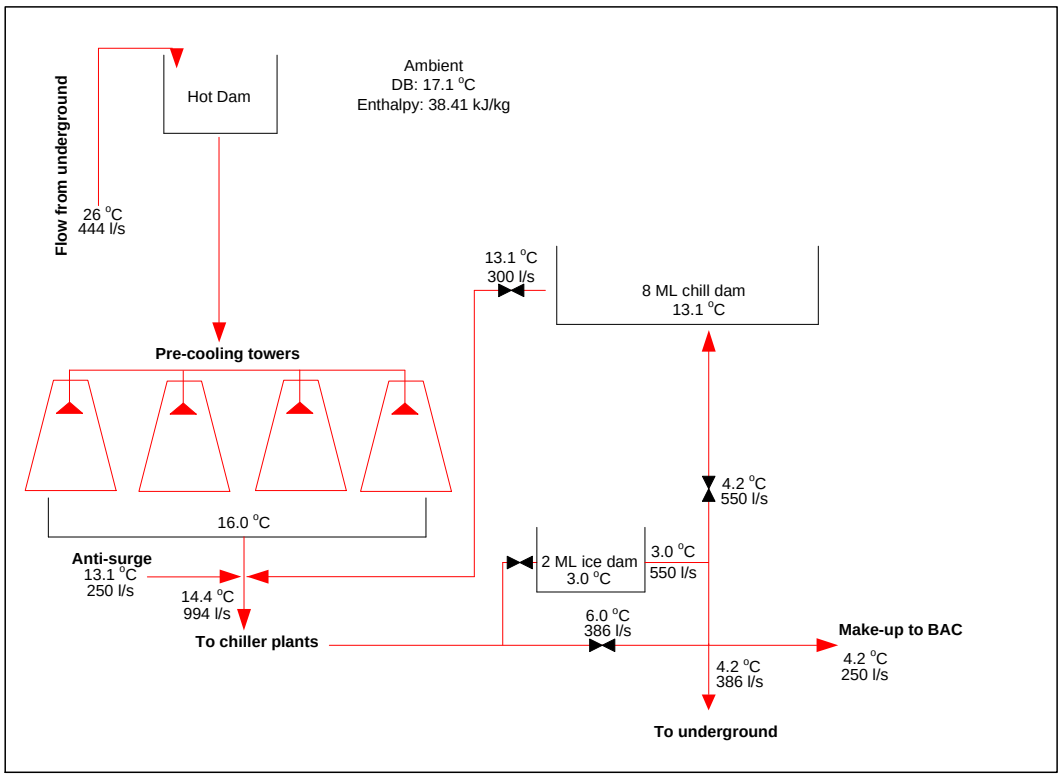

Figure 25: Existing flow through the chilled water plant

Tests were conducted on redirecting the water flow through the 8 Mℓ dam before being sent underground. The results achieved during the testing of the approach are illustrated in Figure 26. The suggested flow through the system required no additional installation of equipment. The valve on the pipeline allowing flow from the 8 Mℓ dam to underground was opened and the valve from the chiller to underground was closed.

Forcing the water through the 8 Mℓ chill dam enables a constant chill capacity. With constant flow through the chill dam the temperature in the dam increases with 0.5 ˚C. This is due to radiation from the surrounding environment on the 8 Mℓ dam and pipelines entering the 8 Mℓ dam. However, if the chill dam is stagnant for a while, as the existing system is operated, water temperature in the 8 Mℓ dam can rise to 13.1 ˚C.

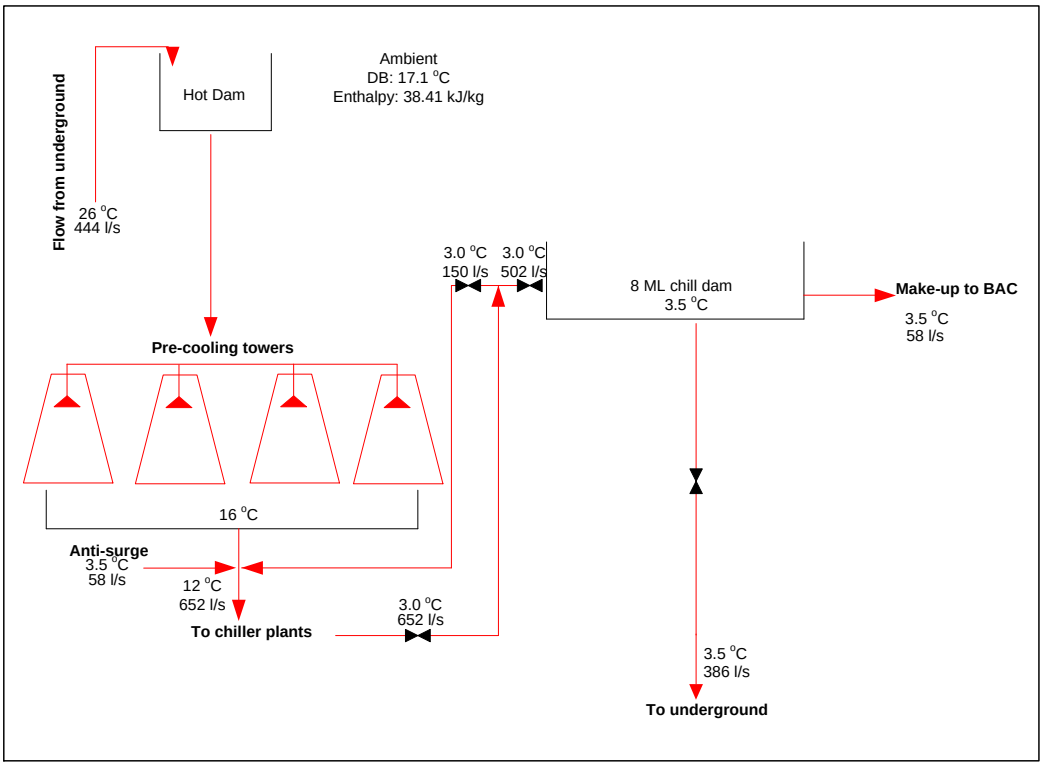

Figure 26: Suggested flow through chilled water plant

In Figure 26 the decommissioning of the ice storage dam also forms part of the savings approach. The flow from the pre-cooling towers and the 8 Mℓ dam mixes at a valve, as shown in Figure 27. The measured mass flow from the pre-cooling tower and the 8Mℓ dam is not available. The water feed to the chillers is maintained at a constant 12 ˚C.

In Figure 25 the existing flow route involves chilled water from the chillers to flow underground, and some of it to the 8 Mℓ chill dam. The study led to the flow from the chillers to the 8 Mℓ chill dam, and a fraction to mix with the pre-cooling flow entering the chillers. From the 8 Mℓ chill dam, water is sent underground and as make-up to the BACs. The water flows through the 8 Mℓ dam before being sent underground, creating a chilled water buffer below 4 ˚C.

The pipeline from the pre-cooling towers that feeds the chillers can handle a maximum flow of 1 050 ℓ/s. In the existing evaporator circuit, large volumes of chilled water is required from the 8 Mℓ dam to lower the temperature of the feed to the chillers. This is due to the high water temperature in the 8 Mℓ dam.

The existing evaporator circuit of Mine M is illustrated in Figure 28. The flow and temperature throughout the circuit is illustrated with data collected from the mine. The COP

of the chillers and motor rating of the pumps and chillers are shown in Figure 28. The total evaporator pump power was calculated as 865 kW. The total chiller compressor motor power was calculated as 12 350 kW. Figure 27 illustrates the known and unknown values that are calculated to deliver a water feed to the chillers at 12 ˚C.

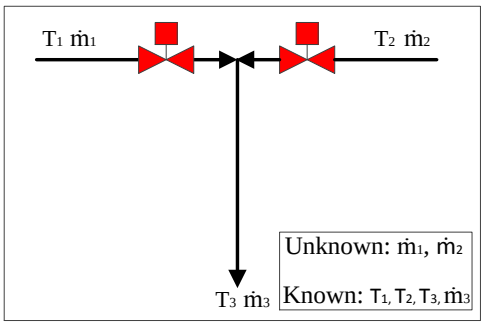

Figure 27: Pre-cooling tower and chill dam water mixture to chillers

Due to the mass flow required from the pre-cooling towers and chillers to deliver a constant 12 ˚C, a mass balance and energy balance were used to formulate Equation 8 and 9. Equation 8 is used to calculate the required flow from the chillers. Equation 9 is used to calculate the amount of water required from the pre-cooling tower to maintain a constant water feed of 12 ˚C to the chillers.

T_1 represents the pre-cooling temperature and $\dot{m}_1$ the pre-cooling mass flow. T_2 represents the chiller outlet temperature and $\dot{m}_2$ the mass flow from the chillers.

$$\dot{m}_2 = \frac{\dot{m}_3(T_3 - T_1)}{(T_2 - T_1)} \tag{8}$$

$$\dot{m}_1 = \frac{\dot{m}_3(T_3 - T_2)}{(T_1 - T_2)} \tag{9}$$

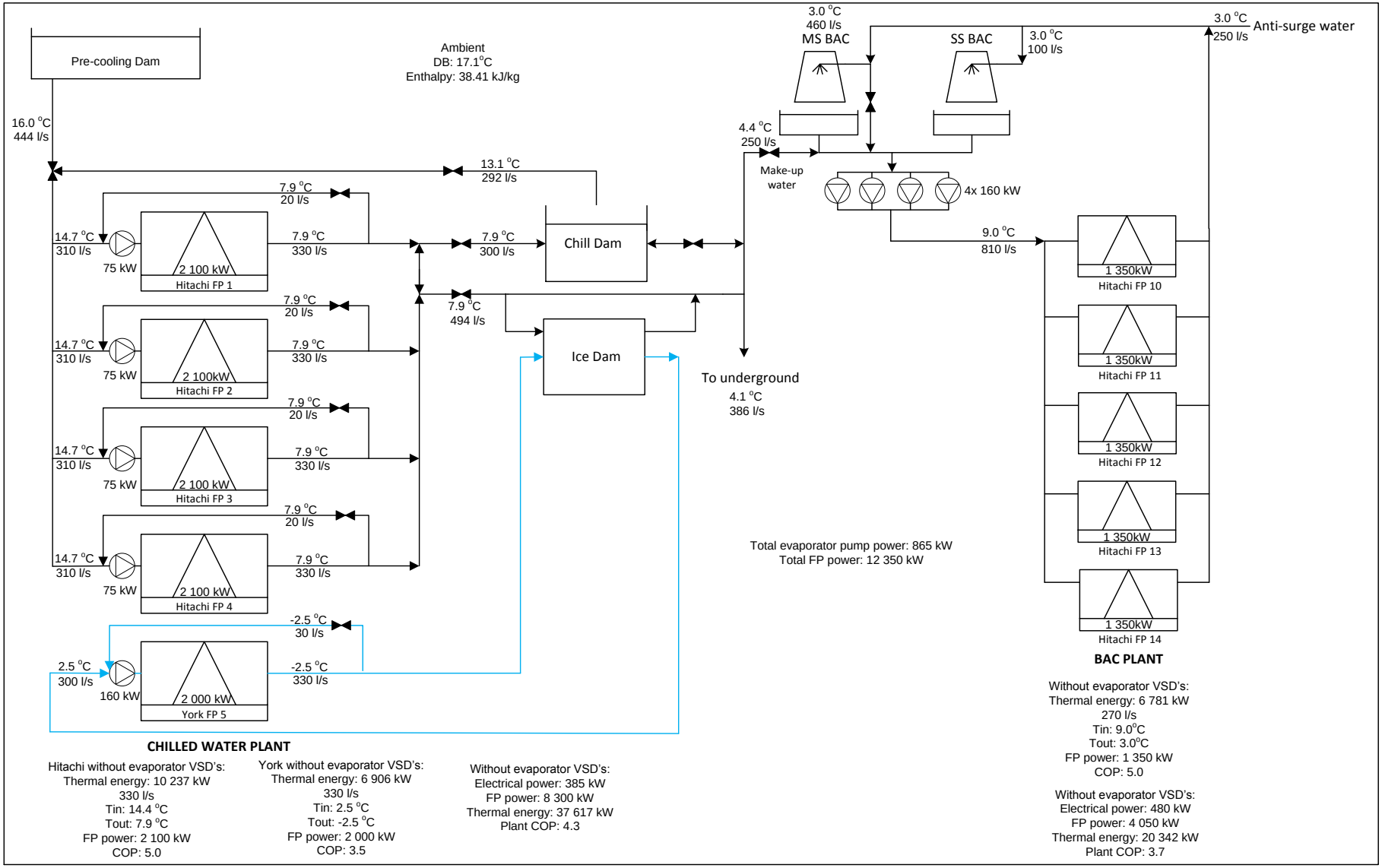

Figure 28: Evaporator water-flow diagram

Converting the ice storage system to a chilled water system resulted in layout changes as shown in Figure 29. The effect of varying the flow through the evaporator circuit and the pumps that require VSDs are also illustrated in Figure 29. Due to the reduced pumping load, the pump's power consumption is also reduced. The pump power can be calculated with Equation 11.

$$Pd = \frac{\dot{m}^2}{\rho \mathrm{A}} \tag{10}$$

$$Pump\ Power = \frac{Pd\dot{m}}{\rho \eta} \tag{11}$$

Equation 10 is used to calculate the flow admittance (A). The results are found in Table 9. These values were used in Equation 11 to calculate the pump power when the flow through the pump is reduced.

Table 9: Pump flow admittance results

Pump description	**Pump power (kW)**	**Flow admittance (m^4)**
Evaporator pump (Chilled water plant)	75	0.64
Condenser pump (Chilled water plant)	160	1.04
Evaporator pump (BAC plant)	160	0.16

The temperature to underground resulted in a reduced temperature. The flow to underground remained according to demand. Only two VSDs were brought into the savings approach of the BAC evaporator side. This was due to limited funding available for installations. The total saving by varying the flow through the evaporator circuit was estimated at 987 kW, as shown in Figure 29.

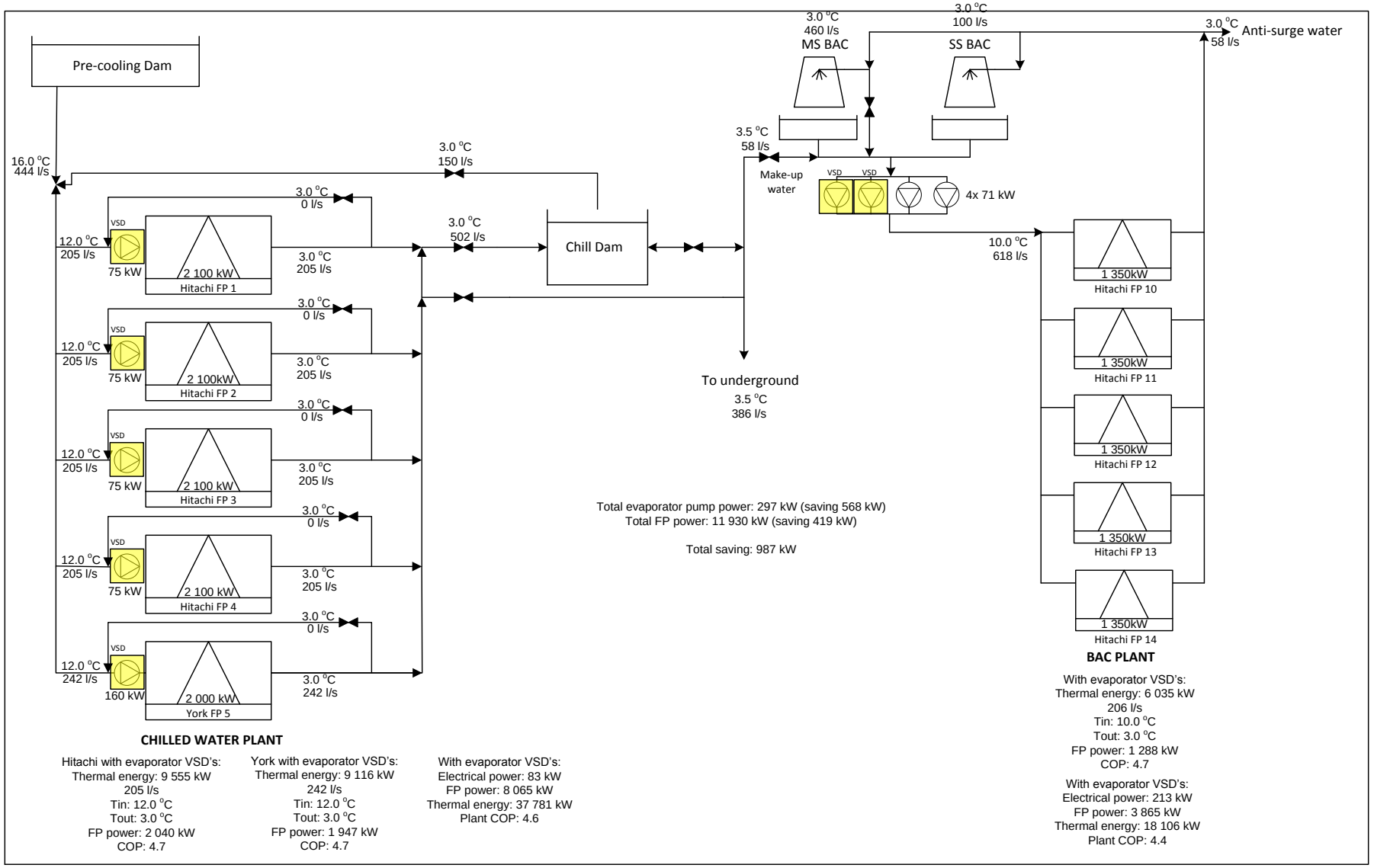

Figure 29: Evaporator circuit after changes

Due to the condenser circuit being in a closed loop, the circuit was separated from the evaporator side. The existing flow and temperature through the chilled water plant condenser circuit is illustrated in Figure 30.

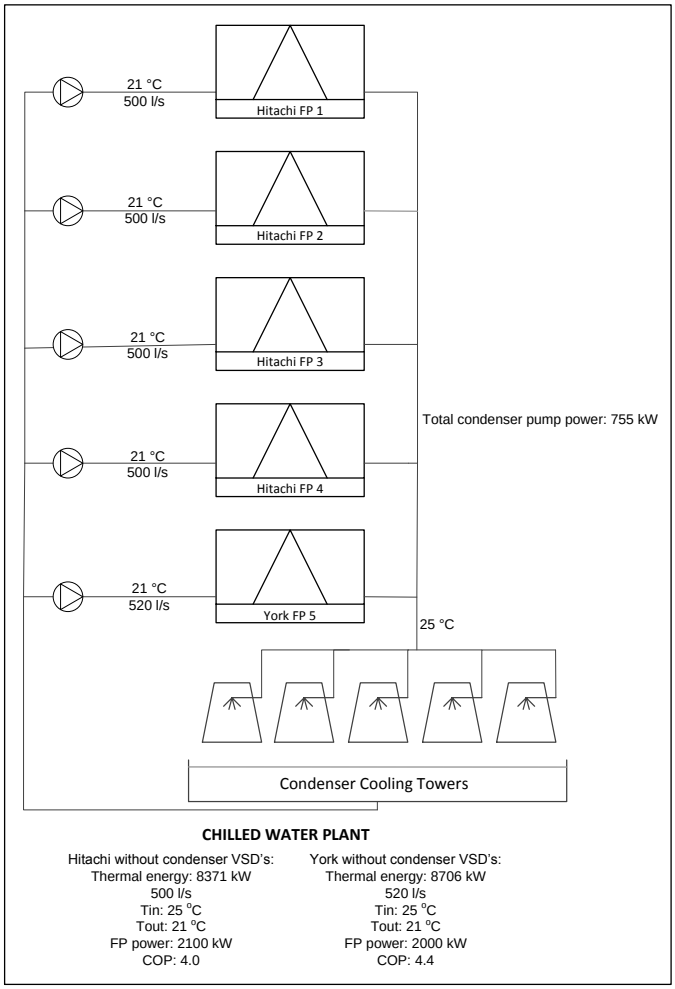

Figure 30: Condenser circuit before changes

The condenser circuit of the BAC was not considered during the savings approach. This was due to limited funding available for installations. The savings approach of the chilled water plant condenser circuit is illustrated in Figure 31. By varying the flow through the condenser circuit, a 362 kW saving was estimated, as illustrated in Figure 31.

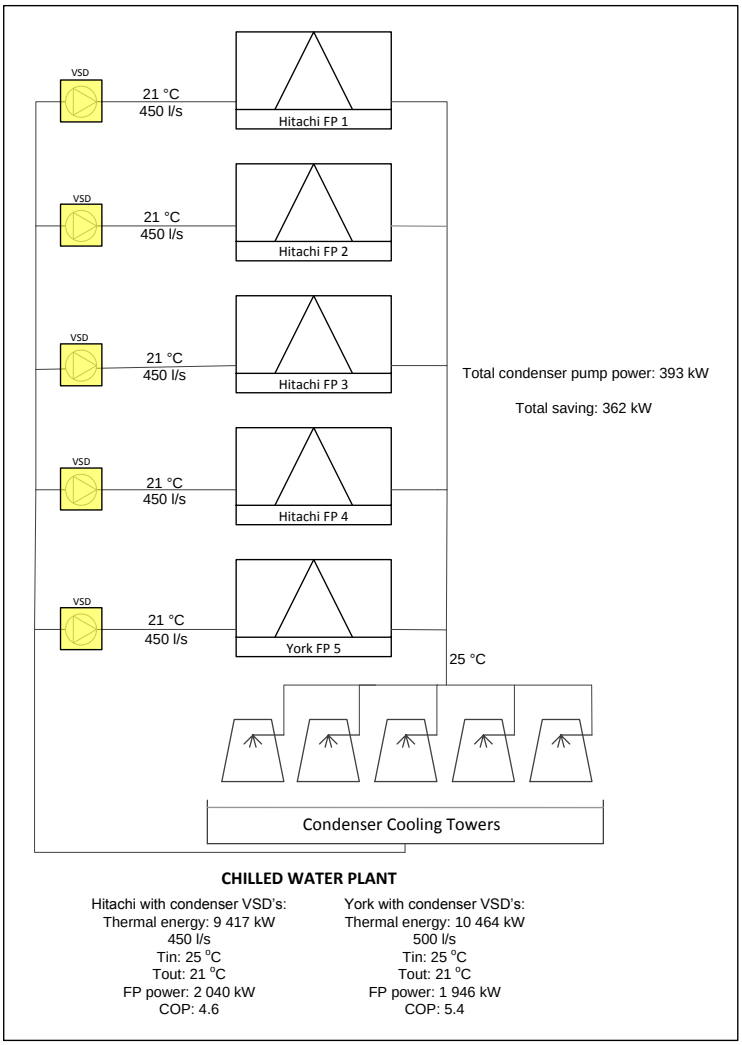

Figure 31: Condenser circuit with varying water-flow changes

The total power saving on the chilled water plant and the BAC plant was calculated with available data as 1 349 kW. A simulation model was required to estimate the 24-hour energy efficiency that could be achieved.

3.5 SIMULATED REFRIGERATION SYSTEM RESULTS

After investigations were completed and a possible electricity savings approach was identified a simulation of the refrigeration system was required. Different components before the glycol chiller operation, during and after the glycol chiller have an effect on the performance of the chiller.

To identify possible 24-hour savings on Mine M's refrigeration system a simulation model of the refrigeration system was developed. The refrigeration system of Mine M was developed

in a simulation package called Process Toolbox™. The specific simulation model was selected because of its capability as an integrated dynamic simulation model that is able to balance energy and mass on a refrigeration system. The simulation validated whether the energy-savings investigated was plausible. Raw data collected from Mine M was brought into the simulation models.

The simulation is divided into 120 intervals of one hour each. The 120 intervals represents five simulation days. The first day is an initial summer day that allocates initial values to the refrigeration system components. The second to fifth day is divided into the four seasons, namely summer, autumn, winter and spring.

Each season day therefore represents 91.2 days of the three month season. Results of the initial summer day are not displayed, as they are convergence values. Results of the four seasons are, however, displayed in the simulation model.

The existing refrigeration system was simulated with data collected from the mine, as explained in Section 3.4. Thereafter the proposed operation of the refrigeration system was simulated. The proposed simulation was controlled as explained in Section 3.4. The layouts of the existing and proposed simulation models are shown in Appendix D, Figure 68 and Figure 69 respectively.

The four seasons brought into calculation allows different weather conditions throughout the year to be brought into account. Different boundary conditions are considered when designing the simulation. The results of the warmer summer months and colder winter months are displayed in this chapter. These boundary conditions are shown in Table 10.

Table 10: Simulation baseline assumptions

Description	Summer (Dec – Feb)	Winter (Jun – Aug)
Eskom Electricity tariff	Megaflex 2013/2014	Megaflex 2013/2014
Hourly climate data	Witwatersrand 2013	Witwatersrand 2013
Outlet water temperature (˚C)	3	3
Average Hitachi evaporator flow (ℓ/s)	300 x 4 (24hr/day)	300 x 3 (24hr/day)
Average York evaporator flow (ℓ/s)	350 (24hr/day)	350 (24hr/day)
Hitachi chiller in operation (00:00 – 23:00)	3	3
York chiller in operation (00:00 – 23:00)	1	1

Description	Summer (Dec – Feb)	Winter (Jun – Aug)
Condenser cooling towers in operation	5	5
Pre-cooling towers in operation	4	4
BACs in operation	2	0
Hot water dam temperature (˚C)	26	26
Pump efficiency rating	0.75	0.75
Motor efficiency rating	0.95	0.95
Cooling tower fan efficiency rating	0.65	0.65

The existing system was simulated to determine a baseline. The simulation layout of the existing refrigeration system is illustrated in Appendix D, Figure 68. Figure 69 in Appendix D shows a simulation of the refrigeration system when the glycol plant is converted into a water chiller and the ice dam is decommissioned.

The assumptions for the proposed simulation remain the same as the baseline simulation. The baseline and proposed chilled water temperature to underground is simulated within 0.4% from each other. The simulated baseline included the York chiller with a COP of 3 to produce ice in the ice storage dam. The proposed simulation included the York chiller with a COP of 4.8 to produce chilled water.

In Chapter 2 research is done to determine how to vary the flow through the system. The solution was through the use of a VSD. The proposed simulation of the refrigeration system requires VSDs on the condenser and evaporator pumps. This allows for a comparison to be made between the results of the simulation without VSDs (baseline simulation) to the simulation with VSDs (proposed simulation).

The baseline simulation resulted in the evaporator outlet temperature of 6 ˚C. The water was then further chilled to 3 ˚C by flowing it through the ice storage dam. The proposed simulation was simulated to deliver water at 3 ˚C, the required chilled water temperature to underground. PID control was placed on the evaporator and condenser pump to vary the flow through the chiller, as explained in Section 3.4. The control connection is illustrated on the proposed simulation layout, Figure 69 in Appendix D.

The reduced York chiller compressor power baseline is compared with the proposed simulation. The results are illustrated in Figure 32. It is shown that, during the afternoon

when ambient conditions are at their highest, the compressor load increases. During evening and early morning the cooling load is reduced. The proposed simulation resulted in a 9% electricity saving.

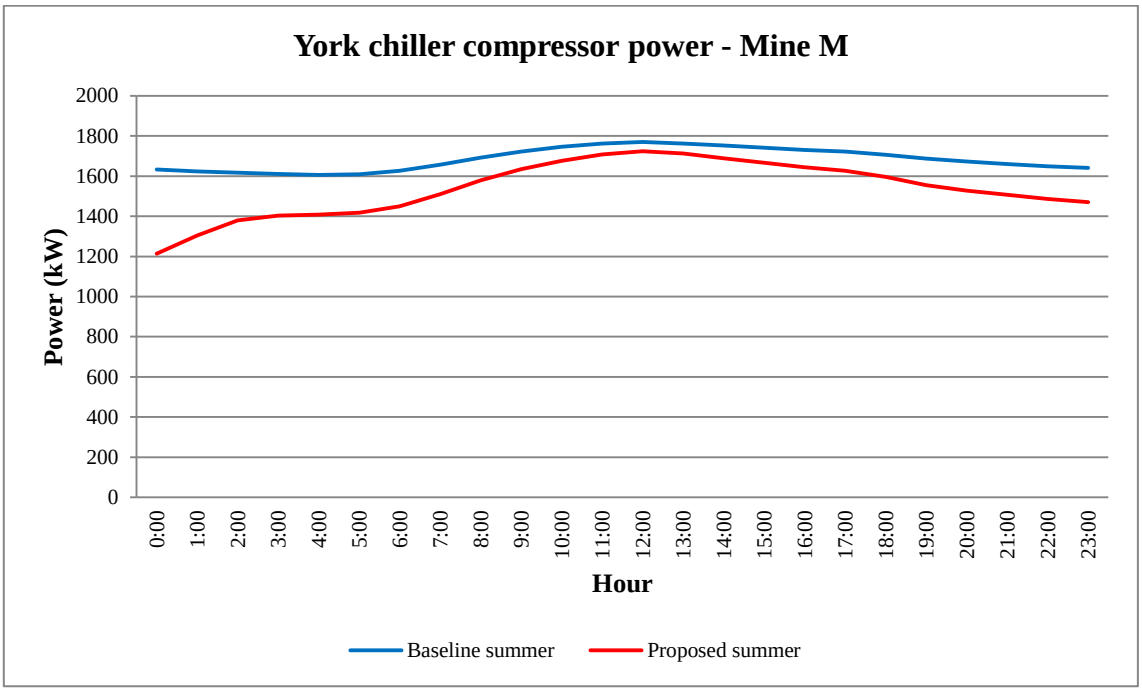

Figure 32: York chiller compressor power

The cost to operate the York chiller during baseline simulation is compared to the proposed simulation illustrated in Figure 33. A cost decrease of 7.8% is achieved. The proposed simulation resulted in a daily electricity cost of R16 500.00 to operate the York chiller.

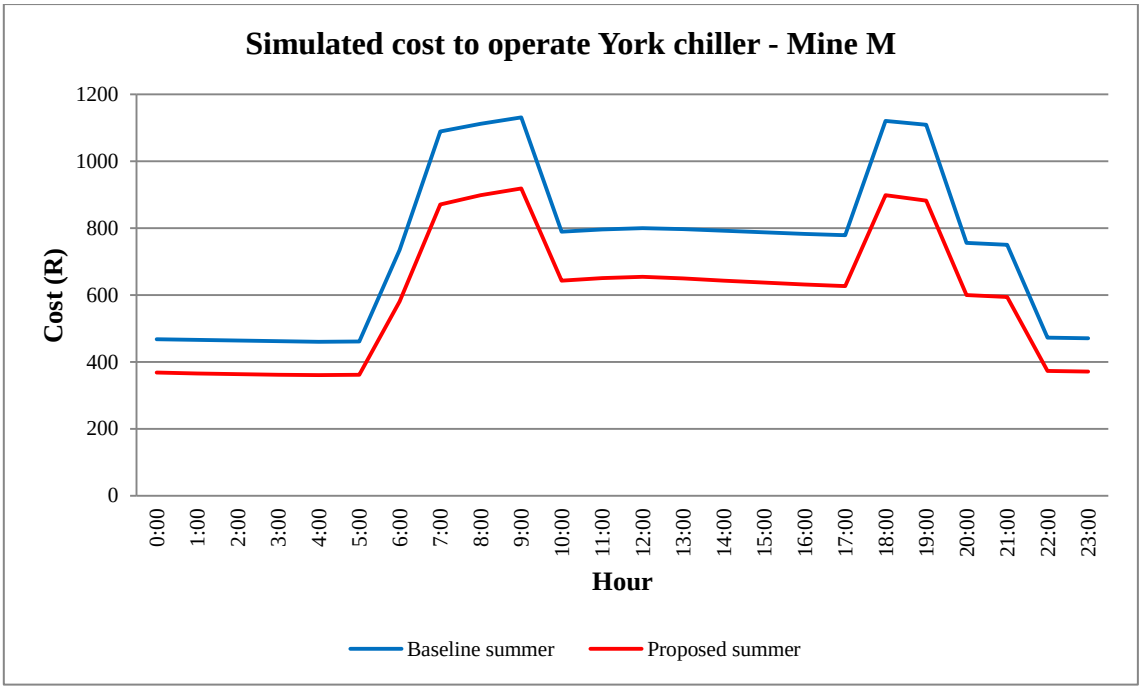

Figure 33: Simulated cost to operate York chiller

The energy savings achieved by comparing the proposed summer simulation with the baseline summer simulation model resulted in a power saving of 1 944 kW. The simulation further resulted in an annual electricity cost saving of R5 169 536 .00. The summer 24-hour power profile of the baseline and proposed simulation are shown in Figure 34.

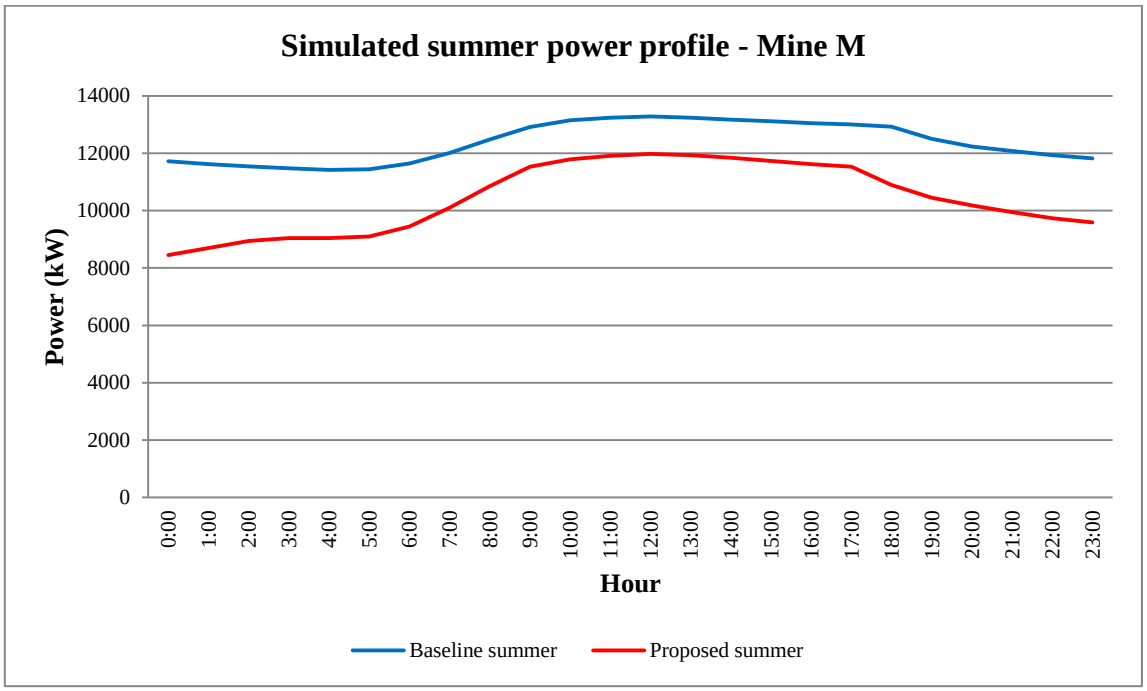

Figure 34: Simulated summer power profile

The winter 24-hour power profile of the simulated baseline and proposed simulation are shown in Figure 35.

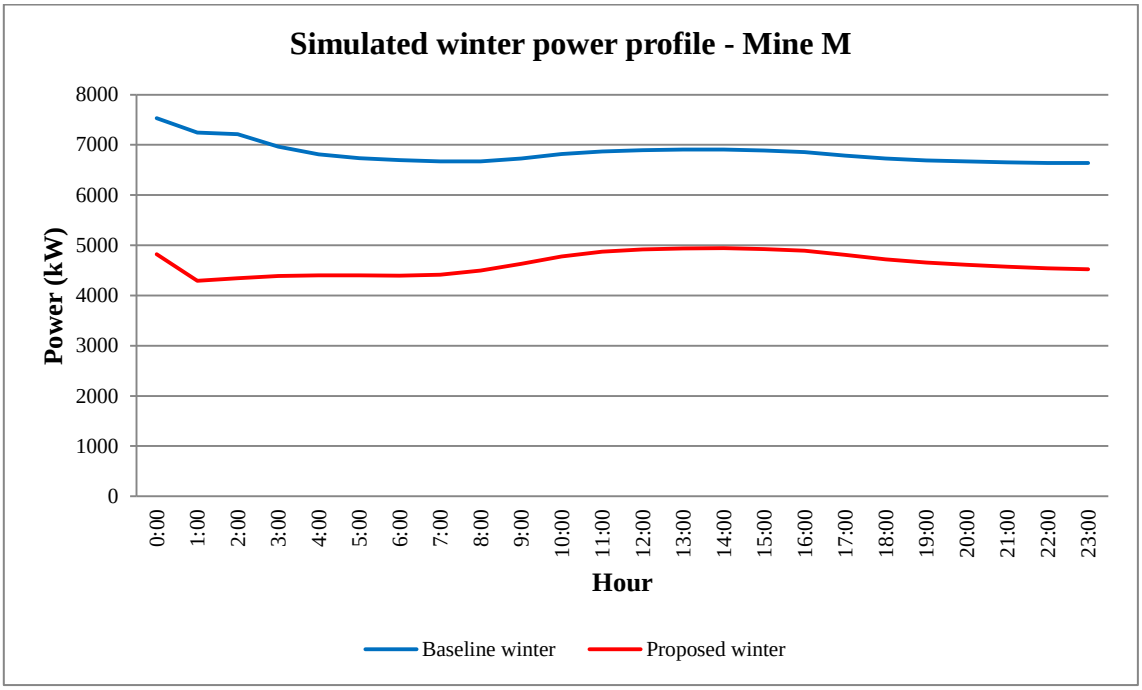

Figure 35: Simulated winter power profile

Converting the ice storage system according to the simulation model resulted in a 146 kW power saving. Installing variable speed drives on the evaporator and condenser pumps of the five fridge plants led to a further 1 458 kW saving. This is however close to the savings calculated in the savings approach of Section 3.4, which resulted in a 1 349 kW saving. An additional 340 kW saving was achieved through the installation of VSDs on two of the four evaporator pumps at the BAC plant. The total power saving according to the simulation resulted in 1 944 kW during the summer months.

The estimated results obtained with the savings approach was verified with the simulation model. This resulted in a 44% difference. Results obtained with the simulated control strategy indicated a power saving and cost-saving on the refrigeration system of Mine M. The implementation and results are described in Chapter 4.

Validation and verification of simulation

Actual data logged on 15 January 2013 was selected and simulated to verify and validate the simulation model used. The actual power consumed on the refrigeration system was compared to the simulated results. The results gained showed that the simulation model was

99.55% accurate, according to actual data. This verifies that the simulation model used during this study is an accurate model.

3.6 CONCLUSION

This chapter started with a case study on the surface refrigeration system of Mine M. The various cooling components used on Mine M to chill water and air are described. Mine M makes use of two methods to chill water. The one is thermal ice storage and the other only requires a traditional water chiller.

A significant energy-saving potential on the chilled water plant and BAC plant of Mine M was investigated. A savings approach was developed and power savings were estimated at 1 349kW. A simulation model was then required to verify the power savings achieved with the savings approach.

The 1 944kW simulation power saving achieved is also plausible, due to the high installed capacity of 18 615 kW. Total savings comprised of converting the ice storage system to a chilled water system, as well as direct evaporator and condenser pump savings and chiller compressor load reduction.

The load on the compressor was reduced by reducing the daily water volume needed to be chilled by the chillers, which contributed to a large energy saving. The water volume required to be chilled was reduced by reducing the back pass to the chiller. The back pass was reduced by varying the flow according to an evaporator temperature outlet SP.

Through simulation results, the service delivery for underground demand remained unchanged, with a 0.4% difference in the temperature of the chilled water to underground. The proposed simulation temperature and volume sent underground remained within the required limits.

According to these results it is concluded that the ice storage system should be converted to a chilled water system. Power savings will then be the result of VSDs installed on the evaporator and condenser pump motors. This will result in energy being saved without affecting underground conditions. In conclusion, this chapter illustrates that the simulated control strategy results in power- and cost savings on Mine M. The implementation and results are discussed in the next chapter.

CHAPTER 4: IMPLEMENTATION AND RESULTS

[9]

Implementations done on the refrigeration system of Mine M is explained in this chapter. Results of the thermal ice storage system during operation are shown. Implemented changes on the thermal ice storage system to convert it to a chilled water system are explained. After implementation, the results of the chilled water system operation are given. The amount of energy savings achieved by operating a chilled water system over a thermal ice storage system is seen in this chapter. Varying the flow through the chillers resulted in an energy saving.

[9] D. Uys, Personal photograph. "York chiller", West Wits, 2014.

4.1 INTRODUCTION

According to the simulation model developed in Chapter 3 on Mine M's refrigeration system, it is proven through simulation results that conversion of the ice storage system to a chilled water system will result in power- and cost savings.

In 2005 Mine M committed to an initiative to reduce their electricity demand by 12% by 2015 [81]. The total annual electricity consumption at Mine M is R 100 million [21]. The ice-storage facility on Mine M was introduced in 2007. It is therefore recent technology used on the surface refrigeration of Mine M [21].

This chapter describes the implemented changes on the deep level gold mine, Mine M. After comparing the results of the simulation models it was found viable to implement the changes on the refrigeration system. During the implementation the ice storage dam was decommissioned. The York chiller was therefore converted from producing ice to producing chilled water. This was followed by installing variable speed drives on the evaporator and condenser pumps, as explained in Section 3.5.

In this chapter a comparison of the baseline results and pre-implemented results, are compared to the actual results after implementation. The period used for the baseline results is January 2013 to March 2013. This period falls within the warmest months and was chosen due to the refrigeration system working the hardest during this period.

The performance assessment period was chosen as January 2014 to March 2014 for accurate comparison with pre-implemented data. Performance assessment is a three-month period when the actual energy savings are compared to the proposed savings. The three-month performance assessment results are shown in Table 14, Table 15 and Table 16 of Appendix C respectively.

The existing ice storage operation consists of one York chiller. The evaporator inlet and outlet flow, condenser in and outlet flow, total chiller power and COP will be compared. The effect of converting the ice storage system on the flow to underground and temperature to underground was also studied.

A summer and winter baseline of the pre-implemented power data was compiled. The actual power data post implementation was then compared to the baseline in order to establish

whether the case study resulted in an energy saving. The results of the glycol plant operating before implementation is discussed in Section 4.2.

It was important to monitor the underground conditions on the deep level mine, due to the surface cooling system that affects the underground conditions. Temperature sensors measured the dry-bulb temperature and relative humidity on different levels underground.

It was found that the underground wet-bulb temperature was under the required temperature as explained in Section 1.3. Equipment was successfully installed on site and controlled and monitored via the SCADA and EMS. This chapter focuses mainly on converting the York chiller into a water chiller that is implemented in parallel with the Hitachi chillers.

4.2 EXISTING GLYCOL SYSTEM RESULTS

Random summer weekdays are selected to determine the operating schedule of the York chiller. From Figure 36 it is evident that the York chiller runs most of the time to cool glycol. Interpreting Figure 36, it is observed that the York chiller operates during peak hours. Operating the York chiller to cool water enables stoppage during peak hours, shifting more energy out of peak demand.

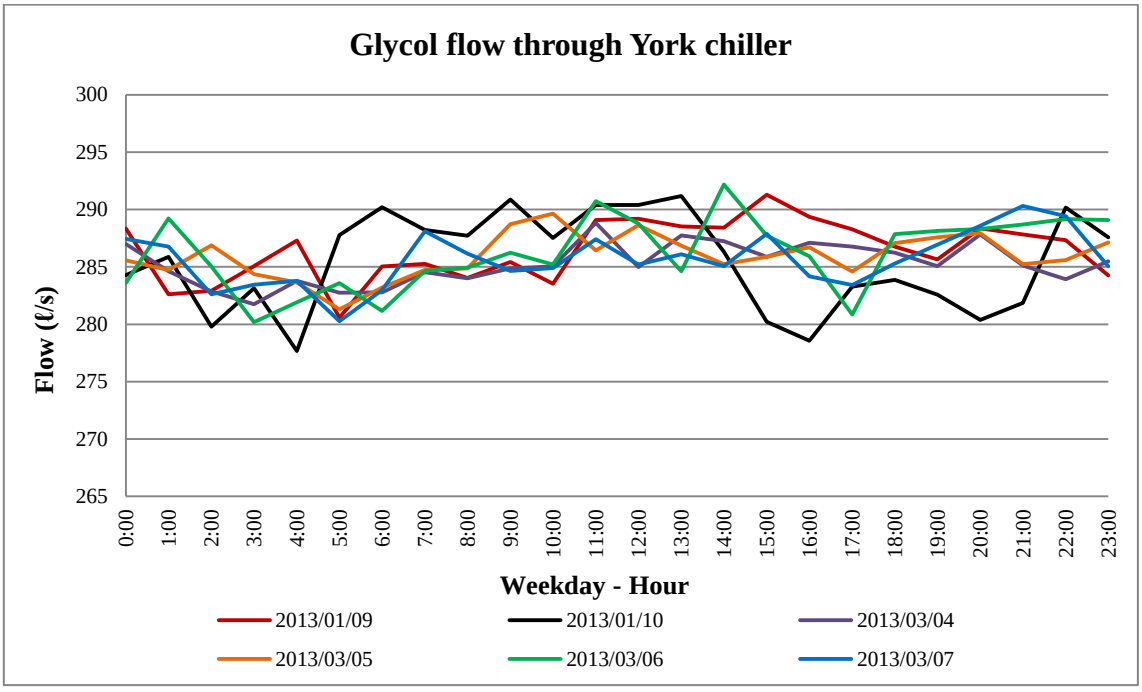

Figure 36: Glycol flow through York chiller evaporator

The average inlet and outlet temperature of the glycol chiller over a 24-hour profile is shown in Figure 37. The average glycol flow through the evaporator side of the glycol plant is 268 ℓ/s. The delta temperature across the evaporator inlet and outlet is on average 4.5 ˚C.

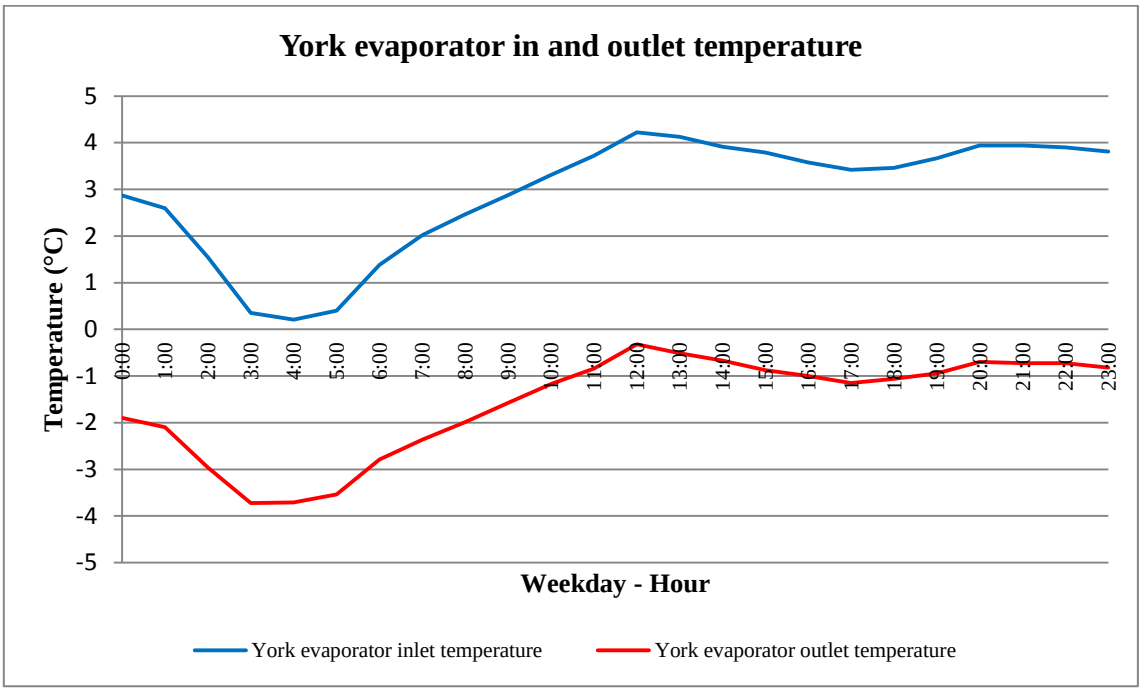

Figure 37: Glycol plant inlet and outlet evaporator water temperature.

The York chiller water temperature difference across the evaporator inlet and outlet versus the compressor power is illustrated in Figure 38. The average power consumed by the York chiller is 2 658 kW. The York chiller is operated 24-hours a day to produce glycol.

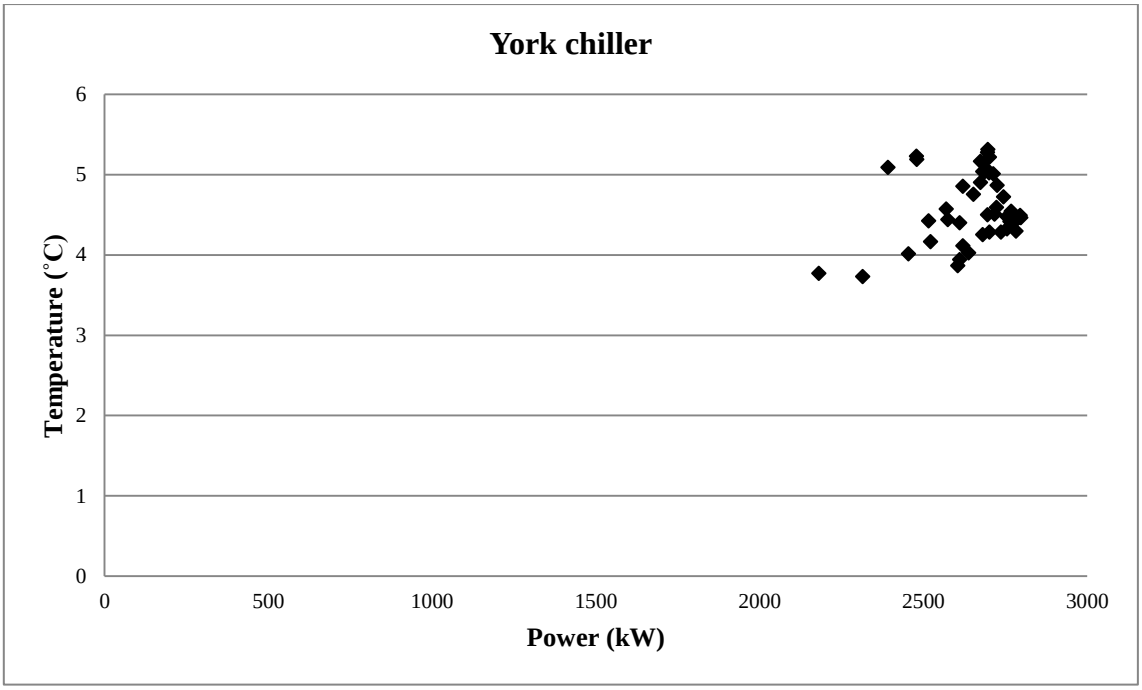

Figure 38: York water temperature difference across evaporator inlet and outlet versus compressor power

The cooling capacity of the York chiller was calculated using Equation 5 from Section 2.3. The average cooling capacity was calculated as 5 400 kW. A 24-hour profile of the York cooling capacity is illustrated in Figure 39.

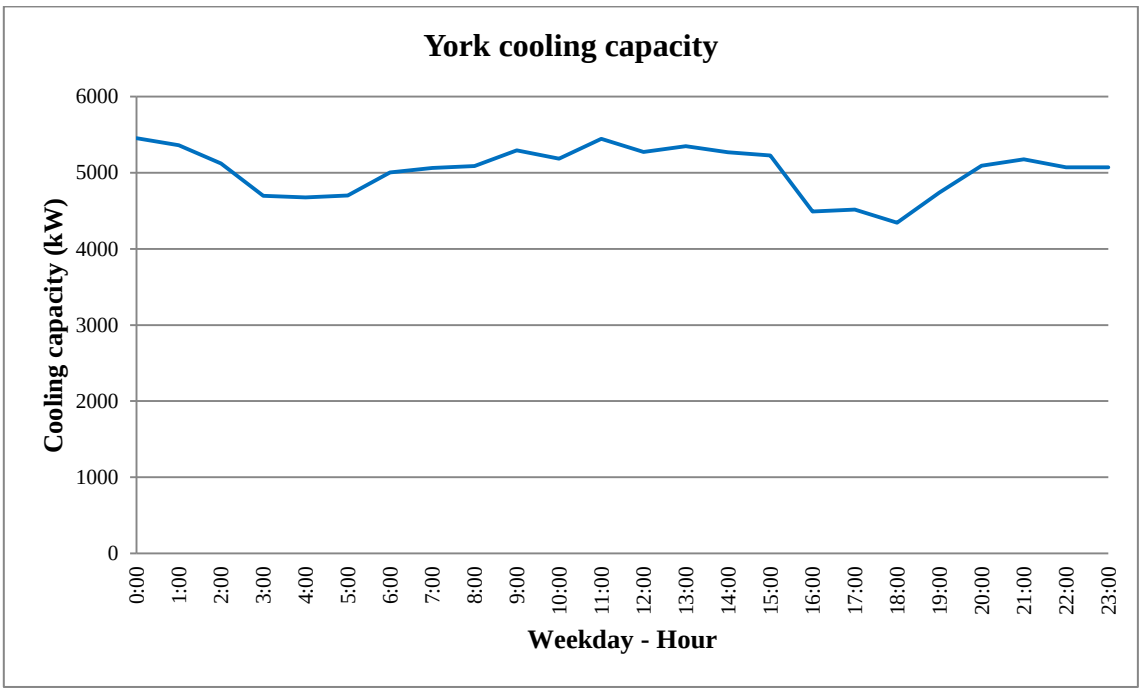

Figure 39: Cooling capacity of the glycol chiller

The inlet and outlet water temperature inside the ice dam is shown in Figure 40. The evaporator outlet water from the Hitachi chillers is cooled with a delta temperature of 3 ˚C. The surface ambient temperature has an effect on the heat loss into and out of the ice storage dam. The 24-hour profile of the surface ambient dry-bulb temperature is illustrated in Figure 40.

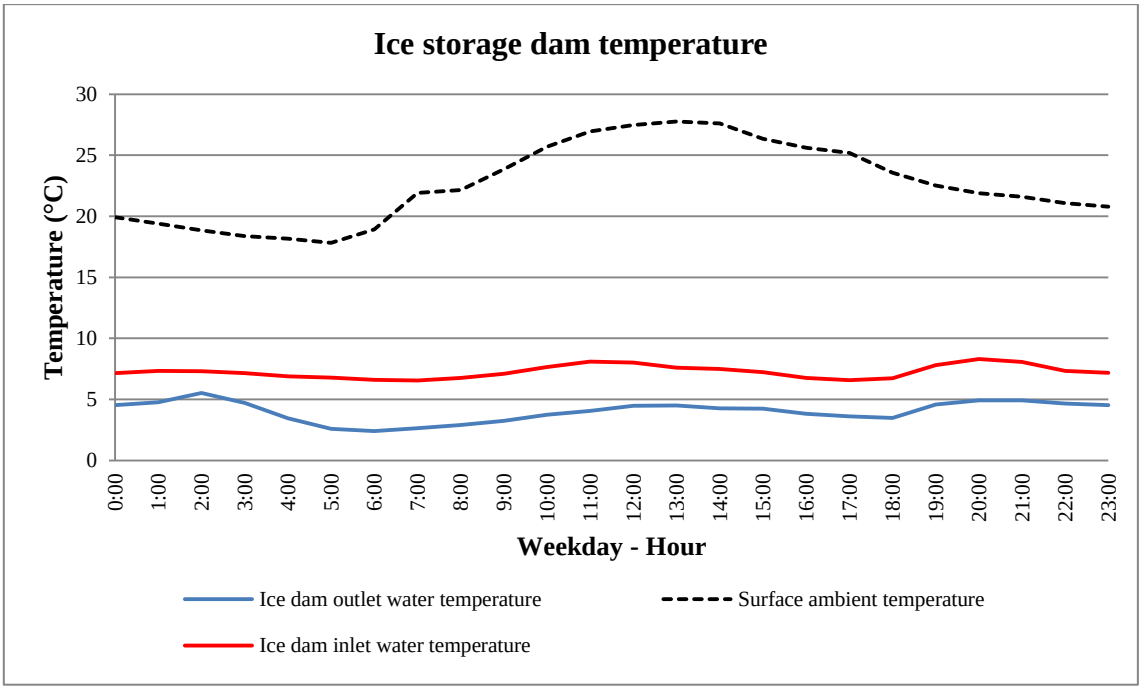

Figure 40: Ice dam water inlet and outlet temperature and surface ambient temperature

4.3 IMPLEMENT CHANGES ON DEEP LEVEL MINE

Ice storage conversion

After investigations, simulation and results were compared, the on-site implementations on Mine M followed. The site implementations required instrument installations, software development and the conversion of the existing thermal ice storage to a chilled water flow configuration.

Water leaving the chillers either flow underground or to the 8 Mℓ chill dam. Water stored in the 8 Mℓ dam assists in lowering the temperature of the pre-cooling feed to the chillers. The chilled water stored in the 8 Mℓ dam loses thermal energy and needs to be chilled again. The water in the dam is stagnant due to no flow through the dam. This leads to temperature rises in the dam, which no longer contributes to lowering the pre-cooling feed to the chillers.

The EMS software package explained in Section 3.4 was installed on a server located in the control room of Mine M. As explained in Chapter 3, it was proposed to the mine to decommission the ice storage dam. The way to go about it was to take the ice dam offline. Bypassing the ice dam required closing the valve on the feed to the ice dam pipeline.

Water leaving the chillers is sent to the 8 Mℓ dam and as pre-cooling feed to the chillers respectively. The chilled water leaves the chillers and mixes directly with the pre-cooling water feeding the chillers. There is however less time for thermal energy losses, which allows for a lower inlet temperature to the chillers. The conversion resulted in continuous flow through the 8 Mℓ dam to the underground and as make-up water to the BAC.

The pipeline configuration was converted in parallel with the other four Hitachi plants. Chilled water from the chillers fed into a single column. The chilled water was forced through the 8 Mℓ chill dam before being sent underground, or as BAC make-up water. Five chillers in parallel gave the mine enough cooling capacity to effortlessly meet underground demand.

The York chiller on Mine M is shown in Figure 41. The condenser is indicated on top of the evaporator. The refrigerant flows through the condenser and is compressed in the compressor. From the compressor refrigerant is expanded as it is fed into the evaporator. This is a closed loop cycle of refrigerant flow. The pipeline for the refrigerant on the evaporator inlet and condenser outlet was removed when the upgraded compressor and gearbox were installed, as illustrated in Figure 41.

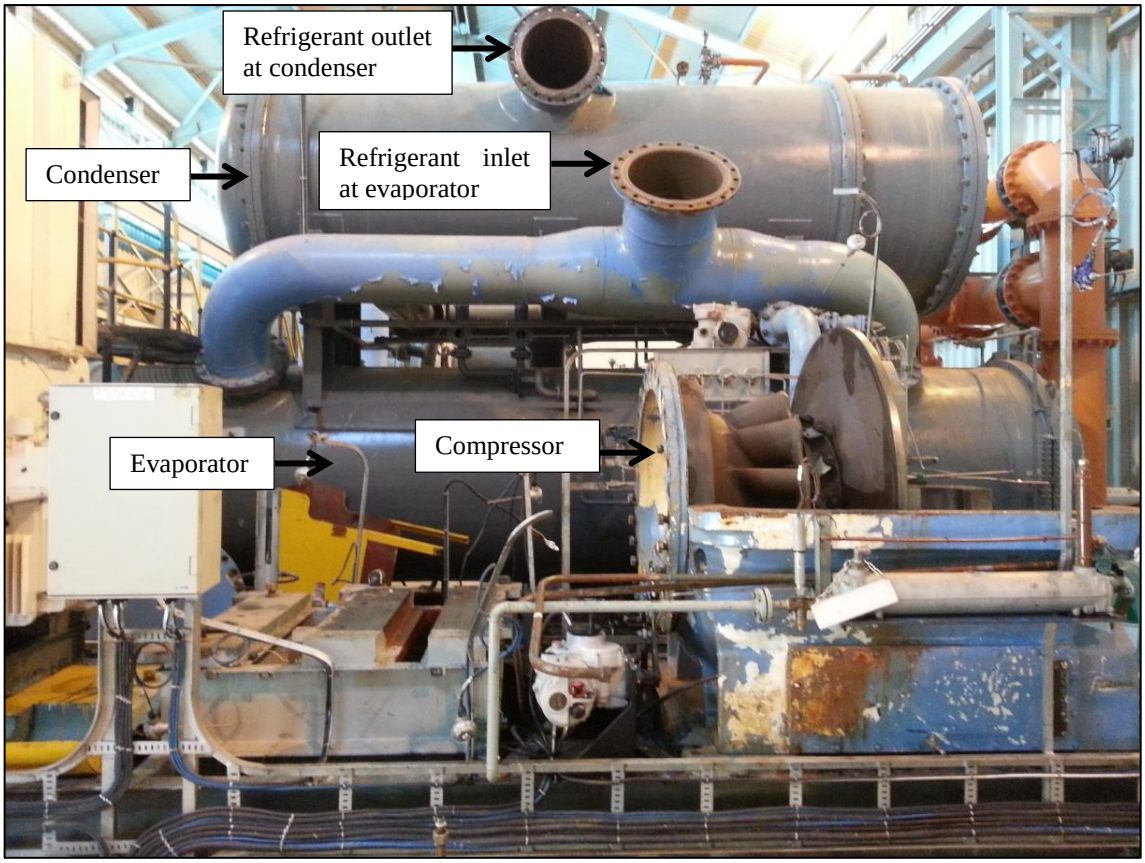

Figure 41: Removed pipeline to implement York chiller gearbox configuration

A different gearbox is required when cooling refrigerant to 2 ˚C instead of cooling refrigerant to -5 ˚C. In order to compress R-134a to cool glycol, the compressor gearbox requires a certain blade configuration. Thinner compressor blades lead to less resistance on the blade, enabling the blade to rotate faster. More compression can be achieved by rotating the blade faster. This enables colder refrigerant temperatures during the expansion phase.

In order to cool the R-134a to below -5 ˚C, a thinner blade is therefore required. When cooling the refrigerant to 3 ˚C, less compression is required. Slower speeds are therefore necessary, and a thicker compressor blade can be used. Figure 64 in Appendix A shows the compressor impeller required to cool glycol.

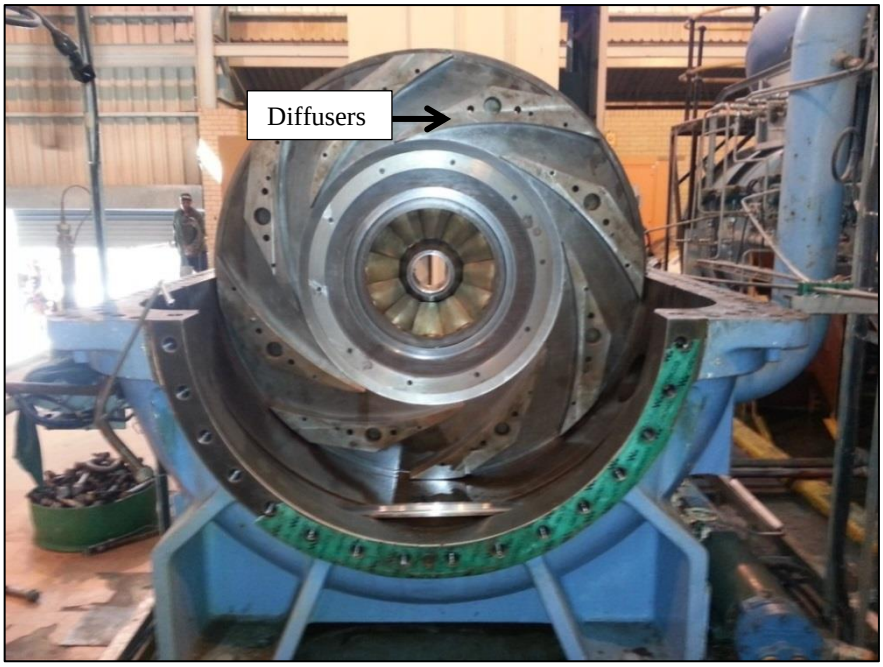

Figure 42: York compressor guide vanes

The diffusers of the compressor to compress R-134a that cools water are shown in Figure 42. After the converted compressor was installed, a pressure test was performed on the compressor at 8 bars[10]. This allowed for the identification of any leaks before the compressor was filled with R-134a. The compressor and gearbox were cut and manufactured over a period of six months, due to certain delays encountered with cutting and balancing the gearbox. The gearbox configuration is shown in Figure 43.

Figure 43: York gearbox configuration

[10] Flip Stols_Chiller Fitter_Anglogold Ashanti
Email: flipstols@gmail.com

Figure 44 shows the compressor impeller and inter-stage blades of the compressor, collected from site for conversion.

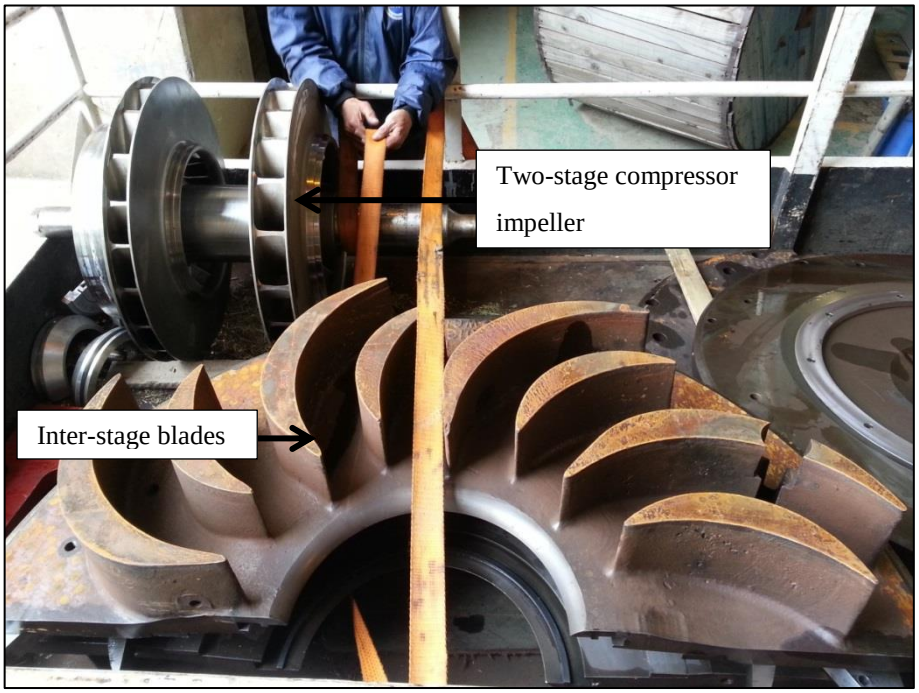

Figure 44: York guide vanes and compressor impeller collected from site for conversion

In order to convert the York chiller in parallel with the Hitachi chillers, the evaporator pipeline needed to be reconnected. The evaporator flow used to circulate in a closed loop. The condenser outlet flow was connected in parallel with five condenser cooling towers. As discussed in Chapter 2, one condenser tower with an operational fan gives sufficient delta temperature for one chiller.

VSD installation

The variable flow strategy discussed and simulated in Chapter 3 required the installation of VSDs. The layout of the refrigeration system where the VSDs were installed is illustrated in Figure 24 of Section 3.4. VSDs were installed on the Hitachi and York chiller evaporators and condenser pumps. The VSD panels installed on the 160 kW condenser pump and 75 kW evaporator pump are shown in Figure 45.

Figure 45: Inside of the York condenser (left) and evaporator (right) VSD

The system design parameters of the chilled water plant and BAC plant are given in Chapter 3, Table 3 and 4 respectively. VSDs were installed on the BAC circuit on two of the four evaporator pumps on the Pamodzi chillers. Chillers 10 to 14 on the BAC plant are referred to as the Pamodzi chillers.

The installation of the VSDs did not interfere with the existing cooling system operation. Each chiller was taken offline for a day to terminate the pump motor cable onto the VSD. Commissioning of each VSD was completed before performance assessment started. Figure 46 shows the existing 160 kW evaporator pump (at the top left) and 275 kW condenser pump (at the bottom right) of the York chiller. Each pump requires its own VSD.

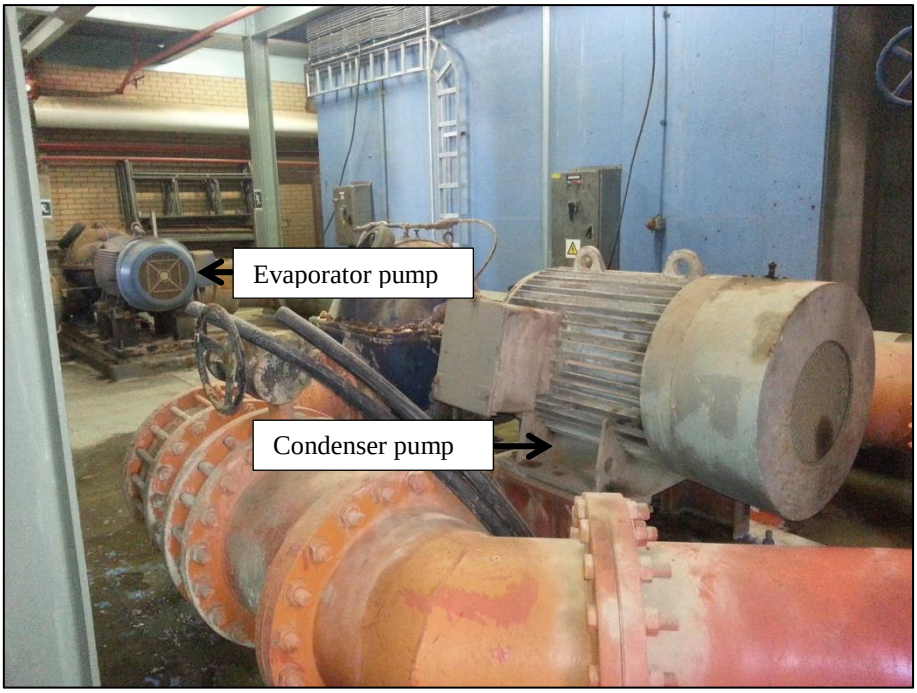

Figure 46: Evaporator and condenser pumps of York chiller at Mine M

Figure 47 illustrates the two VSDs installed on the evaporator pumps of the BAC plant. Each VSD panel possesses an internal extraction fan that cools the drive. If the VSD is not internally cooled, the heat will build up and damage electrical equipment in the panel. If the VSD is overheated, it will trip on high temperature. The VSD then needs to cool down before start up can proceed.

Figure 47: VSDs installed on Pamodzi evaporator pumps

4.4 RESULTS AFTER IMPLEMENTATION

Service delivery results

It is important to interpret the results of the service delivery before and after implementation. As described in Chapter 2, it is important to meet the underground demand when performing an energy-saving project. The three major service deliverables that need to be met is chilled water flow, temperature to underground and underground ambient temperature.

Data of January, February and March 2013 are compared to the performance assessment data of January, February and March 2014. It is important to compare months with the same ambient condition range. Figure 48 shows the flow to underground before implementation, compared to the flow to underground after implementation.

From Figure 48 it is evident that a similar underground demand was achieved after implementation. The flow to underground before (426 ℓ/s) and after implementation (438 ℓ/s) varies with 2.6%. Installing the VSDs and converting the ice storage dam therefore had no significant effect on the amount of flow to underground.

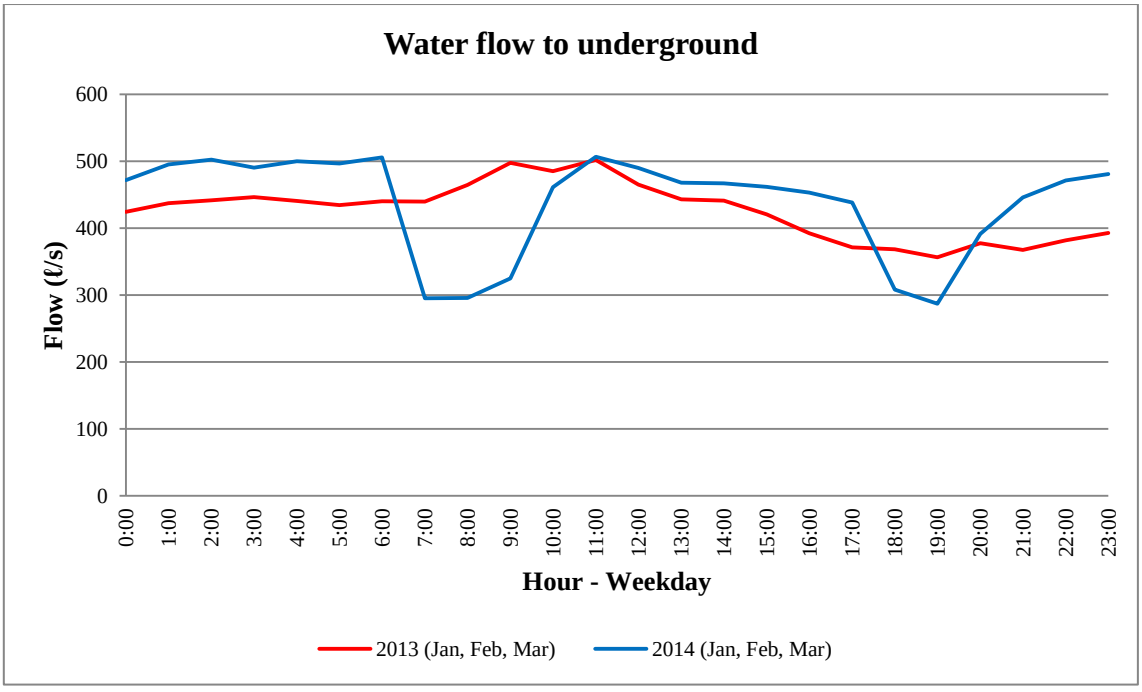

Figure 48: Chilled water flow to underground before and after implementation

In Figure 49 the temperature to underground after implementation shows a decrease of 1.4 ˚C in temperature. After implementation a lower and more constant temperature was sent

underground, as shown in Figure 49. Implementation, however, resulted in a decrease in chilled water temperature sent underground.

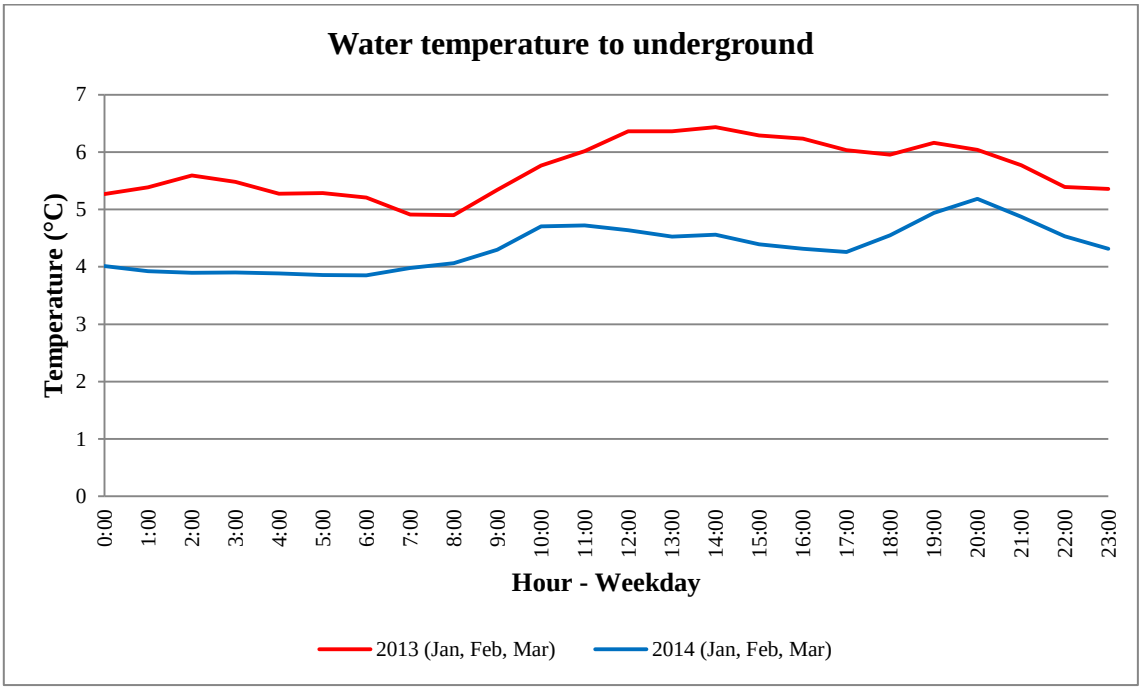

Figure 49: Temperature of chilled water to underground before and after implementation

The underground conditions before and after implementation on the refrigeration and BAC circuit is shown in Figure 50. Underground conditions of Mine M were monitored before implementation, December 2013. The December data was used to develop a baseline for the performance assessment data to be compared against. Figure 50 illustrates 24-hour profiles of the baseline and performance assessment period.

Temperature sensors were placed on levels 83 and 120, and on the surface. The sensors measured the dry-bulb temperature and relative humidity. Equation 2 of Section 2.2 was used to calculate the wet-bulb temperature. The temperature on level 83 was on average at 23.2 ˚C wet-bulb and at 25.8 ˚C wet-bulb on level 120. These temperatures are well below the ideal maximum, as explained in Chapter 2. The average surface ambient temperature was measured at 16.9 ˚C wet-bulb.

From the graph there is a slight drop in underground temperature when the baseline period is compared to the performance assessment period. The VSDs on the evaporator circuit of the BAC plant therefore have no significant effect on the underground wet-bulb temperatures.

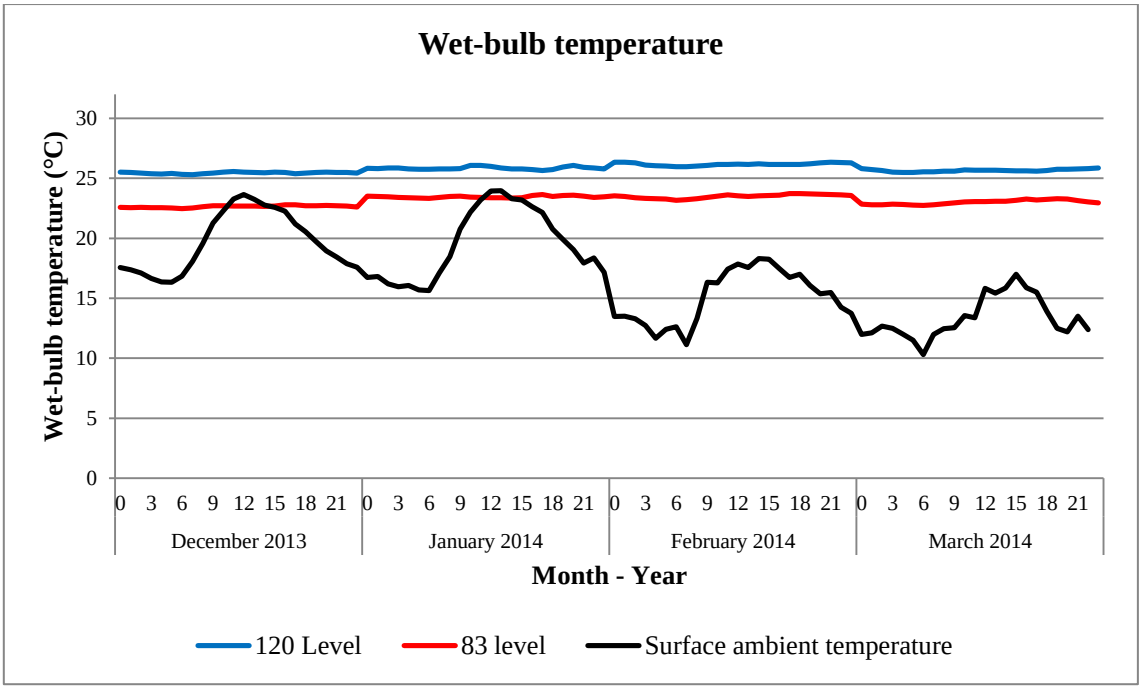

Figure 50: Surface ambient and underground wet-bulb temperatures of Mine M

VSD results

It is important to measure the harmonic effect of the VSDs on the electricity sent back into the system. Electricity spikes are managed to a minimum to prevent disturbance in the system. The total harmonic distortion (THD) level was measured before VSD installation in August 2013. The harmonic level on each panel over a period of 18 days was in the order of 1.2%, peaking at around 1.5%. The installed VSDs have built-in motor chokes and line chokes.

After installing the VSDs on the four Hitachi chillers and one York chiller, harmonic levels were measured on the VSDs. The harmonic levels on each of the 500-volt boards increased from 0.9%, drives switched off, to 3.2% when the drives were switched on. The worst case situation was created by switching three of the five chillers on, with all five evaporator pumps operating. The maximum THD level on a single board increased from 2.5% to 3.3%. Table 11 shows the results gathered during the harmonic tests.

Table 11: Harmonic levels of different size VSDs

VSD size (kW)	Pump size (kW)	Current (A)	Frequency (Hz)	THD (%)
MCC panel 1				
75	75	74	43	3.2
160	160	200	49	3.2
MCC panel 2				
75	75	77	41	2.7
160	160	173	45	2.7
MCC panel 3				
75	75	70	41	2.7
160	160	180	48	2.7
MCC panel 4				
75	75	60	41	2.7
160	160	188	47	2.7
MCC panel 5				
160	160	102	32	1.5
315	275	279	42	1.5

Control strategy

The control of the refrigeration system implemented on Mine M is described in Section 2.2 and 3.4. Performance of the control strategies was validated through evaluation of performance results. Figure 51 illustrates the output frequency from the VSD on evaporator pump three, controlled on the evaporator outlet temperature. The frequency varies to maintain the outlet temperature according to the SP of 4 ˚C. The SP was selected by the mine.

As the outlet temperature increases, the frequency output of the drive decreases. During the morning- and evening peak the electricity load on the compressor is shifted, resulting in an increase in temperature. Figure 50 illustrates that, as the temperature decreases, the frequency output of the VSD increases.

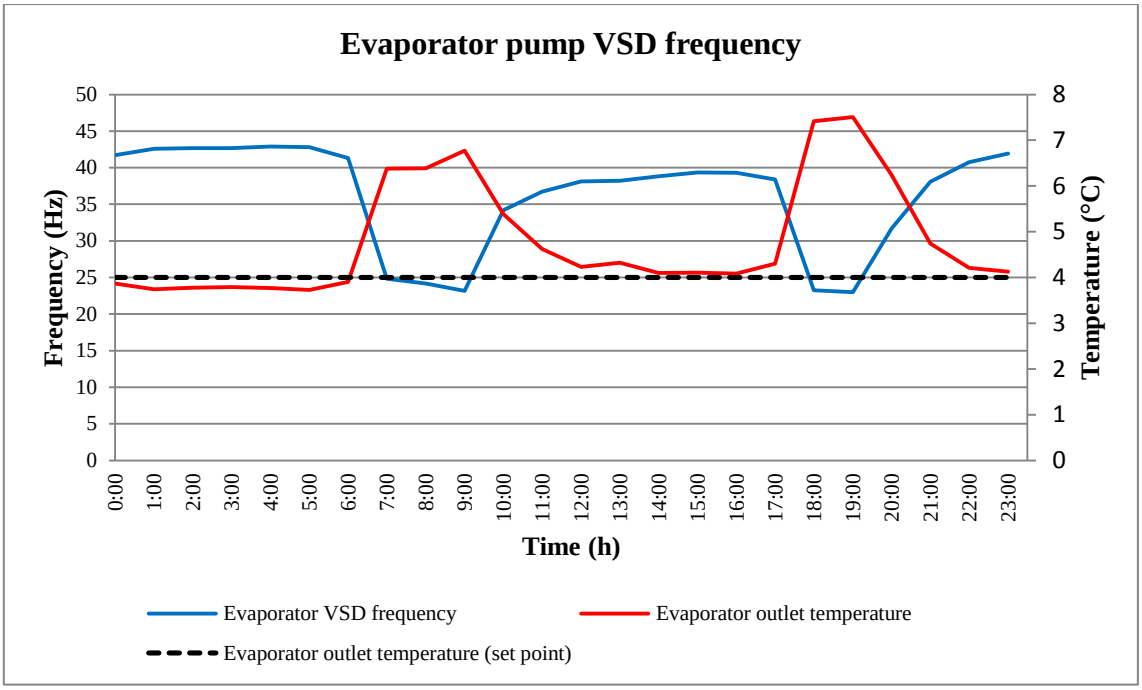

Figure 51: Chiller three evaporator pump VSD frequency

Figure 52 illustrates the VSD frequency output on the condenser pump of chiller three. Interpretation of the results found that, as the temperature difference between inlet and outlet temperature decreases, the frequency to the VSD decreases accordingly.

The control of the VSD on the condenser pump motor maintained the temperature difference across the condenser at a 6 ˚C SP. As the delta temperature increased, the frequency output of the VSD increased accordingly. The condenser pump is switched off during peak hours. This is evident from the delta temperature that decreases during these hours.

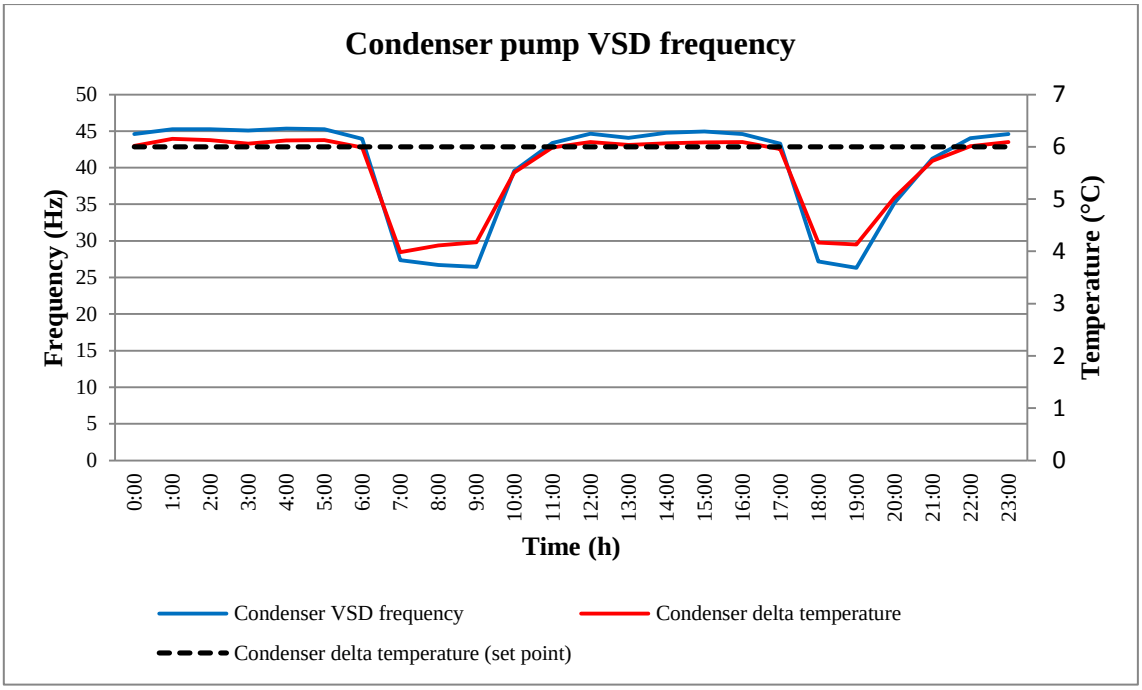

Figure 52: Chiller three condenser pump VSD frequency

The flow through the pump is dependent on the frequency output from the VSD. Figure 53 illustrates the decrease in flow delivered by the evaporator pump as the frequency of the VSD decreases. A linear correlation between the flow and the frequency is interpreted. The normal frequency operation range of the VSD is between 30 and 45 Hz.

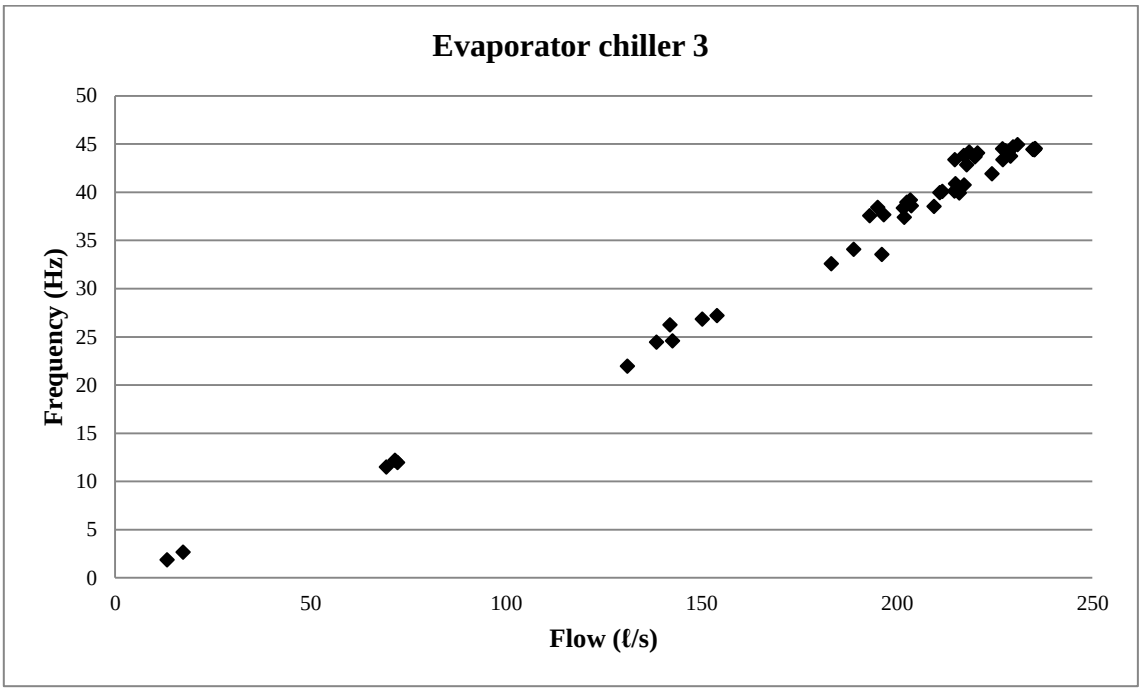

Figure 53: VSD frequency versus pump flow rate

The COP of the York chiller producing glycol was on average at 2, with a cooling capacity of 5 400 kW, as illustrated in Figure 54. After converting the York chiller to a water chiller, the COP increased with 103%. Additionally, the cooling capacity of the York chiller after implementation increased with 73%, as shown in Figure 54.

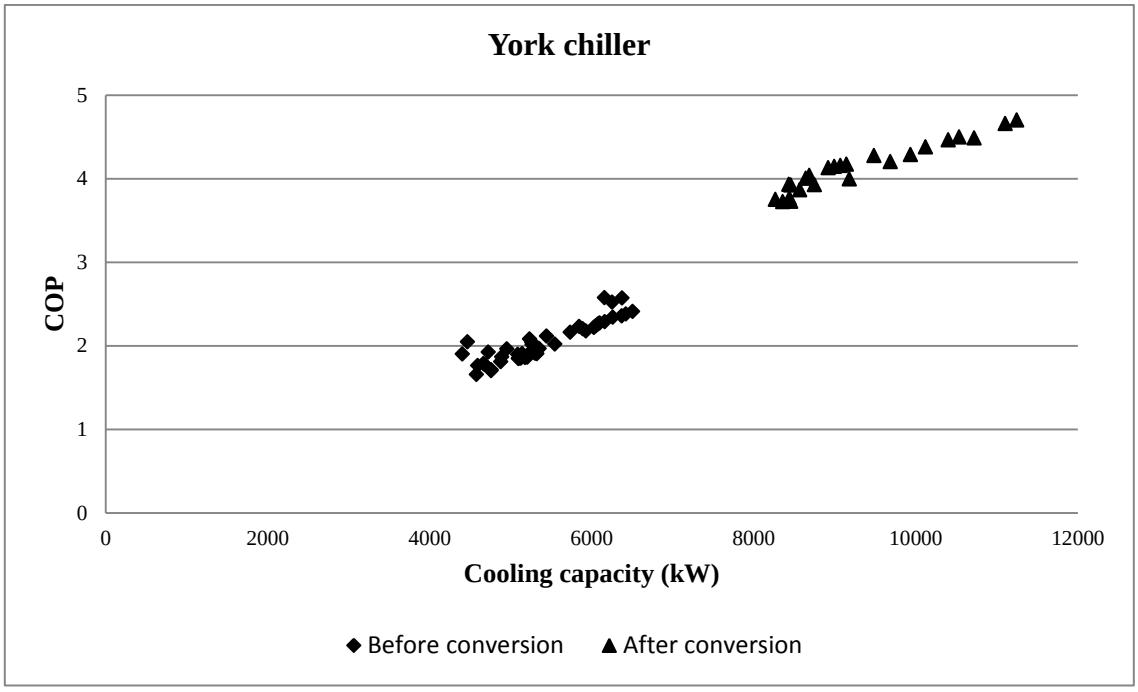

Figure 54: COP and cooling capacity of York chiller

The COP of the York chiller against the glycol flow through the chiller is shown in Figure 55. After implementation the COP increased to 4.1, with an average water flow of 251 ℓ/s through the chiller.

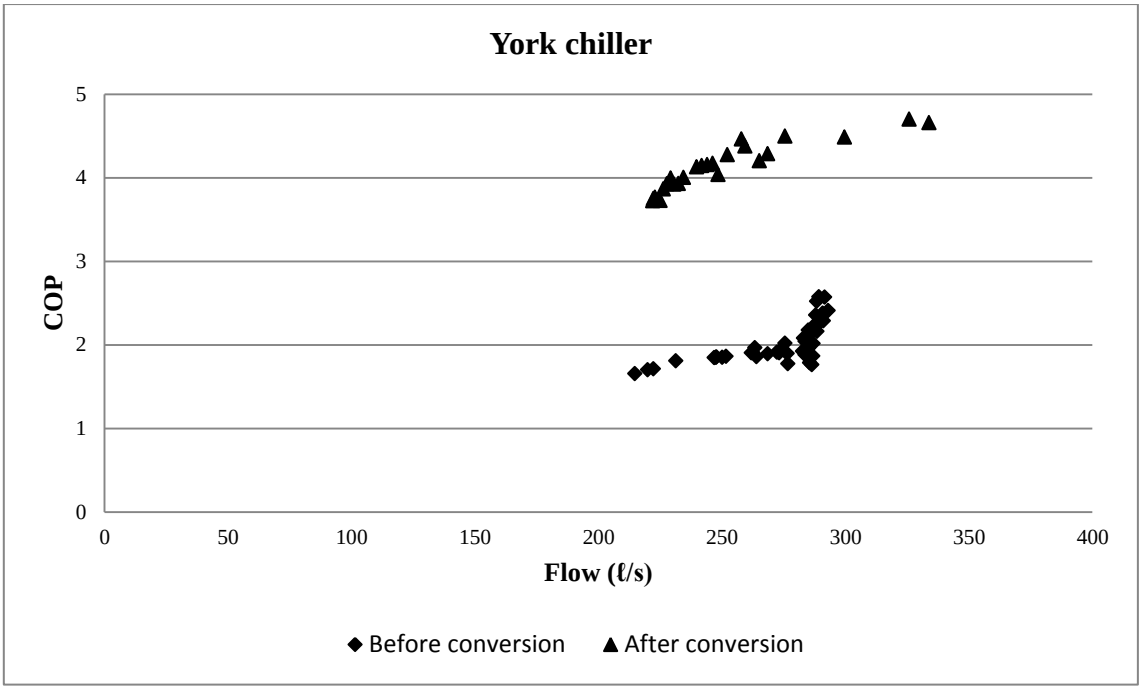

Figure 55: York chiller COP against glycol flow

The evaporator outlet temperature and flow of the York chiller before and after the conversion is illustrated in Figure 56. There is no significant difference between the evaporator flow before and after implementation. A temperature increase in evaporator outlet is, however, interpreted when converting from cooling glycol to cooling water.

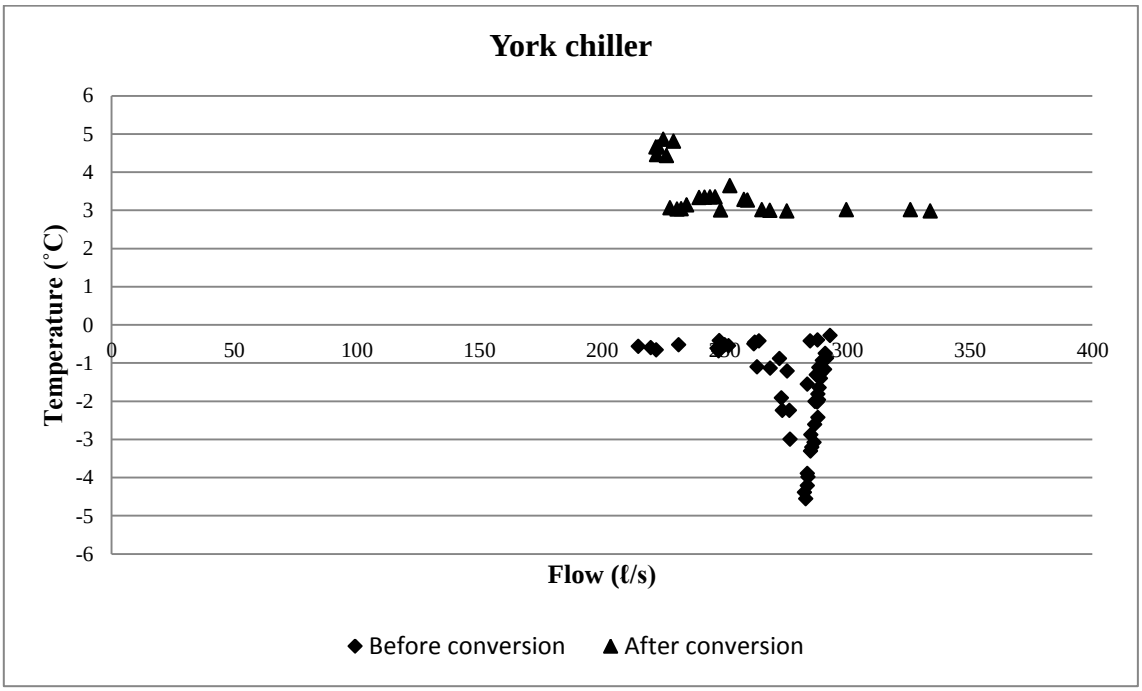

Figure 56: York chiller evaporator water outlet flow and temperature before and after conversion

The temperature difference across the evaporator against the chiller compressor power consumed is illustrated in Figure 57. The temperature difference across the evaporator side of the York chiller was 4.5 ˚C before conversion and 9.0 ˚C after conversion. This is a 96% temperature difference increase across the evaporator.

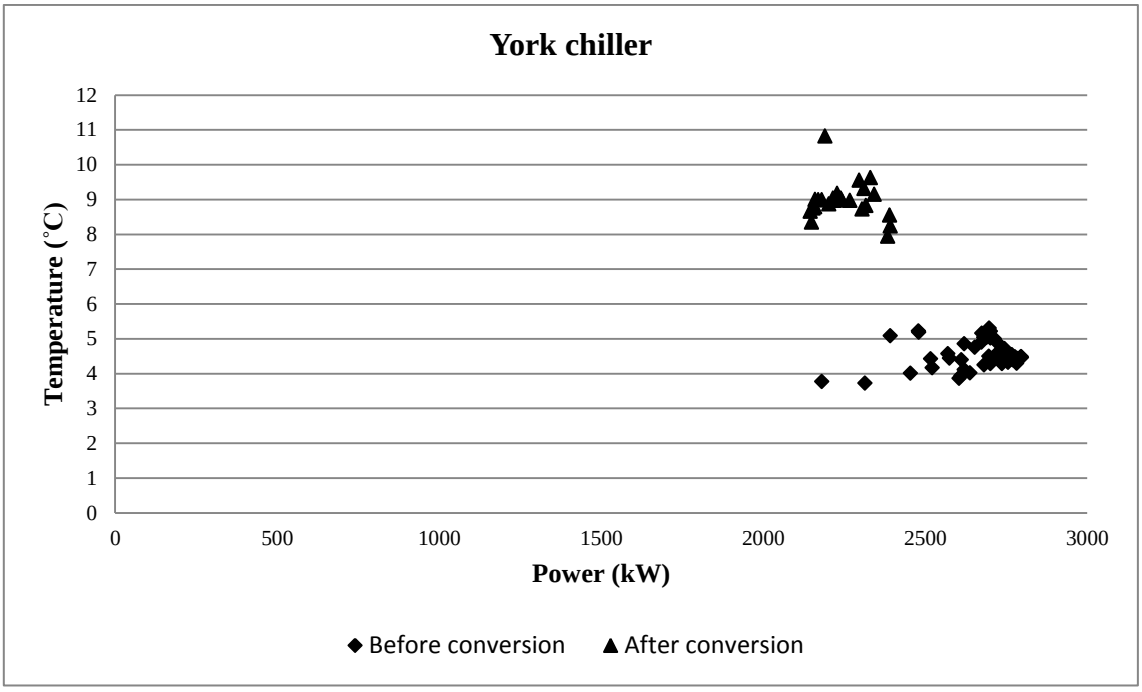

Figure 57: York chiller temperature difference across evaporator versus chiller compressor power

Results compared in this chapter included service delivery and control results. It is important to monitor the service delivery changes after such an implementation and compare results with pre-implemented results. Implementations had no significant effect on the service delivery. Results further indicated that the control on the evaporator and condenser functioned according to the control strategy.

4.5 ELECTRICAL ENERGY SAVINGS

Measurement and verification

In order to determine accurate electricity savings a power baseline must be developed. The baseline serves as electricity reference to measure the electricity savings achieved during and after performance assessment. Eskom appoints a measurement and verification team (M&V) to confirm the savings that the ESCO company achieved.

M&V is a team that analyses the energy consumed before and after implementation and is contracted to quantify and report the impact of the results achieved via the energy savings project delivered on the mine to Eskom[11].

To ensure that accurate and consistent savings are claimed, M&V requires three months of electricity usage before and after an implementation. Power baselines before implementation were sent to the M&V team for comparison with their power readings.

On a cooler day in winter, less energy will be consumed on the refrigeration system compared to a warm summer day. A winter and a summer baseline were therefore compiled to calculate the savings obtained with the implementation. In this case study the load of the refrigeration system will consequently be isolated from the rest of the mine's equipment. Three months is used for the summer baseline and three months for the winter baseline.

Figure 58 illustrates the summer baseline and Figure 59 the winter baseline. This ensures that the actual warmer summer months are compared to the summer baseline and the actual winter months are compared to the winter baseline.

The period used for the summer baseline is January, February and March 2013, and for the winter June, July and August 2013. The baseline is further subdivided into weekdays, Saturdays and Sundays. Gold mining is a continuous process, operating 24-hours, 7 days a week. However, Eskom's focus is to reduce the power usage on weekdays, therefore only weekday savings will be accounted for.

[11] http://www.eskom.co.za/IDM/MeasurementVerification/Pages/Measurement_Verification.aspx

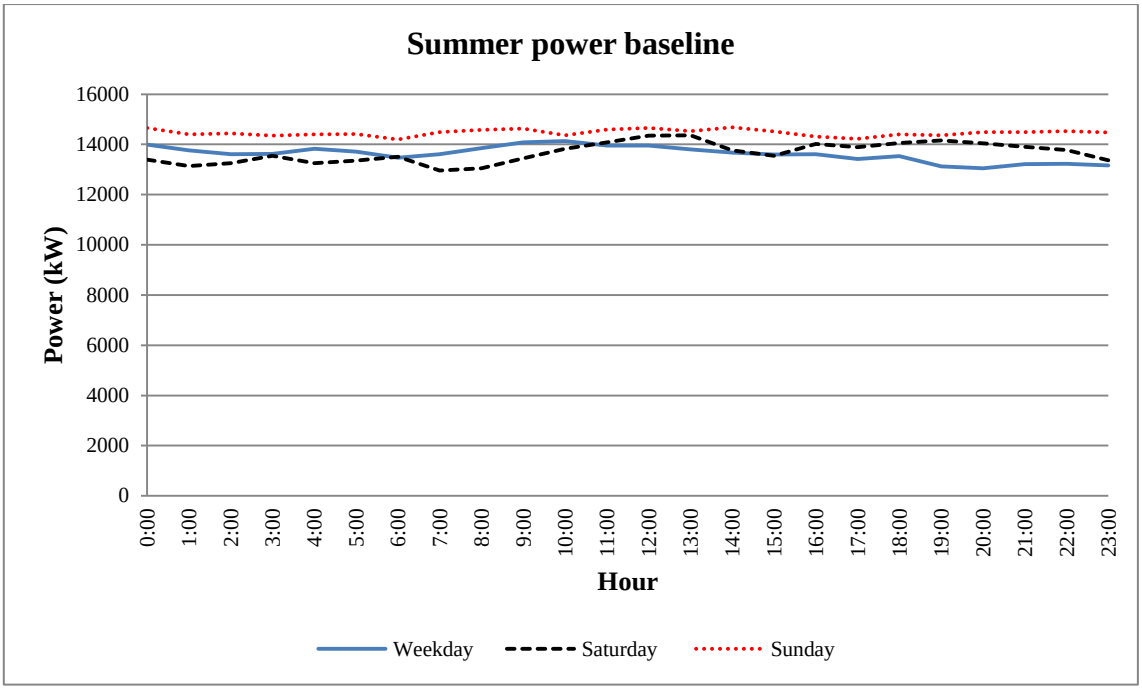

Figure 58: Average summer baseline for weekdays, Saturdays and Sundays

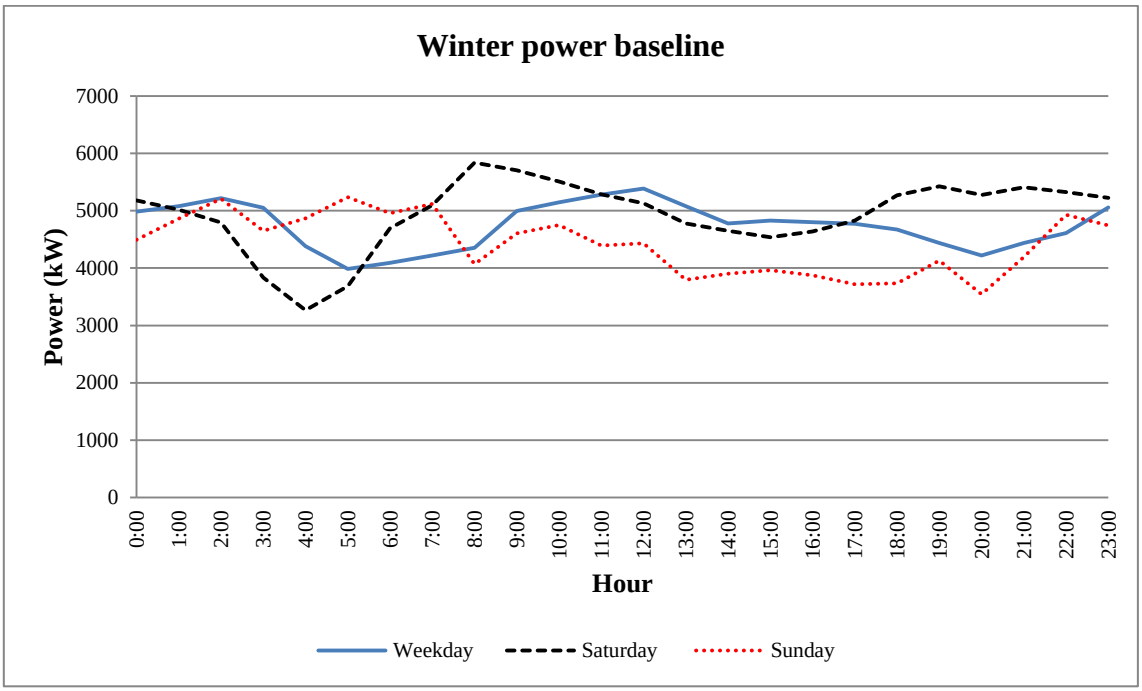

Figure 59: Average winter baseline for weekdays, Saturdays and Sundays

Due to cooling demand and temperature that have a direct impact on the amount of power consumed on the refrigeration system, a baseline must be scaled. Data is collected via various methods, as explained in Section 3.4. During the baseline development, two variables that affect the power usage were used as variables in the scaling calculation of the baseline. These variables include:

- x_1: Total flow of chilled water from the chillers (ℓ/day)
- x_2: Ambient temperature (˚C)

The scaled formula is developed using a Microsoft office LINEST function. The actual daily energy consumption is compared to the scaled baseline in order to determine the energy savings for the specific day. The power consumption is calculated by inserting the actual data into the variables of the scaling formula.

LINEST is a function that uses the least squares method to calculate the best straight line that fits the data. Equation 12 is the summer scaling formula calculated in LINEST with January, February and March data. Equation 13 is the winter scaling Equation calculated with June, July and August data.

$$y = 0.000108x_1 - 665.66x_2 + 344126.3 \quad (12)$$

$$y = -0.5181x_1 - 0.146x_2 + 147393.2 \quad (13)$$

Power savings

The conversion of the glycol ice storage chiller to a water chiller resulted in a 618 kW saving illustrated in Figure 60. This included the chiller compressor and the evaporator and condenser pumps. The total energy consumed by the glycol chiller was 2 600 kW. After implementation the glycol chiller gave the mine an additional chiller as backup. The York chiller will not be operated for long periods of time, resulting in an indirect power saving of 2 600 kW.

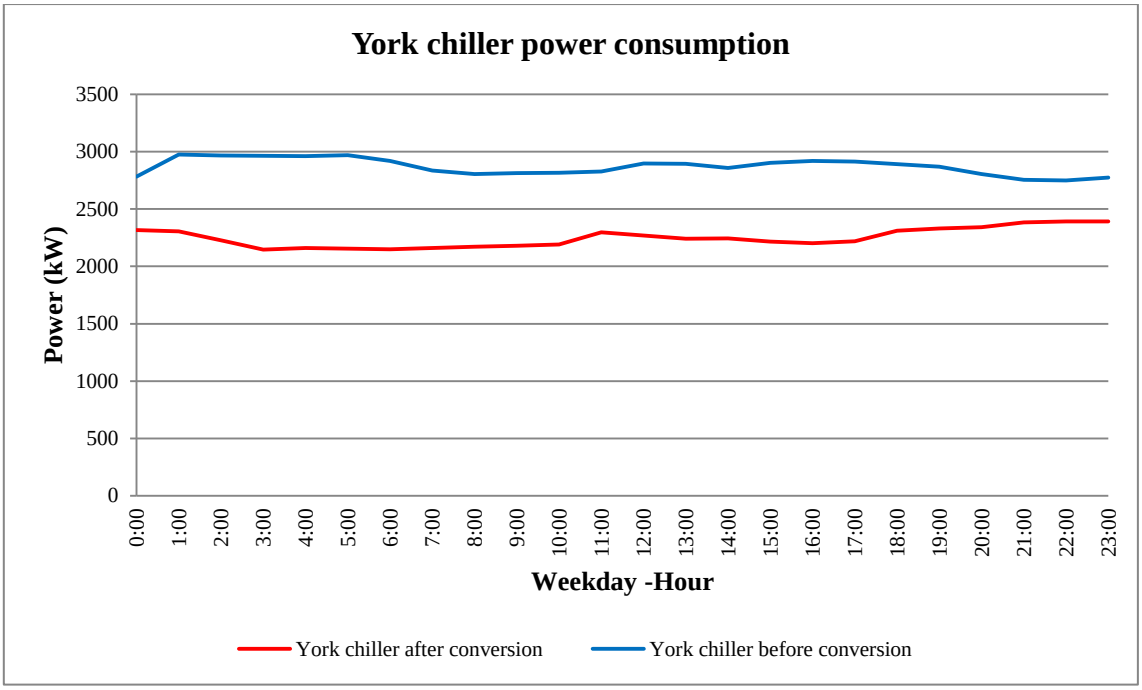

Figure 60: Power consumption of York chiller before and after conversion

The actual power usage of the entire system after implementation is illustrated in Figure 61. The weekday power saving during performance assessment amounted to 1.5 MW. The conversion of the ice storage system to a chilled water system enabled the possibility of a load shift during peak hours, due to the available water storage capacity. The engineer on Mine M pro-actively contributed to a load shift energy saving during the morning peak and evening peak hours, as shown in Figure 61.

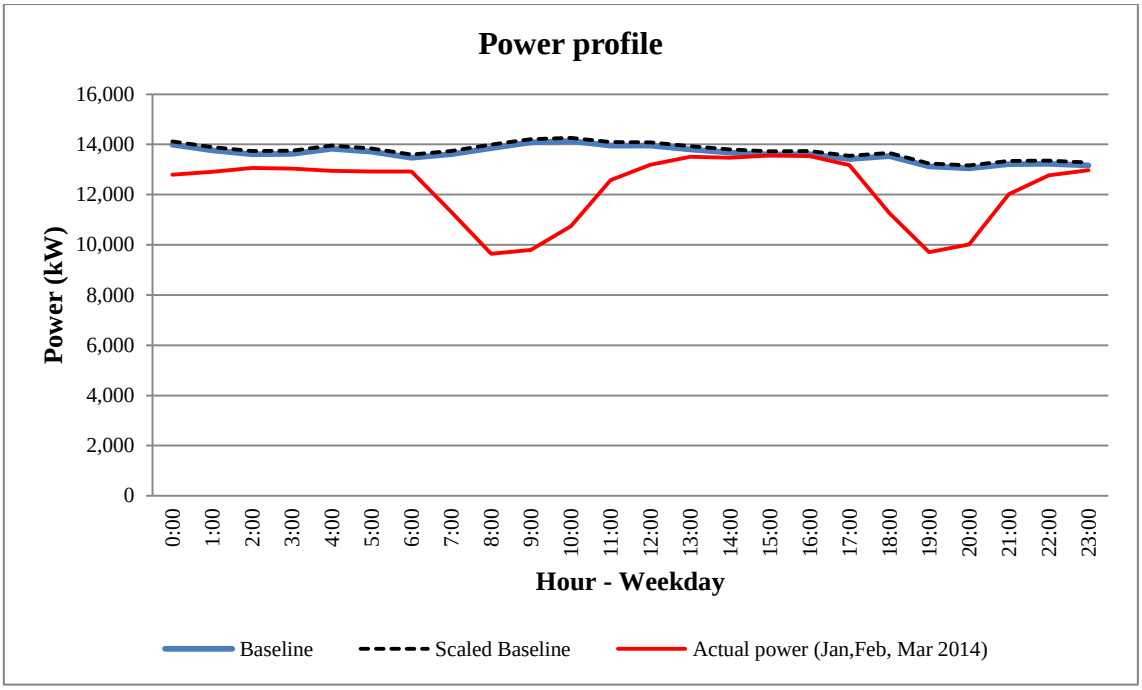

Figure 61: Power consumed after implementation on Mine M

The electricity savings achieved on the refrigeration system can be divided into the closed loop BAC plant and the chilled water plant. Results of the savings are seen in Figure 62. The load shift reduced the energy efficiency with a further 3.4 MW during morning peak and 2.2 MW during evening peak. The power saving on the BAC plant and chilled water plant is shown in Figure 62.

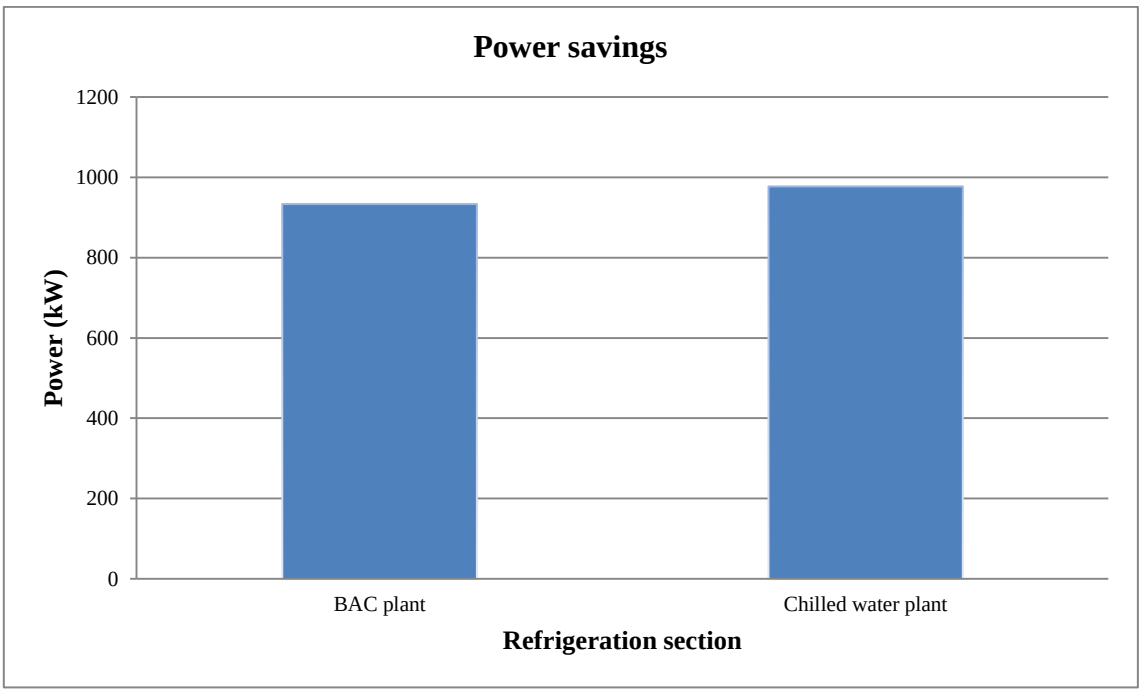

Figure 62: Power savings on the refrigeration system

Cost savings

As explained in Chapter 1, the gold mine electricity tariff falls under the Megaflex non-local authority tariff. Gold Mine M is within 300 km from the nearest Eskom distributor. The on-site substation voltage supplied to the refrigeration system is 6.6 kV. The active energy charge cost used in this study is shown in Table 12.

The tariff structure is split into high demand and low demand. The high demand accounts for the winter months June to August, when electricity consumption is at its highest, as explained in Chapter 1. The low energy demand tariff accounts for the summer, autumn and spring months, when energy consumption is not as high as the winter months.

Table 12: Megaflex tarrif for high demand (Jun-Aug) and low demand (Sep-May) [7]

	Megaflex	
Hour	High demand (Jun-Aug) [c/kWh] VAT incl	Low demand (Sep-May) [c/kWh] VAT incl
00:00	33.12	28.68
01:00	33.12	28.68
02:00	33.12	28.68
03:00	33.12	28.68
04:00	33.12	28.68
05:00	33.12	28.68
06:00	60.99	45.20
07:00	201.33	65.68
08:00	201.33	65.68
09:00	201.33	65.68
10:00	60.99	45.20
11:00	60.99	45.20
12:00	60.99	45.20
13:00	60.99	45.20
14:00	60.99	45.20
15:00	60.99	45.20
16:00	60.99	45.20
17:00	60.99	45.20
18:00	201.33	65.68
19:00	201.33	65.68
20:00	60.99	45.20
21:00	60.99	45.20
22:00	33.12	28.68
23:00	33.12	28.68

The cost savings during performance assessment is shown in Table 13.

Table 13: Performance assessment achieved savings

Month	Weekday power savings (kW)	Monthly cost savings (R)
January	1197	309 953.00
February	1436	430 833.00
March	1886	497 641.00

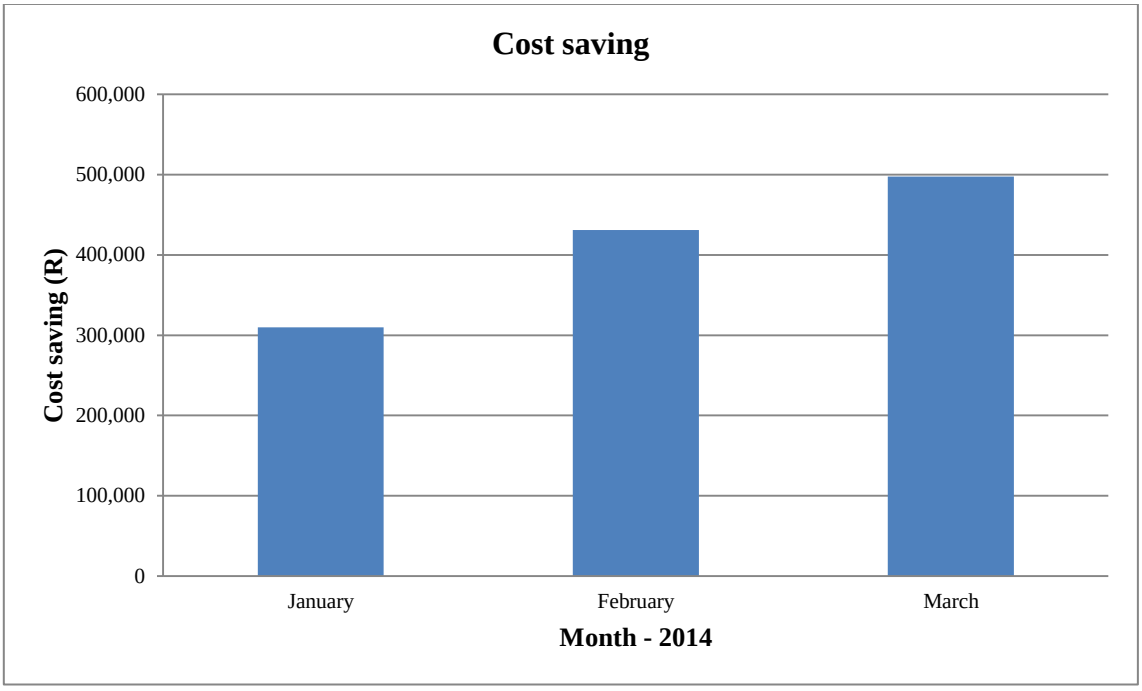

Figure 63: Electricity cost-savings of the refrigeration system - Mine M

Through the reduced power saving of 1.5 MW on Mine M, resulted in an annual reduced carbon emission of 17 895 ton using Equation 4 in Section 2.2. The implementation resulted in an annual summer weekday cost saving of R3 202 148.78.

Validation and verification of results

The total savings of each day differs due to equipment failure. The actual savings achieved are 29.6% of the simulated savings. This is, however, associated to human error on the actual operations. As previously stated, the installed capacity is 18.6 MW. The actual summer power saving is 1.5 MW and the simulated power saving is 1.9 MW. Comparing the actual and simulated power savings with the installed capacity resulted in a 2.4% difference. This

result validates the actual energy savings achieved on Mine M through the conversion of the ice storage system to a chilled water system and through installing VSDs.

4.6 CONCLUSION

This chapter started with the implementations on the refrigeration system of Mine M. Existing operation results of the glycol system was compared with the chilled water system after implementation. Results after implementation showed no significant change in the service delivery before implementation. The COP, however, increased with 103% after implementation. The temperature difference across the evaporator increased with 96% after conversion.

The temperature and flow underground, as well as the underground surrounding wet-bulb temperature, are not affected through the implementation of the energy-saving strategy. The difference in the actual power saving and simulated savings can be ascribed to human error on site. The VSD installations and control of the VSDs are successfully installed and implemented on Mine M.

Results after implementation was successfully collected and verified by M&V. It is concluded that the energy efficiency implementation on the refrigeration system of Mine M resulted in a 1.5 MW power saving during the performance assessment.

CHAPTER 5: CONCLUSION AND RECOMMENDATION

[12]

This chapter conveys the conclusion and recommendations of this study. It is concluded that converting an ice storage system to a chilled water system resulted in an energy saving. For additional savings it is further recommended that load shift is conducted on the BAC during peak hours.

[12] D. Uys, Personal photograph. "Main shaft and service shaft", West Wits, 2014.

5.1 CONCLUSION

The gold mining industry contributes to a large extent to South Africa's economy. The need to supply electricity to gold mines is therefore of great importance. There are however, numerous opportunities to reduce the energy consumption on a deep level gold mine, particularly the refrigeration system. It was found that cooling contributes to 23% of electricity consumed on gold mines exceeding depths of 1 600 m.

Due to constant high underground virgin rock temperatures, underground cooling water is required throughout the year. Each mine's refrigeration system is unique. However, the fundamentals of energy-saving strategies can be applied to the refrigeration system of various deep level gold mines. Each component in the refrigeration system is linked to each other and has a purpose to aid in producing chilled water. If the cooling capability of one of these components is hindered, the effect will be realised throughout the refrigeration system.

Energy efficiency is achieved by reducing the flow through the chiller and indirectly reducing the pump power and compressor power of the chiller. It was found that a VSD can be used to reduce the frequency to the motor, reducing the flow produced by the pump. VSDs have proven to deliver outstanding results in the energy-saving field. VSDs have proven to increase the lifespan of the pump motor and pump bearings.

The required time for ice formation is dependent on the glycol outlet temperature. At the lowest glycol temperature, sufficient ice formation can take up to eight hours. Limited research has been conducted on the thermal ice storage of deep level mines, therefore additional simulations and investigation approaches were followed.

The load on the compressor was reduced by reducing the daily water volume needed to be chilled by the chillers, which contributed to a 1 944 kW power saving. The volume of chilled water required to be chilled was reduced by reducing the back pass to the chiller. The back pass was reduced by varying the flow according to an evaporator temperature outlet SP. Power savings were also realised by varying the flow through the condenser according to a delta temperature SP across the condenser.

It is estimated that the centrifugal pumps used on the mine to distribute the water through the chillers constantly operate at full speed. However, most of the time extreme conditions are

not present and therefore it is not necessary for the pump to operate at full speed. This extreme condition occurs for a maximum of three months during the summer season. In conclusion, varying the flow through the evaporator reduces the electricity load on the pump.

Through simulation results, the service delivery for underground demand remained unchanged, with a 0.4% difference in the temperature of the chilled water to underground. The proposed simulation temperature and volume sent underground remained within the required limits.

According to these results it was concluded that the ice storage system should be converted to a chilled water system. Additional power savings will then be the result of VSDs installed on the evaporator and condenser pump motors. This will result in energy being saved without affecting underground conditions.

The temperature and flow underground, as well as the underground surrounding wet-bulb temperature, are not affected by the implementation of the energy-saving strategy. The difference in the actual power saving and simulated savings can be ascribed to human error on site. The VSD installations and control of the VSDs have been successfully installed and implemented on Mine M.

Results after implementation were successfully collected and verified by M&V. It is concluded that the energy efficient implementation on the refrigeration system of Mine M resulted in a 1.5 MW power saving during the performance assessment. It is concluded that the VSDs were not adversely affecting the electrical distribution system. The maximum harmonic level measured by the drive was 3.3% with all the pumps running, significantly lower than the NRS standard of 8%.

In conclusion, through the results of the implementation, Method B is the superior strategy for consuming less electricity to produce chilled water on Mine M. Making use of Method B does not negatively affect the cooling demand.

5.2 RECOMMENDATION

From the underground temperature results it is evident that the wet-bulb temperature measured is well below the environmental limit of 27.5 ˚C. It is recommended that a load shift or peak clip is implemented on the bulk air coolers for further electricity savings. As

indicated in Chapter 3, the BACs have an installed capacity of 1 440 kW. By switching off the bulk air cooler fans, evaporator pumps, condenser pumps and Pamodzi chillers' compressors during morning and evening peak, an additional saving can be achieved.

More studies on whether it is cost effective to increase mine depths should be done. This will determine if it is financially viable to implement new cooling technologies and machinery. Ultimately the economy and gold price of South Africa will be the determining factor whether gold mine depths in South Africa will break the 5 km barrier.

It is recommended that regular maintenance is performed on the VSDs and refrigeration equipment. Regular maintenance will ensure that the system operates at maximum efficiency. Set point changes and control needs to be updated when the demand changes.

REFERENCES

[1] Eskom Ltd, "Integrated results presentation for the year ended 31 March 2013," in *Johannesburg, Sunninghill, Megawatt Park*, 2013, pp. 6–10.

[2] E. A. Abdelaziz, R. Saidur, and S. Mekhilef, "A review on energy saving strategies in industrial sector," *Renewable and Sustainable Energy Reviews*, vol. 15, no. 1, pp. 150–168, Jan. 2011.

[3] D. W. Westfall, "Can South Africa generate growth in manufacturing ?," Arlington, USA, 2012.

[4] Eskom Ltd, "Generation plant mix_Fact sheet," Johannesburg, Sunninghill, Megawatt Park, 2012.

[5] SAinfo, "South Africa's energy supply," *South African Yearbook*, 2012. [Online]. Available: http://www.southafrica.info/business/economy/infrastructure/energy.htm#.U3ENGPmSykE. [Accessed: 12-May-2014].

[6] PWC, "SA Mine: Highlighting trends in the South African mining industry," Cape Town, 2012.

[7] Eskom Ltd, "Schedule of standard prices for Eskom tariffs 1 April 2013 to 31 March 2014 for non-local authority supplies and 1 July 2013 to 30 June 2014 for local authority supplies," Johannesburg, Sunninghill, Megawatt Park, 2013.

[8] A. Middelberg, J. Zhang, and X. Xia, "An optimal control model for load shifting – With application in the energy management of a colliery," *Applied Energy*, vol. 86, no. 7–8, pp. 1266–1273, Jul. 2009.

[9] R. Stephen, "Demand side management in South Africa," in *Energy efficiency made simple*, 2nd ed., Bedfordview: Crown, 2008, pp. 23–25.

[10] A. Hajiah and M. Krarti, "Optimal control of building storage systems using both ice storage and thermal mass – Part I: Simulation environment," *Energy conversion and management*, vol. 64, no. 1, pp. 499–508, Dec. 2012.

[11] C. Beggs, *Energy: Management, supply and convervation*, 7th ed. Oxford: New York: Butterworth-Heinemann, 2002, pp. 48–49.

[12] Eskom Ltd, "Integrated results for the year ended 31 March 2014," in *Johannesburg, Sunninghill, Megawatt Park*, 2014, pp. 8–20.

[13] Department of minerals and energy, "Energy efficiency strategy of the Republic of South Africa," Johannesburg, Sunnyside, 2005.

[14] Reegle, "Energy profile: South Africa," *Ciograsp*, 2011. [Online]. Available: http://cigrasp.pik-potsdam.de/countries/833900607/energy_profile. [Accessed: 12-May-2014].

[15] Economy, "Mining production rises in January at slower rate than month before," *Business day live*, 2014. [Online]. Available: http://www.bdlive.co.za/economy/2014/03/13/mining-production-rises-in-january-at-slower-rate-than-month-before. [Accessed: 12-May-2014].

[16] D. Ogunlade, *Energy policies for sustainable development in South Africa options for the future*, 1st ed. 2006, pp. 104–105.

[17] PWC, "SA Mine: Highlighting trends in the South African mining industry," Cape Town, 2013.

[18] BP plc, "BP energy outlook 2035," in *Energy outlook 2035, Durban*, 2014, pp. 67–80.

[19] Eskom Ltd, "The energy efficiency series," Johannesburg, Sunninghill, Megawatt Park, 2010.

[20] A. J. Gunson, B. Klein, M. Veiga, and S. Dunbar, "Reducing mine water network energy requirements," *Journal of cleaner production*, vol. 18, no. 13, pp. 1328–1338, Sep. 2010.

[21] Anglogold Ashanti Ltd, "Energy recovery at Mponeng using ice," 76 Jeppe Street, Newtown, Johannesburg, South Africa, 2007.

[22] L. Mackay, S. Bluhm, and J. van Rensburg, "Refrigeration and cooling concepts for ultra-deep platinum," *The Southern African institute of mining and metallurgy*, vol. 1, no. 4, pp. 285–292, 2010.

[23] A. Holman, "Benefits of improved performance monitoring of mine cooling systems," M.S. dissertation, Dept. Mech. Eng., North-West University, 2014.

[24] J. Vosloo, L. Liebenberg, and D. Velleman, "Case study: Energy savings for a deep-mine water reticulation system," *Applied Energy*, vol. 92, no. 1, pp. 328–335, Apr. 2012.

[25] U.S. Department of energy, "Pump life cycle costs: A guide to LCC analysis for pumping systems," Washington, 2001.

[26] Bureau of energy efficiency, *Pumps and pumping system*, 2nd ed. Dehradun, 2005, pp. 113–134.

[27] Chamber of mines of South Africa, "The importance of gold mining in South Africa," 2008. [Online]. Available: http://chamberofmines.org.za/mining-industry/gold. [Accessed: 17-May-2014].

[28] Gold investing news, "2013 Top 10 gold producing contries," 2014. [Online]. Available: http://goldinvestingnews.com/43146/2013-top-gold-producing-countries.html. [Accessed: 28-Sep-2014].

[29] Anglogold Ashanti Ltd, "Gold in South Africa," 76 Jeppe Street, Newtown, Johannesburg, South Africa, 2004.

[30] Chamber of mines of South Africa, "South African mining industry overview 2011," Marshalltown, 2011.

[31] L. Mogotsi, "Challenges facing the South African gold mining industry," *Alchemist*, vol. 1, no. 38, pp. 15–17, 2003.

[32] N. S. Jennings, "Mining: An overview," *ILO Encyclopaedia of occupational health and safety*. 2011.

[33] R. M. Stewart, "South African miners dig deeper to extend gold veins' life spans," *The wall street journal*, 2011. [Online]. Available: http://online.wsj.com/articles/SB10001424052748703584804576144062424424614. [Accessed: 07-Jun-2014].

[34] M. Bleby, "A trip down the world's deepest mine," *Business day live*, 2012. [Online]. Available: http://www.bdlive.co.za/articles/2011/06/21/a-trip-down-the-world-s-deepest-mine;jsessionid=92F5CB3634FA6684C74874B961022960.present2.bdfm. [Accessed: 11-Jun-2014].

[35] S. Leveritt, "Heat stress in mining," 1998. [Online]. Available: http://www.ergonomics.org.au/downloads/EA_Journals/Heat_Stress_in_Mining_-_leveritt.pdf. [Accessed: 27-Sep-2014].

[36] G. E. du Plessis, "A variable water flow strategy for energy savings in large cooling systems," Ph.D. thesis, Dept. Mech. Eng., North-West University, 2013.

[37] R. C. W. Webber, R. M. Franz, W. M. Marx, and P. C. Schutte, "A review of local and international heat stress indices , standards and limits with reference to ultra-deep mining," *The South African institute of mining and metallurgy*, vol. 1, no. 1, pp. 313–324, 2003.

[38] A. J. Schutte and M. Kleingeld, "Demand-side energy management of a cascade mine surface refrigeration system," M.S. dissertation, Dept. Mech. Eng., North-West University, 2007.

[39] B. D. J. Brake, "The application of refrigeration in mechanised mines," *The AusIMM proceedings*, vol. 306, no. 1, pp. 1–9, 2001.

[40] C. Thomaz, "Cooling solution for Africa's deep-level mines," *Mining Weekly*, Carletonville, pp. 3–5, 2009.

[41] G. E. du Plessis, L. Liebenberg, and E. H. Mathews, "Case study: The effects of a variable flow energy saving strategy on a deep-mine cooling system," *Applied Energy*, vol. 102, no. 1, pp. 700–709, Feb. 2013.

[42] A. M. Donoghue and G. P. Bates, "The risk of heat exhaustion at a deep underground metalliferous mine in relation to body-mass index and predicted VO2max.," *Occupational medicine*, vol. 50, no. 4, pp. 259–63, May 2000.

[43] Anglogold Ashanti Ltd, "Carbon disclosure project module," 76 Jeppe Street, Newtown, Johannesburg, South Africa, 2012.

[44] South African Weather, "Fochville," 2014. [Online]. Available: http://www.southafricanweather.co.za/aat/default.asp?city=fochville&province=North West&area=77078. [Accessed: 19-Jul-2014].

[45] M. J. Mcpherson, *Subsurface ventilation and environmental engineering*. 1993, pp. 651–652.

[46] M. J. Howes, "Ventilation and cooling in underground mines," *ILO Encyclopaedia of occupational health and safety*. 2011.

[47] Accuweather, "Weather Carletonville, South Africa," 2014. [Online]. Available: http://www.accuweather.com/en/za/carletonville/298074/air-travel-monthly/298074?monyr=1/01/2014. [Accessed: 27-Sep-2014].

[48] J. Greyling, "Techno-economic application of modular air cooling units for deep," M.S. dissertation, Dept. Mech. Eng., North-West University, 2008.

[49] ASHRAE, *Handbook on equipment*. Atlanta: American Society of Heating, Refrigeration and Air conditioning Engineers, 1997, pp. 36.1–36.19.

[50] A. J. Schutte, R. Pelzer, and E. H. Mathews, "Improving cooling system efficiency with pre-cooling," *Electricity +Control spot on*, 2010.

[51] R. E. Sonntag, C. Borgnakke, and G. J. Van Wylen, *Fundamentals of Thermodynamics*, 7 th. John Wiley & Sons, New Jersey, 2009.

[52] J. Mix, "HVAC efficiency definitions," Canada, United States, 2006.

[53] V. Manser, "What is a cooling tower?," *Cooling Technology Institute*, 2014. [Online]. Available: http://www.cti.org/whatis/coolingtowerdetail.shtml. [Accessed: 08-Nov-2014].

[54] K. Liebendorfer and J. Furlong, "Bulk air cooling the optimum solution for turbine inlet air chilling," Phillipi, South Africa, 2008.

[55] J. du Plessis, M. Butterworth, and R. Mcintyre, "Ventilation and cooling strategy for a deep mechanised mine - South Deep in South Africa," 41 Sloane Street, Bryanston, Johannesburg, 2012.

[56] Baltimore aircoil company, *Plume abatement*. Phillipi, South Africa, 2011, pp. 87–88.

[57] R. Stull, "Wet-bulb temperature from relative humidity and air temperature," *Journal of Applied Meteorology and Climatology*, vol. 50, no. 11, pp. 2267–2269, Nov. 2011.

[58] J. Hall, "Process pump control," *Chemical Engineering*, pp. 30–31, 01-Nov-2010.

[59] The Engineering Toolbox, "Pump affinity laws," 2014. [Online]. Available: http://www.engineeringtoolbox.com/affinity-laws-d_408.html. [Accessed: 28-Jul-2014].

[60] J. Chaurette, "Fluide design," 2004. [Online]. Available: http://www.pumpfundamentals.com/yahoo/affinity_laws.pdf. [Accessed: 28-Jul-2014].

[61] I. Halkijevic, Z. Vukovic, and D. Vouk, "Frequency pressure regulation in water supply systems," *Water Science & Technology: Water Supply*, vol. 13, no. 4, pp. 896–899, Aug. 2013.

[62] E. Mathews, M. Kleingeld, and D. Krueger, "A successful DSM project implemented on the refrigeration plant at Kopanang gold mine," *ICUE, Cape Town*, 2006.

[63] United Nations Environment Programme, "Refrigeration and air conditioning systems," Elsevier, Nairobi, Kenya, 2006.

[64] Hydraulic institute, "Variable speed pumping: A guide to successful applications," United States of America, Washington, 2004.

[65] S. Perju and L. V. Hasegan, "Reducing energy consumption by upgrading pumping stations in water distribution systems," *Environmental Engineering and Management Journal*, vol. 12, no. 4, pp. 735–740, 2013.

[66] E. Ozdemir, "Energy conservation opportunities with a variable speed controller in a boiler house," *Applied Thermal Engineering*, vol. 24, no. 7, pp. 981–993, May 2004.

[67] Associated Power Technologies Inc, "Total harmonic distortion and effects in electrical power systems," *Zhurnal Eksperimental'noi i Teoreticheskoi Fiziki*, pp. 1–4, 2011.

[68] A. Van Niekerk, D. C. Uys, and J. F. Van Rensburg, "Implementing DSM interventions on water reticulation systems of marginal deep level mines," *Industrial and Commercial Use of Energy*, 2014.

[69] K. Stouffer, K. Scarfone, and J. Falcon, *Guide to industrial control systems (ICS) security recommendations of the national institute of standards and technology*. Gaithersburg, Maryland, 2011, pp. 2.1 – 2.4.

[70] Eskom Ltd, "Eskom integrated report 2011," 2011. [Online]. Available: http://financialresults.co.za/2011/eskom_ar2011/add_info_tables.php. [Accessed: 05-Sep-2014].

[71] A. Saito, "Recent advances in research on cold thermal energy storage," *International Journal of Refrigeration*, vol. 25, no. 1, pp. 177–189, 2002.

[72] I. W. Eames, M. Worall, and S. Wu, "An experimental investigation into the integration of a jet-pump refrigeration cycle and a novel jet-spay thermal ice storage system," *Applied Thermal Engineering*, vol. 53, no. 2, pp. 285–290, May 2013.

[73] I. Bellas and S. A. Tassou, "Present and future applications of ice slurries," *International Journal of Refrigeration*, vol. 28, no. 1, pp. 115–121, Jan. 2005.

[74] Environmental systems process Ltd, "Thermal energy storage design guide," Peterborough, United Kingdom, 2001.

[75] IDE Technologies, "Vacuum ice maker," 2014. [Online]. Available: http://www.environmental-expert.com/products/vacuum-ice-maker-196328#down. [Accessed: 14-Jul-2014].

[76] Anon, "Thermal storage - glycol systems," 2014. [Online]. Available: http://cipco.apogee.net/ces/library/xctg.asp. [Accessed: 13-Sep-2014].

[77] A. Hajiah and M. Krarti, "Optimal controls of building storage systems using both ice storage and thermal mass – Part II: Parametric analysis," *Energy Conversion and Management*, vol. 64, no. 1, pp. 509–515, Dec. 2012.

[78] Baltimore aircoil company, "Why ice thermal storage for air conditioning projects," 2010. [Online]. Available: http://www.baltimoreaircoil.com/english/products/ice-thermal-storage/air-conditioning/designselection. [Accessed: 08-Aug-2014].

[79] B. Rismanchi, R. Saidur, H. H. Masjuki, and T. M. I. Mahlia, "Energetic, economic and environmental benefits of utilizing the ice thermal storage systems for office building applications," *Energy and Buildings*, vol. 50, pp. 347–354, Jul. 2012.

[80] M. Creamer, "Ice lowers cost of cooling deep mines, says engineer," *Mining weekly*, 2008. [Online]. Available: http://www.miningweekly.com/article/ice-lowers-cost-of-cooling-deep-mines-says-engineer-2008-05-30. [Accessed: 06-Aug-2014].

[81] S. Cutifani, "Case study : AngloGold Ashanti and climate change," 76 Jeppe Street, Newtown, Johannesburg, South Africa, 2008.

APPENDICES

APPENDIX A – CHILLED WATER COMPRESSOR IMPELLER

Figure 64: Compressor impeller

APPENDIX B – LOGGED DATA

Figure 65: Installed DENT power logger

Figure 66: Current clips of DENT logger installed

Figure 67: Tiny Tag temperature and humidity loggers

APPENDIX C – PERFORMACE ASSESMENT DATA

Table 14: Data of performance assessment - January

	January (Weekday) average										
Hour	Flow to underground (ℓ/s)	Make up flow (ℓ/s)	Total flow (ℓ/s)	Ambient Temp (°C)	Baseline (kW)	Scaled baseline (kW)	Actual power chillers (kW)	Actual power BAC (kW)	Total power (kW)	Saving (kW)	Cost saving (R)
00:00	398.23	32.90	431.13	20.10	13988.35	14080.25	11964.57	580.59	12545.16	1535.10	440.27
01:00	445.22	34.74	479.96	19.67	13765.00	13855.43	12087.80	583.28	12671.08	1184.36	339.67
02:00	452.09	33.31	485.40	19.28	13608.60	13698.01	12303.60	584.93	12888.53	809.48	232.16
03:00	410.52	34.76	445.28	18.99	13623.00	13712.50	12404.29	584.42	12988.71	723.80	207.58
04:00	428.43	33.58	462.01	18.76	13831.60	13922.47	12302.19	582.96	12885.15	1037.32	297.50
05:00	428.85	33.78	462.63	18.53	13711.05	13801.13	12198.24	581.59	12779.83	1021.30	292.91
06:00	511.92	31.82	543.74	19.03	13466.60	13555.07	12325.40	581.81	12907.20	647.87	292.84
07:00	406.48	29.61	436.09	19.98	13606.75	13696.14	11549.42	579.84	12129.27	1566.88	1029.13
08:00	429.93	24.59	454.52	21.30	13858.45	13949.50	10864.30	581.38	11445.68	2503.82	1644.51
09:00	449.59	26.03	475.62	22.70	14080.80	14173.31	10802.59	572.38	11374.97	2798.34	1837.95
10:00	470.66	21.33	491.99	24.40	14129.25	14222.08	11193.49	582.30	11775.79	2446.29	1105.72
11:00	513.18	24.81	537.99	25.61	13961.50	14053.23	12410.02	574.69	12984.71	1068.51	482.97
12:00	424.90	24.68	449.58	26.48	13950.70	14042.35	12628.76	574.47	13203.23	839.12	379.28
13:00	372.37	30.21	402.57	26.99	13802.30	13892.98	12559.57	573.81	13133.38	759.60	343.34
14:00	406.68	26.69	433.37	27.09	13669.40	13759.21	12465.16	574.63	13039.79	719.42	325.18
15:00	370.79	30.26	401.04	26.79	13599.30	13688.65	12664.24	577.94	13242.18	446.47	201.80
16:00	348.69	28.16	376.85	25.92	13609.30	13698.71	12823.81	577.53	13401.35	297.36	134.41
17:00	347.40	30.82	378.23	24.82	13419.05	13507.21	12475.55	585.49	13061.04	446.17	201.67
18:00	352.69	27.49	380.17	24.11	13531.50	13620.40	11146.35	590.95	11737.31	1883.09	1236.82
19:00	279.45	30.33	309.78	23.37	13124.50	13210.73	10343.75	594.78	10938.53	2272.20	1492.38
20:00	322.65	33.63	356.28	22.61	13045.45	13131.16	10464.39	593.83	11058.22	2072.94	936.97
21:00	323.32	26.57	349.89	21.89	13215.90	13302.73	11723.97	586.68	12310.64	992.08	448.42
22:00	374.26	28.08	402.35	21.21	13231.80	13318.73	12269.65	583.44	12853.09	465.64	133.55
23:00	378.68	29.53	408.21	20.77	13160.75	13247.21	12485.96	580.87	13066.83	180.38	51.73

Table 15: Data of performance assessment - February

	February (Weekday) average										
Hour	Flow to underground (ℓ/s)	Make up flow (ℓ/s)	Total flow (ℓ/s)	Ambient Temp (°C)	Baseline (kW)	Scaled baseline (kW)	Actual power chillers (kW)	Actual power BAC (kW)	Total power (kW)	Saving (kW)	Cost saving (R)
00:00	511.59	6.42	518.01	19.78	13988.35	14104.39	12118.12	963.77	13081.89	1022.51	293.25
01:00	531.15	6.30	537.46	19.24	13765.00	13879.19	12297.83	962.95	13260.78	618.41	177.36
02:00	545.53	7.33	552.86	18.90	13608.60	13721.49	12594.11	964.13	13558.24	163.25	46.82
03:00	541.79	9.86	551.65	18.54	13623.00	13736.01	12674.47	963.75	13638.22	97.79	28.05
04:00	542.29	7.61	549.90	18.45	13831.60	13946.34	12471.80	962.26	13434.06	512.28	146.92
05:00	536.68	9.56	546.24	18.09	13711.05	13824.79	12250.20	960.46	13210.66	614.14	176.13
06:00	504.04	9.07	513.11	18.19	13466.60	13578.31	12453.19	962.37	13415.56	162.75	73.56
07:00	196.58	8.76	205.33	18.99	13606.75	13719.63	9924.56	965.49	10890.05	2829.58	1858.47
08:00	198.08	10.42	208.50	20.12	13858.45	13973.41	7274.63	963.45	8238.09	5735.33	3766.96
09:00	221.03	8.39	229.42	21.44	14080.80	14197.61	7556.40	955.56	8511.95	5685.65	3734.34
10:00	473.02	8.52	481.55	22.69	14129.25	14246.46	9016.16	962.49	9978.65	4267.81	1929.05
11:00	533.96	7.53	541.49	24.44	13961.50	14077.32	11821.98	938.42	12760.40	1316.92	595.25
12:00	543.08	9.85	552.94	25.20	13950.70	14066.43	12873.73	960.31	13834.04	232.39	105.04
13:00	516.23	12.24	528.47	25.82	13802.30	13916.80	13274.37	961.08	14235.45	-318.65	-144.03
14:00	521.10	7.74	528.85	25.95	13669.40	13782.80	13179.00	958.49	14137.49	-354.69	-160.32
15:00	524.24	10.47	534.71	25.76	13599.30	13712.11	13092.51	945.19	14037.70	-325.58	-147.16
16:00	498.01	11.81	509.81	25.30	13609.30	13722.20	12874.82	960.68	13835.50	-113.31	-51.21
17:00	474.50	9.85	484.35	24.69	13419.05	13530.37	12143.99	960.70	13104.69	425.68	192.41
18:00	233.49	10.17	243.66	23.53	13531.50	13643.75	9828.58	962.29	10790.88	2852.88	1873.77
19:00	240.74	8.92	249.66	22.35	13124.50	13233.38	7589.31	960.40	8549.70	4683.67	3076.24
20:00	437.34	8.31	445.65	21.58	13045.45	13153.67	8322.17	963.40	9285.57	3868.10	1748.38
21:00	524.74	8.21	532.95	20.73	13215.90	13325.53	11609.66	963.40	12573.06	752.48	340.12
22:00	538.24	8.15	546.39	20.30	13231.80	13341.57	12428.90	964.26	13393.16	-51.59	-14.80
23:00	541.15	7.98	549.13	19.94	13160.75	13269.93	12520.17	963.47	13483.64	-213.71	-61.29

Table 16: Data of performance assessment - March

	March (Weekday) average										
Hour	Flow to underground (ℓ/s)	Make up flow (ℓ/s)	Total flow (ℓ/s)	Ambient Temp (°C)	Baseline (kW)	Scaled baseline (kW)	Actual power chillers (kW)	Actual power BAC (kW)	Total power (kW)	Saving (kW)	Cost saving (R)
00:00	504.74	23.18	527.91	17.87	13988.35	14172.84	11808.53	966.50	12775.03	1397.81	400.89
01:00	508.44	23.23	531.67	17.60	13765.00	13946.54	11842.85	966.50	12809.35	1137.19	326.15
02:00	509.83	24.25	534.07	17.34	13608.60	13788.08	11784.54	966.84	12751.38	1036.70	297.33
03:00	518.02	24.22	542.24	17.01	13623.00	13802.67	11537.85	965.28	12503.13	1299.54	372.71
04:00	529.04	25.23	554.28	16.95	13831.60	14014.02	11547.08	964.97	12512.06	1501.96	430.76
05:00	524.38	26.09	550.48	16.78	13711.05	13891.88	11824.46	963.98	12788.43	1103.45	316.47
06:00	500.41	26.64	527.06	16.76	13466.60	13644.21	11470.48	964.18	12434.66	1209.55	546.72
07:00	282.65	26.36	309.00	17.25	13606.75	13786.21	9977.72	966.19	10943.91	2842.29	1866.82
08:00	258.31	25.40	283.70	17.48	13858.45	14041.22	8305.07	963.91	9268.98	4772.24	3134.41
09:00	304.46	23.99	328.45	18.53	14080.80	14266.51	8553.85	965.59	9519.44	4747.07	3117.88
10:00	439.56	23.88	463.44	20.27	14129.25	14315.60	9492.89	963.03	10455.92	3859.68	1744.57
11:00	472.71	25.05	497.76	21.57	13961.50	14145.63	11045.52	958.30	12003.81	2141.82	968.10
12:00	501.47	25.32	526.79	22.97	13950.70	14134.69	11580.10	961.20	12541.30	1593.39	720.21
13:00	514.74	25.86	540.59	23.23	13802.30	13984.33	12186.97	963.92	13150.89	833.45	376.72
14:00	472.37	23.32	495.69	21.91	13669.40	13849.68	12268.23	963.18	13231.41	618.27	279.46
15:00	489.54	25.19	514.73	22.62	13599.30	13778.66	12433.73	962.35	13396.08	382.58	172.93
16:00	511.82	25.84	537.66	22.41	13609.30	13788.79	12417.98	962.25	13380.22	408.56	184.67
17:00	492.52	22.77	515.30	21.30	13419.05	13596.03	12427.02	956.51	13383.52	212.50	96.05
18:00	338.55	20.66	359.21	19.93	13531.50	13709.96	10300.63	950.20	11250.83	2459.13	1615.16
19:00	341.16	25.42	366.58	19.19	13124.50	13297.59	8701.56	949.04	9650.60	3647.00	2395.35
20:00	414.26	23.64	437.90	18.84	13045.45	13217.50	8725.74	960.04	9685.78	3531.72	1596.34
21:00	488.98	23.33	512.31	18.38	13215.90	13390.20	10223.11	959.90	11183.01	2207.19	997.65
22:00	500.62	24.18	524.80	18.19	13231.80	13406.31	11109.79	964.50	12074.29	1332.02	382.02
23:00	522.82	24.38	547.19	17.96	13160.75	13334.32	11395.37	960.19	12355.56	978.76	280.71

APPENDIX D – SIMULATION LAYOUTS

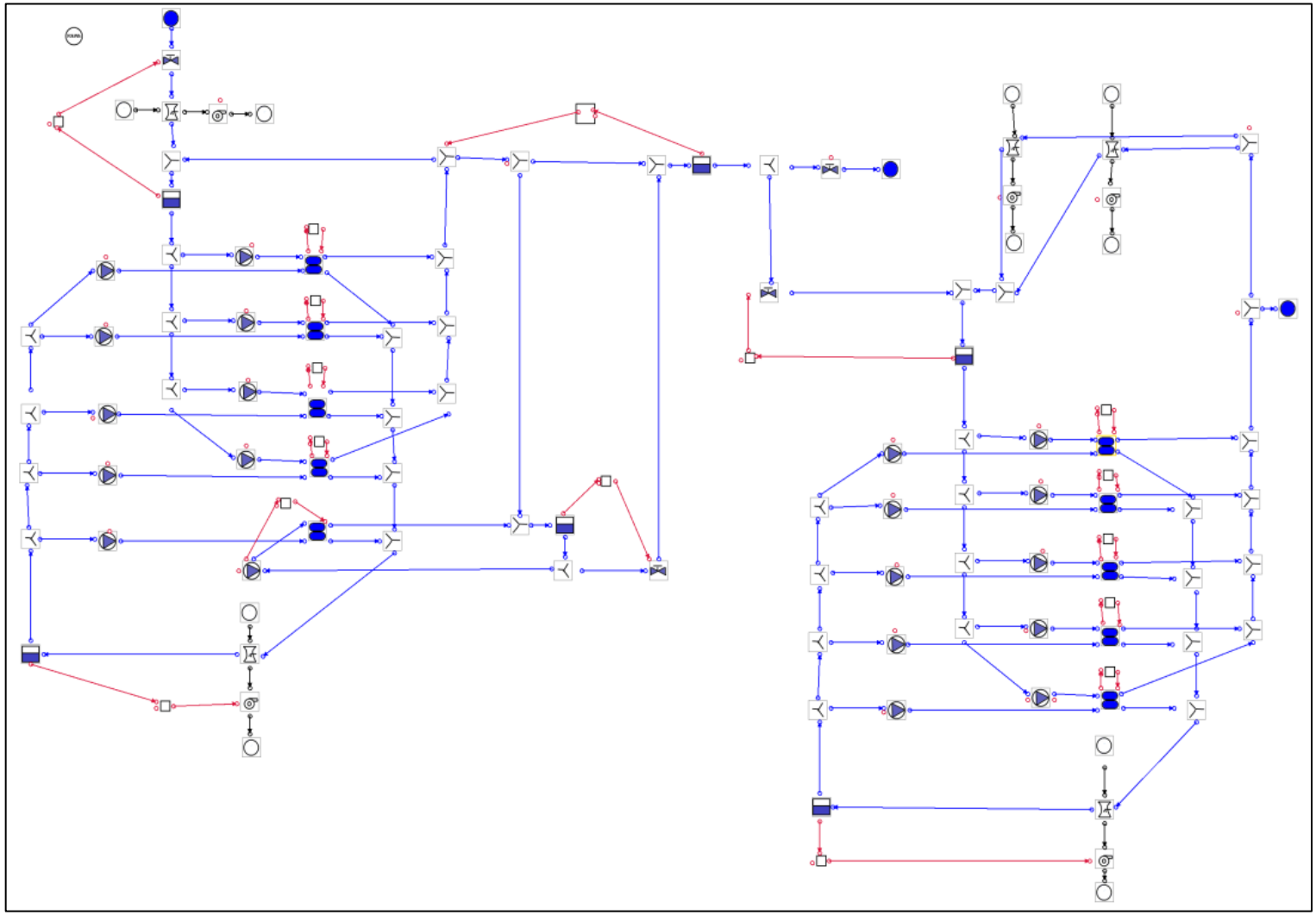

Figure 68: Simulation layout of Mine M with baseline operation

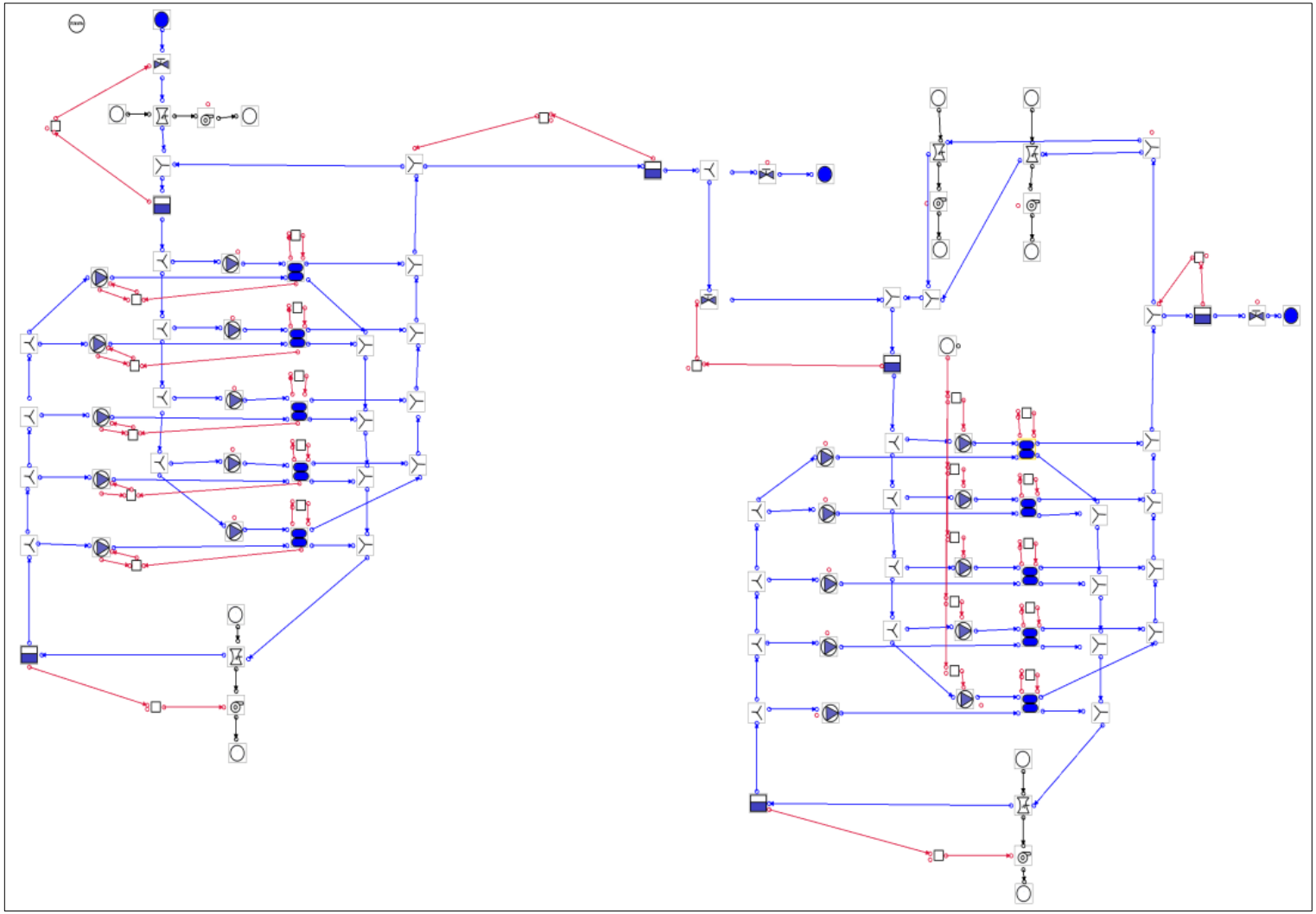

Figure 69: Simulation layout of Mine M to identify savings potential